APPROVAL SHEET

Title of Dissertation: Effects of culture dimensionality and hypoxia on human neural stem cells

Name of Candidate: Sasan Sharee Ghourichaee

Doctor of Philosophy, 2016

Dissertation and Abstract Approved: _____

Jennie B. Leach

Associate Professor

Chemical, Biochemical & Environmental Engineering

Date Approved: _____

ABSTRACT

Title of Document:	Effects of culture dimensionality and hypoxia on human neural stem cells
	Sasan Sharee Ghourichaee, Doctor of Philosophy, 2016
Directed By:	Dr. Jennie B. Leach, Associate Professor, Chemical, Biochemical, and Environmental Engineering, UMBC

Neurodegenerative diseases result in the loss of brain cells, causing difficulties in movement and mental functioning of patients. Currently, there is no effective therapy with the capability of modifying disease symptoms in the long-term. Transplantation of human neural stem cells (NSCs) is a novel treatment modality with the ability to regenerate the damaged neural tissue. NSCs possess two unique characteristics: the ability to renew themselves through cell division (self-renewal), and the capability to differentiate into major brain cell types (neurons, astrocytes, and oligodendrocytes). Therefore, NSCs present a renewable source of cells with tissue-specific regenerative capacity and, hence, are promising therapeutic candidates.

However, limited availability of stem cells, lack of standardized protocols for cell preparation as well as low survival of NSCs after transplantation are among important challenges that restrict the translational potential of NSC-mediated therapy. We hypothesize that the discrepancy between *in vitro* culture methods and the native brain microenvironment may be an underlying reason for this restricted translational potential. For enhanced therapeutic efficacy, the *in vitro* culture methods utilized for propagation of the cells need to be improved. Culture dimensionality, reduced oxygen concentration (hypoxia), growth factors, and interactions between cells and the extracellular matrix are among important culture parameters that differ between *in vitro* and *in vivo* situations. In this work, we present quantitative data supporting that these culture parameters can individually and synergistically regulate NSC survival, proliferation, differentiation, and cellular output. This work is a major step towards understanding key factors that regulate NSC fate and provides a foundation for improved strategies to more efficiently harness the regenerative potential of human NSCs.

EFFECTS OF CULTURE DIMENSIONALITY AND HYPOXIA ON HUMAN NEURAL STEM CELLS

By

Sasan Sharee Ghourichaee

Dissertation submitted to the Faculty of the Graduate School of the

University of Maryland, Baltimore County, in partial fulfillment

of the requirements for the degree of

Doctor of Philosophy

2016

Dedication

To my dear mom, dad, brother, and Mr. Fatemi Niya

Acknowledgements

I would like to thank my advisor Dr. Jennie Leach for her support, patience, and precious guidance. Without her support, I could never achieve this degree. Her multitasking skills, patience, and analytical thinking have always impressed me. In addition, I would like to thank Dr. Elizabeth Powell for all her help, care, and support. Her knowledge and passion for science are exemplary. I also thank Dr. Mariajose Castellanos for teaching me how to be an effective teacher. Many thanks to Dr. Douglas Frey and Dr. Julia Ross for serving on my committee and for being fantastic professors. I am very grateful to you all.

Many thanks to my dear lab mates Helena and Swarna for all their kindness, support, and invaluable care. You are my sisters. Special thanks to my dear friends in the department: Ke, Payam, Bill, Kiran, Utsav, Hilda, Michael, Cindy, Lili, Karthik, Aru, Natasha, Sevda, Marwa, Zahra, and Yang. You are all like family to me and there will always be a place in my heart for all of you. Many thanks to my dear friends Victor, Denise, and Kassy without whom life would be very hard in the department.

No matter how much I try I will always fail to thank my mother, father, and brother. I love you all so very much. All I have is because of you and your prayers. Thank you!!!

Table of Contents

List of Tables

List of Figures

Chapter 1: Summary of Work

The pathology of neurological disorders and injuries is associated with the loss of neurons, astrocytes, and oligodendrocytes in the brain that results in functional impairments [1]. Even though the currently available therapies provide modest symptomatic relief for patients, they are not effective in the long-term and are not able to stop the disease progression [2]. Therefore, a need exists for development of novel disease-modifying therapies that yield long-lasting improvements of the disease symptoms. Human neural stem cells (NSCs) possess an enormous potential to be utilized in novel cell-replacement therapies for neurodegenerative diseases and injuries. NSCs possess two cardinal properties: the ability to renew themselves through mitotic division and the capability to differentiate into neurons and glia (astrocytes and oligodendrocytes) [3]. However, the translational potential of NSC-based therapy is restricted due to the lack of standardized *in vitro* cell preparation protocols, limited survival of the NSCs after transplantation into the diseased brain, and limited availability of cost-effective and scalable NSC *in vitro* expansion methods.

Several clinical applications of transplantation of NSCs in human subjects with neurological disorders has resulted in heterogeneous results ranging from no clinical benefits to major improvements [4]. The variation in clinical outcomes may stem from non-standardized *in vitro* cell preparation methods. The temporal output of a population of NSCs may include undifferentiated stem cells, terminally differentiated neurons and glia , and dead cells [5]. Due to the plasticity of NSCs, environmental cues play a crucial role in determining the cellular composition of NSC cultures over time [6]. In the absence of standardized cell preparation protocols,

the cellular composition of the NSC *in vitro* cultures may differ significantly, resulting in transplants with varying degrees of cell type heterogeneity and consequently variable clinical outcomes. To tackle this challenge, in **Chapter 3** of this dissertation, I investigated the independent and synergistic effects of three important environmental factors (culture dimensionality, oxygen concentration, and growth factors) on the survival, growth, and differentiation potential of human NSCs. My experimental design included two dimensional (2D) vs three dimensional (3D) cultures and normoxic (21% O_2) vs hypoxic (3% O_2) conditions in the presence and absence of growth factors. Additionally, I constructed mathematical models that provide predictions for the rates of human NSC growth and differentiation under these culture conditions. My results indicate that the synergistic effect of culture dimensionality and hypoxic oxygen concentration in the presence of growth factors enhances the growth of viable and undifferentiated human NSCs. Moreover, the same synergistic effect in the absence of growth factors promotes the differentiation of human NSCs into neural and glial progenies. The results of this work will aid to develop standardized *in vitro* cell culture protocols with the capability of generating stem cell populations with well-defined cellular output over time.

Another important challenge constraining the therapeutic efficacy of NSC-mediated therapy is the low survival of the implanted stem cells. Previously published studies report a survival amount of between 10% to 40% of the total transplanted NSCs [7, 8]. Consequently, to enhance the long-term effectiveness of the cell-replacement therapy there is a need to increase the retention time of NSCs post transplantation. Recent studies indicate that the *in vitro* culturing of stem cells under

hypoxia (hypoxic preconditioning) prior to transplantation significantly improves their survival and regenerative potential [9]. For instance, mesenchymal stem cells and embryonic stem cells cultured under hypoxia exhibited a higher survival and differentiation potential in comparison with the cells cultured normoxia [10, 11]. The human brain is a hypoxic environment with an oxygen concentration between 3% to 4% as opposed to the atmospheric oxygen concentration (normoxia, 21%) that cells are exposed to in culture [12]. Yet, the effects of hypoxic preconditioning on human NSC survival and differentiation is not well understood. In **Chapter 4**, I hypothesized that the *in vitro* hypoxic preconditioning of human NSCs may enhance the survival of the cells and promote their differentiation into neurons and glia. I investigated the survival and differentiation behavior of human NSCs by culturing them under short-term (up to 10 d) and long-term (up to 60 d) hypoxia and compared the results with the control groups cultured under normoxia. My results indicate that short-term hypoxic preconditioning enhances the survival of human NSCs and that long-term hypoxic preconditioning promotes their differentiation into neural progenies without reducing the survival of the cells. Therefore, hypoxic preconditioning provides an effective cell-priming strategy aimed to increase the tissue-repair capability of NSCs and improve the clinical potential of cell-replacement therapy.

Limited availability of cost-effective and scalable methods to rapidly expand numbers of stem cells *in vitro* is the third challenge that limits the translational potential of cell-mediated therapy [13]. Oxygen concentration and the interactions between cells and the extracellular matrix (ECM) are the two important regulators of NSC proliferation [14, 15]. In **Chapter 5** of my dissertation, I tested the hypothesis

that oxygen concentration and the ECM composition can synergistically enhance the growth of human NSCs. To test for this possible synergistic effect, I cultured human NSCs on six substrates (i.e., collagen I, collagen IV, poly-L-ornithine, fibronectin, laminin, and Matrigel) under normoxic (21% oxygen) and hypoxic (3% oxygen) conditions and then determined the total viable cell numbers in culture after 2 and 4 d. The percentages of cells undergoing proliferation and apoptosis varied with culture conditions, with a synergistic interaction between Matrigel substrate and hypoxia that resulted in the greatest number of human NSCs after 4 d compared to other conditions. These findings inform new methods to augment human NSC production by identifying potential substrate biomaterial design criteria as well as culture conditions that favor the generation of larger numbers of undifferentiated cells.

The current dissertation strives to delineate how the important components of native brain tissue (dimensionality, oxygen concentration, growth factors, and cell-ECM interactions) regulate NSC growth and differentiation. By clarifying these regulatory effects, this work opens new doors for producing sufficient quantities of NSCs, generating well-defined cellular transplants, and enhancing the tissue-repair capability of the transplants. Overall, this study provides a foundation for improved strategies to more efficiently harness the regenerative potential of human NSCs.

Chapter 2: Background and Motivation

Stem Cells and their Therapeutic Potential

A crucial factor in the survival of any individual is the repair of damaged tissues due to disease or injury. The idea of wound repair and tissue regeneration is as old as humanity and can be even observed in ancient Greek myths. The Greek titan, Prometheus, was punished by Zeus because of his disobedience in introducing fire and knowledge to human beings. He was tied to a rock and his liver regenerated every day after being eaten by an eagle [16].

Tissue-repair process requires the replacement of dead or damaged cells by the newly generated ones. Furthermore, the newly generated cells must become integrated in the structure of the damaged tissue in order to restore its function [17]. Consequently, tissues with higher proliferative potential and simpler structures more effectively self-repair. For instance, skin (cutaneous) wounds regain their function, usually, within a few weeks after an injury. However, adult mammalian central nervous system due to its highly complex structure and low cell turnover, has a more limited capacity for self-repair [1]. Cell-replacement therapies have the potential to compensate for this endogenous inability by presenting stem cells as promising candidates to be utilized as cellular transplants.

The discovery of stem cells dates to back to 1945 when radiation-induced leukemia was observed among the survivors of Hiroshima and Nagasaki atomic bombings [18]. Hematologists discovered that a specific population of bone marrow cells, soon after infusion, had the ability to reconstitute the destroyed blood cells [19, 20]. This specific population of cells was called hematopoietic stem cells (HSCs).

The HSCs possessed two cardinal characteristics. First, the HSCs were capable of "self-renewal" by producing exact copies of themselves upon division. Secondly, HSCs were "multipotent" and had the ability to differentiate into both red and white blood cells [21]. Therefore, HSCs by providing a renewable source of multipotent cells exhibited an enormous regenerative potential.

It is now recognized that not only blood cells but all tissues and organs in the body arise from stem cells [22]. This is of particular importance for adult human brain where the capacity of repair is very limited. NSCs possess the ability to self-renew and give rise to neurons and glia which are the major cellular constituents of the brain [3]. Consequently, transplantation of NSCs is a promising strategy to regenerate brain tissue that is lost as a result of neurodegenerative diseases or injuries.

Neurodegenerative Diseases and their Impact on Society

Neurodegenerative diseases such as Parkinson's disease (PD), multiple sclerosis (MS), Alzheimer's disease (AD), amyotrophic lateral sclerosis (ALS), and stroke result in the loss of neurons and glia and cause cognitive, motor, and sensory impairments. There are ~8 million patients in the USA who have neurological disorders [23], and worldwide, there are ~47 million patients with dementia [24]. These disorders impose a significant burden on society. For instance, in Europe, there are about 3.7 million patients with PD, MS, ALS, and stroke which carry an estimated economic cost of $106 billion (**Table 2.1**) [25].

Table 2.1. Number of subjects affected and the cost of neurological disorders in Europe in 2010

Type of Disease	Number of Subjects Affected (millions)	Total Cost (billion USD)
PD	1.2	~16
MS	0.5	~16
ALS	0.1	~2
Stroke	2	~72

Generated from [25]

The world health organization projected that the number of years of potential life lost due to these diseases will increase from 92 million in 2005 to 103 million by 2030 [26, 27]. Currently, there are no disease-modifying therapies to restore the lost neurological functions of these patients. Rehabilitation techniques, depending upon the severity of damage to brain, could involve months or years of treatment [28]. Moreover, the medications available to halt the progression of neurodegenerative diseases are not effective in the long term. NSC transplantation has the potential to be the alternative therapeutic strategy.

Application of Neural Stem Cells in Neurodegenerative Diseases

Neural Stem Cells

Adult mammalian brain was long assumed to remain structurally unchanged after early postnatal development and that no new neurons were perceived to be generated during adulthood. In the early twentieth century, Santiago Ramón y Cajal, the father of modern neuroscience, commented in his masterpiece [29], "*Once the*

development was ended, the founts of growth and regeneration of the axons and dendrites dried up irrevocably. In the adult centers, the nerve paths are something fixed, ended, and immutable. Everything may die, nothing may be regenerated. It is for the science of the future to change, if possible, this harsh decree [30] ." This long-held idea, however, was shattered by the discovery and isolation of unique cells from the mammalian brain that possessed the capability to give rise to both neural and glial cells [31-33]. These unique cells established the concept of NSCs as the building blocks of the mammalian brain.

A hallmark of NSCs is their ability to produce exact copies of themselves [3] and also generate differentiated neurons and glia [3, 34-36]. NSCs accomplish this task of self-renewal and multipotency through two division mechanisms: symmetric and asymmetric divisions. By undergoing a symmetric division NSCs produce two daughter cells which are identical to the mother cell and maintain their undifferentiated state (**Fig.2.1A**). Symmetric division allows the NSCs to grow in number and expand the stem cell pool. Asymmetric division produces one daughter stem cell and one intermediate progenitor cell (IPC). The IPCs will, ultimately, generate a terminally differentiated neuron (nIPC), astrocyte (aIPC), or oligodendrocyte (oIPC; **Fig.2.1B**). [5, 37]. The balance between a symmetric and an asymmetric division must be tightly regulated because excessive symmetric division

may cause tumor formation whereas precocious asymmetric division results in premature differentiation and organ misdevelopment [38, 39].

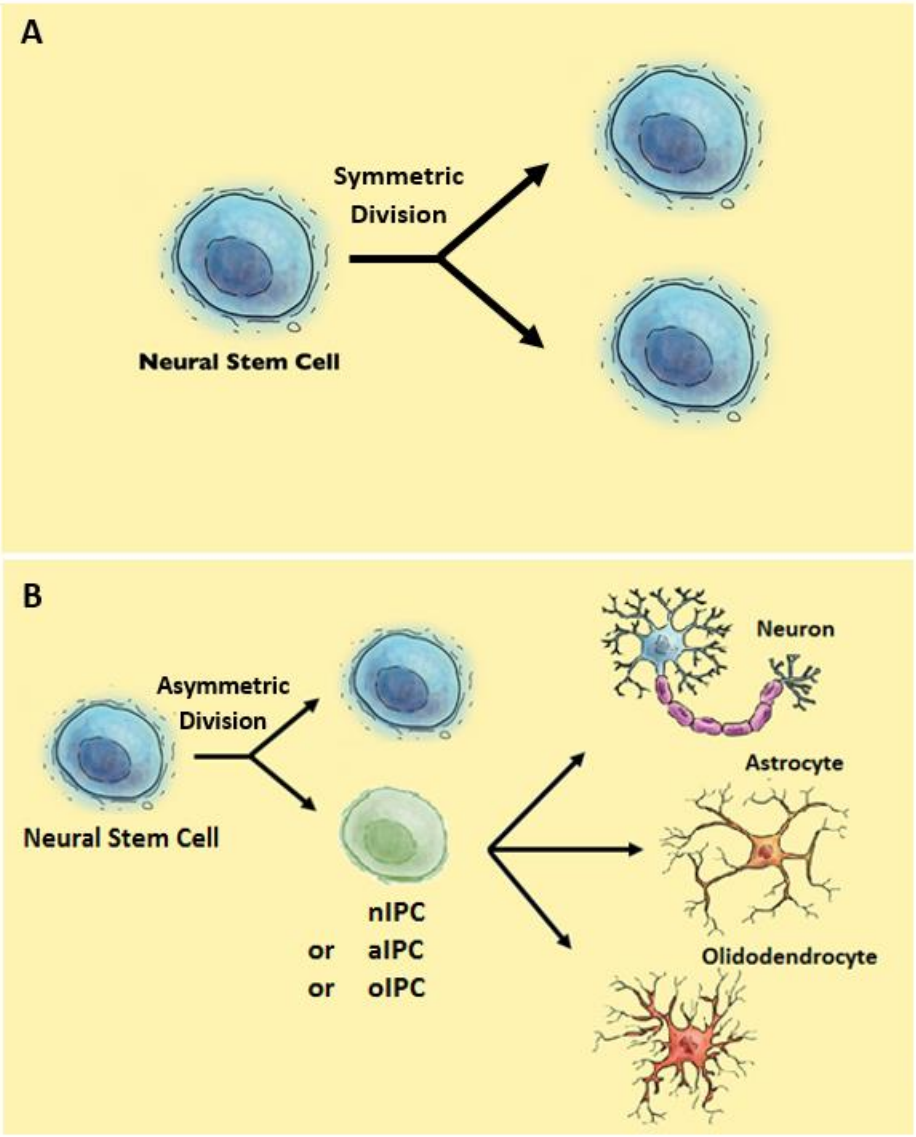

Figure 2.1. Neural stem cell symmetric and asymmetric division and the subsequent cellular output. NSCs can generate two identical copies of themselves by undergoing symmetric division. Therefore, the cellular output of a symmetric division is two undifferentiated stem cells (**A**). Asymmetric division produces an undifferentiated NSC and a neuronal (nIPC), astrocytic (aIPC), or oligodendrocyte (oIPC) intermediate progenitor cell.

The nIPCs, aIPCs, and oIPCs will, eventually, generate terminally differentiated neurons, astrocytes, or oligodendrocytes (**B**). Reproduced from [40].

Neural stem cells reside in a highly specialized microenvironment in the brain known as the neural stem cell niche [35, 41, 42]. There are two NSC niche locations in the mammalian brain: the subventricular zone (SVZ) of the lateral ventricle and the subgranualar zone (SGZ) of the hippocampal dentate gyrus (**Fig.2.2**) [3, 43].

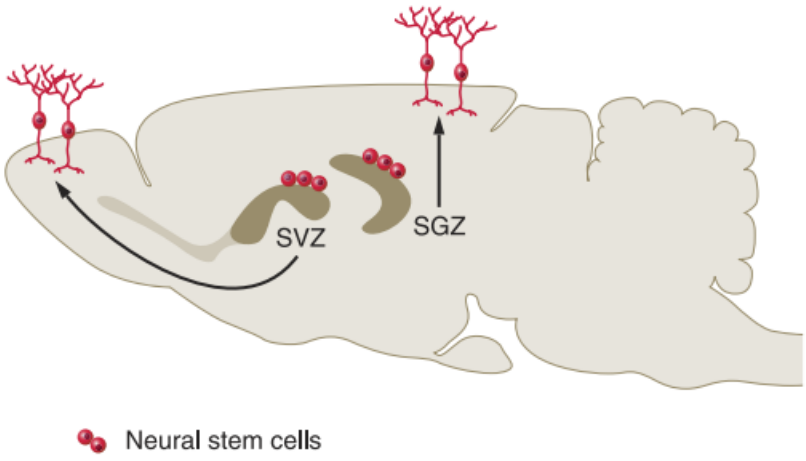

Figure 2.2. The schematic representation of NSC niche locations in the mammalian brain. The subventricular zone (SVZ) and the subgranular zone (SGZ) are the two germinal niches in the adult mammalian brain that retain NSCs and regulate their proliferation and differentiation behavior. Adapted from [44].

The NSC niche exerts tight regulation on key aspects of NSC behavior such as survival, proliferation, and terminal differentiation [45]. Interactions of NSCs with the ECM and neighboring cells as well as the presence of biochemical cues such as growth factors (GFs) and environmental cues such as oxygen are some of the important niche components that regulate the NSC behavior (**Fig.2.3**) [46]. This tight

regulation maintains the balance between the generation of terminally differentiated neurons and glia without depletion of the NSC pool and sustains the brain tissue homeostasis.

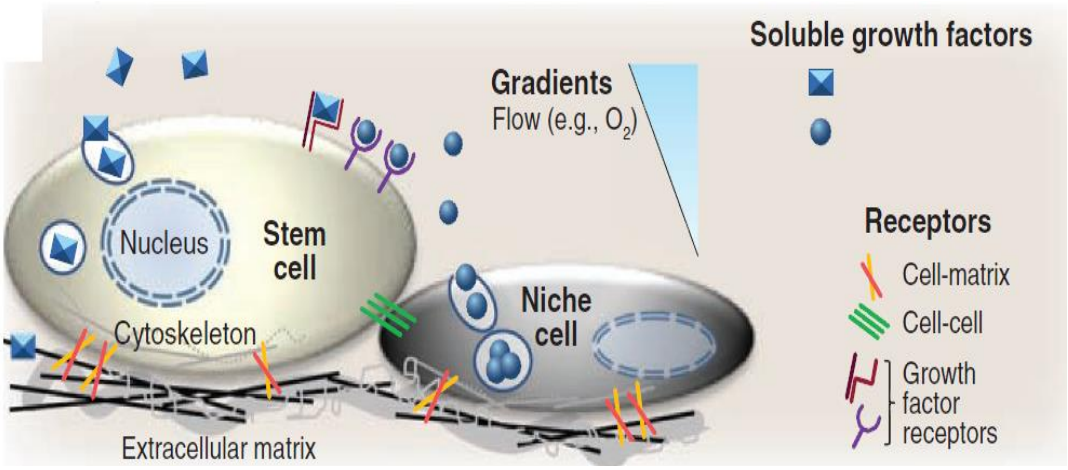

Figure 2.3. The parameters that regulate stem cell behavior in the niche. NSC niche provides a specialized microenvironment for cells in which cell-ECM and cell-cell interactions as well as environmental and biochemical factors regulate the proliferation and differentiation behavior of the NSCs. Adapted from [47].

The discovery of neurogenesis (generation of new-born neurons) from self-renewing multipotent NSCs in the adult human brain [33] created a momentum for performing stem cell transplantation studies on animal and human subjects and yielded promising outcomes [48]. However, it should be noted that the development of NSC-based therapies for neurological diseases is still at its infancy. It is projected that effective cell-replacement therapies will be achieved within the next 20 years [49].

Preclinical Trials of NSC Transplantation

Preclinical studies of NSC transplantation performed on animal disease models have provided promising results [2]. For instance, human NSCs transplanted in a rat model of stroke migrated to the site of lesion, differentiated into neurons [50, 51], and resulted in behavioral recovery [7, 52, 53]. Similarly, transplanted human NSCs into rat [54, 55] and primate [56, 57] models of PD exhibited neuronal differentiation and resulted in enhanced functional recovery. Amelioration of learning and memory deficits in AD-induced rats was also observed as a result of human NSC implantation [58]. These preclinical studies provide a proof of principle that partial reconstruction of the damaged brain tissue via transplantation of NSCs is possible.

Clinical Trials of NSC Transplantation and the Associated Challenges

NSC clinical trials were initiated in 1987 by implanting human fetal NSCs in patients with PD and continued until the late 1990s [4]. These clinical trials resulted in heterogeneous outcomes with major improvement in some cases and modest to no clinical benefits in the others [59-62]. Furthermore, 7-15% of the patients experienced graft-induced dyskinesia (involuntary movement) as a side effect of implantation. The occurrence of dyskinesia was proposed to be the result of excessive outgrowth of the transplanted grafts and a subsequent imbalance in dopamine secretion [63, 64].

The cellular output of NSC cultures can encompass undifferentiated NSCs, IPCs, terminally differentiated neurons and glia, and dead cells which constitute a heterogeneous population of different cell types [65, 66]. This heterogeneity in cell type is directly influenced by the cell preparation protocols. It is proposed that utilization of non-standardized *in vitro* culture methods may have resulted in

generation of transplants with differing cellular compositions, thus, yielding variable clinical outcomes [67]. I hypothesized that the key to acquire well-defined NSC cultures is to characterize both individual and synergistic effects of important environmental and biochemical cues on NSC fate. In this work, I characterized the individual and synergistic effects of culture dimensionality, oxygen concentration, and GFs on the survival, proliferation, and differentiation behavior of NSCs.

Parameters that Influence NSC Temporal Output

Two Dimensional (2D) vs Three Dimensional (3D) Cultures

NSCs have been conventionally cultured on flat surfaces, such as glass coverslips and polystyrene multiwell plates, referred to as two dimensional (2D) culture systems. Thus far, significant advancements in delineating the NSC self-renewal and multilineage differentiation have been achieved by utilizing 2D culture methods [68-71]. However, *in* vivo, NSCs reside in a local niche which has a three dimensional (3D) cytoarchitecture [3] and, now, it is widely recognized that 3D *in vitro* cultures generally mimic the *in vivo* environment more closely than 2D platforms. This is, in particular, due to differences in cell-ECM and cell-cell interactions between 2D and 3D culture methods as well as the presence of gradients of GFs and oxygen [72]. For instance, in 2D cultures, cells are confined to a flat x-y plane and only a segment of the cells can interact with the ECM. The rest of the cell surface is exposed to nutrients and soluble cues that are homogenously distributed in the bulk culture medium. However, *in vivo*, the binding of cells to the ECM occurs in a 3D x-y-z space and in the presence of spatial gradients of nutrients and biochemical

cues [73]. Therefore, cells cultured on 2D surfaces experience an unnatural inherent polarization that affect various cellular behaviors such as growth and differentiation (**Fig.2.4**) [74].

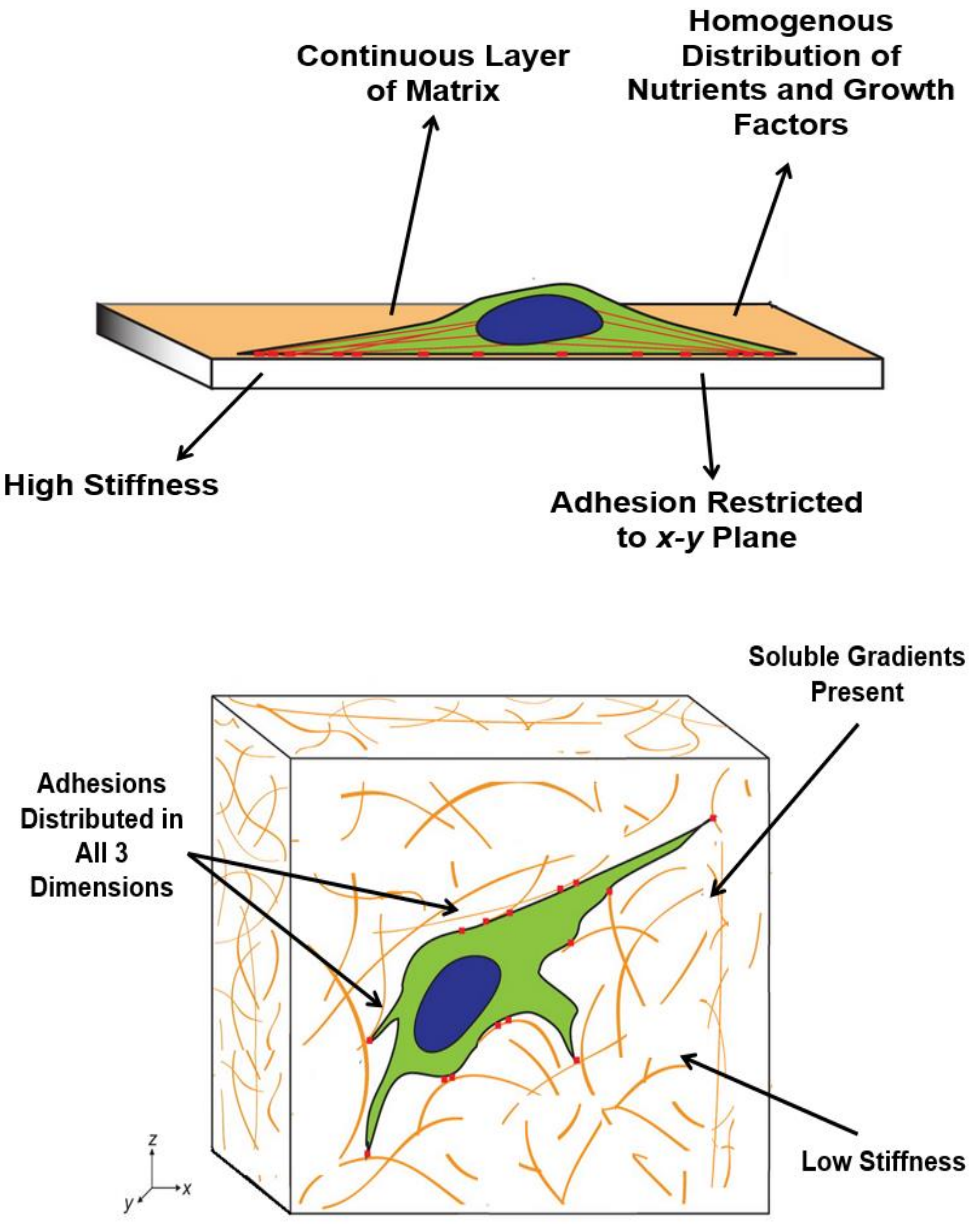

Figure 2.4. Major difference between 2D and 3D culture platforms. Cells experience a strikingly different microenvironment when cultured on an ECM-coated 2D plastic or glass surface compared to a 3D hydrogel constructed with an ECM protein such as collagen. Reproduced from [73].

Hydrogels have, in recent years, emerged as promising biomaterials to be utilized as 3D culture platforms [75]. Hydrogels are cross-linked networks of polymeric chains with the capability to incorporate high water contents. They exhibit high permeability for nutrients and soluble cues, can be formed under cytocompatible conditions as well as resemble the architecture and mechanics of the native *in vivo* microenvironments [76]. Previously published studies, on other cell types such as fibroblasts, indicate that the morphology of cells cultured within 3D collagen hydrogels mimicked the *in vivo* phenotype (bipolar morphology) more closely [77] when compared to the cells cultured on 2D substrates that exhibited a flat shape [78]. Moreover, primary hepatocytes (liver cells) encapsulated within collagen hydrogels exhibited higher viability and liver-specific metabolic functions whereas the cells cultured on 2D surfaces lost viability and metabolic functions after a few days post-isolation [79]. Additionally, our lab has also shown that 3D hydrogels uniquely allow neuronal cells to undergo intrinsic cellular programs akin to those observed *in vivo* (e.g. morphological development) [80, 81].

Stem cells, such as mesenchymal stem cell, encapsulated within 3D collagen hydrogels exhibited enhanced viability and accelerated the healing of mice skin wounds [82]. Furthermore, enhanced proliferation of human embryonic stem cells cultured within 3D agarose hydrogels [83] and increased neuronal differentiation of rat NSCs encapsulated within alginate hydrogels [84] have been reported. I concluded from these findings that culture dimensionality exerts regulatory influences on stem cell growth and differentiation behavior which consequently affects the cellular composition of the culture. Therefore, I sought to clarify the effect of dimensionality

on human NSC cellular composition. To accomplish this, I investigated the survival, proliferation, and differentiation behavior of human NSCs by culturing them in 3D collagen-laminin hydrogels and comparing the results with cells cultured on 2D laminin-coated surfaces.

Normoxic vs Hypoxic Cultures

In 1774, Joseph Priestly demonstrated the importance of oxygen for animal life by placing a mouse alongside a burning candle in a bell jar. The consumption of oxygen by the burning candle caused detrimental effects on the rodent and highlighted the significance of oxygen availability for survival [85]. Oxygen plays a crucial role in the oxidative metabolism of aerobic organisms and significantly influences the signal transduction pathways that control cell survival, proliferation, and phenotypic fate [15, 86]. The concentration of O_2 in the ambient air is 21% (160 mmHg) which is referred to as normoxia. However, even though O_2 concentrations inside the body vary by organ, they are substantially lower than the atmospheric O_2 level (21%) [87]. The partial pressure of the inhaled oxygen (pO_2) continuously decreases as it travels in the blood throughout the body and reduces to 2%-9% (14-65 mmHg) when it reaches various tissues [15]. Therefore, inside the body, tissues experience lowered or hypoxic O_2 concentrations.

The rodent and human brains are hypoxic microenvironments. For instance, in adult rodents, the oxygen concentration in the cortical gray matter is between 2.5% to 5.3% (**Table 2.2**) [88]. Similarly, measurements in the adult human brain depict an O_2 concertation varying from 3% to 4% [12]. Additionally, the mammalian

embryonic development is known to occur at hypoxic O_2 levels (3% O_2) [89, 90]. Therefore, it is conceivable that NSCs experience a hypoxic environment both during development and in the adult brain. However, NSCs have been conventionally cultured under atmospheric oxygen concentration (normoxia) and it has been shown that hypoxia plays an important regulatory role in both NSC proliferation and differentiation [87]. For instance, hypoxia enhances the proliferation of mouse [91], rat [92], and human [93] NSCs. Additionally, previously published studies indicate the positive effect of hypoxic cultures on the neuronal differentiation of rat and human NSCs [92, 93]. Since hypoxia affects proliferation as well as differentiation of the cells, I hypothesized that it may influence the NSC cellular output over time. To test this hypothesis, I cultured human NSCs under both hypoxic (3% O_2) and normoxic conditions in both 2D and 3D platforms to assess the effect of oxygen concentration and the synergistic effect of oxygen-dimensionality on the survival, growth, and differentiation of NSC.

Table 2.2. Regional rat brain tissue partial pressures of oxygen.

Brain Area	Oxygen (%)
Cortex (gray)	2.5-5.3
Cortex (white)	0.8-2.1
Hypothalamus	1.4-2.1
Hippocampus	2.6-3.9
Midbrain	0.55-1

Adapted from [88]

Effect of Growth Factors on Neural Stem Cells

The long-term *in vitro* propagation of NSCs requires continuous supplementation with fibroblast growth factor-2 (FGF2) and epidermal growth factor (EGF) [70]. FGF2 and EGF are proliferative factors and have been shown to be critical for the proliferation of mice [31, 94-96], rat [97, 98], and human [70, 99, 100] NSCs. In the presence of FGF2 and EGF, NSCs maintain their undifferentiated state and undergo continuous proliferation [3]. However, the withdrawal of these growth factors, from NSC culture, induces differentiation of the NSCs towards neurons and glia (**Fig.2.5**) [101].

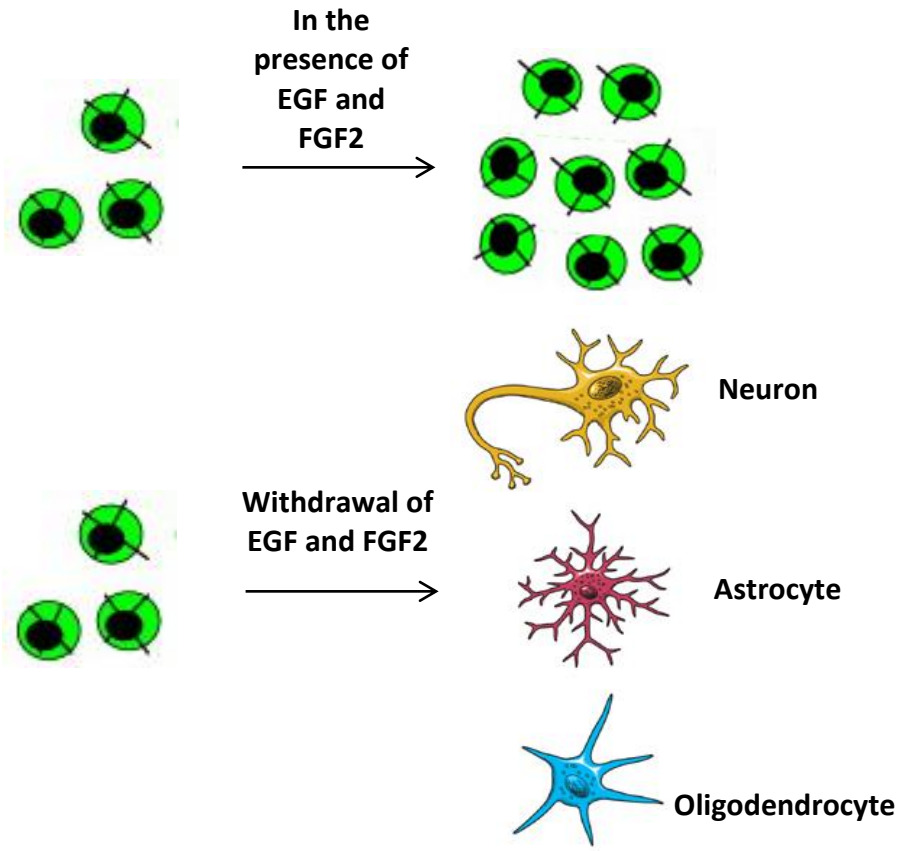

Figure 2.5. The effect of EGF and FGF2 on NSCs. NSCs *in vitro* cultures upon the addition of EGF and FGF2 continuously generate undifferentiated stem cells and expand in number. Upon the withdrawal of EGF and FGF2, NSCs begin to differentiate and will eventually generate terminally differentiated neurons and glia.

The discovery of FGF-2 dates back to 1974 when Holley and Kiernan showed that a protein extracted from cow brain can stimulate the proliferation of fibroblast cells [102]. FGF2 is heparin-binding and belongs to the FGF family of growth factors that encompass 22 members [103]. FGF2 consists of at least 3 peptides and exists in multiple molecular weight isoforms and the isoform with the lowest molecular weight (18 kDa) is secreted [104]. In rodents, FGF2 is expressed in the developing brain as early as embryonic day 10 (E10; E0 is day of mating) and promotes the proliferation

of NSCs [105]. Previously published works indicate that the FGF2 gene is necessary for the maintenance of proliferating NSCs in the embryonic mouse brain [106]. The FGF2 knockout mice had a lower number of NSCs in the SVZ niche [107] which resulted in a decreased number of newly generated neurons and impaired cortical development[108]. FGF2 is believed to act mainly through the cell surface FGF-receptor-1 (FGFR1) [109].

EGF was first discovered by Stanley Cohen in 1962 from mouse salivary glands and shown to increase the epidermal cell proliferation [110]. EGF consists of a single polypeptide with 53 amino acids of which 6 are cysteine [111]. Past studies indicate that both *in vivo* and *in vitro* cultures of NSCs are responsive to the presence of EGF. For instance, the infusion of EGF into the adult mouse brain resulted in an enhanced proliferation of NSCs in the SVZ niche [112, 113]. Moreover, the embryonic mouse NSCs, *in vitro,* exhibited increased proliferation in a medium supplemented with EGF [95]. EGF exerts its proliferative activity by binding to EGF receptor (EGFR) [114]. The expression of EGFR in the embryonic rodent brain occurs as early as E11 [115] and the EGFR knock out mice have shown to exhibit impaired cortical brain development due to decreased NSC proliferation and consequently limited neuronal cell generation [116]. Based upon these findings which show the critical effect of FGF2 and EGF on NSC proliferation, I aimed to clarify the cellular composition of human NSC cultures in the presence and absence of FGF2 and EGF under both normoxic and hypoxic conditions as well as in 2D and 3D cultures.

Hypoxic Preconditioning of NSCs

One of the major factors that decreases the therapeutic efficacy of stem cell-mediated therapy is the extensive cell death that occurs post-transplantation which can be as many as 90% of the total implanted cells [8]. Therefore, there is a need to enhance the survival of the implanted cells to increase their therapeutic potential. *In vitro* exposure of stem cells to hypoxia (hypoxic preconditioning) prior to transplantation may provide a solution for this challenge. For instance, the exposure of rodent mesenchymal stem cells to hypoxic oxygen levels before transplantation into infarcted rat heart tissues resulted in enhanced survival of mesenchymal stem cells and improved cardiac function of rats [10]. In addition, hypoxic preconditioned mouse embryonic stem cells and mesenchymal stem cells after transplantation into ischemic rat brain exhibited enhanced survival, extensive neuronal differentiation, and accelerated the functional recovery of the animal subjects [11]. Promoting the survival and differentiation potential of human NSCs into neurons and glia plays a significant role in increasing their regenerative capacity. Yet, the effect of hypoxic preconditioning on human NSC survival and differentiation potential is unclear. Since NSCs reside within a hypoxic niche *in vivo*, I hypothesized that the *in vitro* exposure of these cells to a hypoxic condition may provide a pro-survival and a pro-differentiation environment. Therefore, I aimed to assess the survival and differentiation of human NSCs under both hypoxic (3% O_2) and normoxic conditions.

Limited Availability of NSCs

Translational potential of cell-replacement therapy is constrained because the amount of stem cells required for therapy highly exceeds the availability from donors

[13]. For instance, mesenchymal stem cells and hematopoietic stem cell clinical-applications need cell doses up to 9×10^6 and 2×10^5 (cells/kg body weight), respectively [117, 118]. Therefore, there is a need for cost-effective and scalable methods for the production of large quantities of stem cells *in vitro*. Hypoxia has been shown to enhance rodent and human NSC growth [92, 93]. Since oxygen is scalable, widely available, and presents no risk of pathogen transmission, manipulating the oxygen concentration in stem cell cultures provides a powerful tool to enhance the proliferation of NSCs. Additionally, one of the important factors that regulates cell proliferation is the interactions between the cells and the ECM [119]. The NSC niche in the brain is composed of various ECM proteins such as laminin, collagen I, collagen IV, and low levels of fibronectin [120]. The relationship between ECM type, oxygen concentration, and NSC proliferation is not well understood. I hypothesized that the synergistic effect of lowered oxygen concentration and substrate composition may enhance the growth of human NSCs. Therefore, I assessed the growth of human NSCs cultured on four purified ECM proteins (laminin, collagen I, collagen IV, and fibronectin) and a cell-adhesive matrix for NSCs which is a tissue-derived ECM (Matrigel).

Neural Stem Cells and the ECM

All cell types are in contact with the ECM. ECM is a complex network of macromolecules including proteins, proteoglycans, glycoproteins, and polysaccharides [121]. Even though it was long believed that the ECM is an inert supportive cellular scaffold, the increasing body of evidence in the last two decades

suggests an instructive role of the ECM on various cellular behaviors such as proliferation [122] and differentiation [123]. The physical properties of the ECM such as porosity, rigidity, insolubility, and topography support tissue structure and integrity and play an important role in cell migration by functioning as a barrier, anchorage-site, or a movement track [124]. From a biochemical point of view, the ECM greatly influences cellular processes such as survival and proliferation by binding to biochemical cues such as growth factors and regulating their bioavailability [125]. For instance, the ECM in NSC niche binds FGF-2 via heparan sulfate proteoglycans, protects FGF-2 from enzymatic degradation, establishes a localized reservoir of FGF-2, and influences NSC proliferation by promoting FGF-2 signaling [126, 127].

Moreover, ECM instructs stem cells by binding to cell-surface receptors of which the major class are integrins [125]. Integrins are heterodimeric transmembrane receptors that consist of an α and a β subunit [128]. Due to their heterodimeric structures, integrins are capable of binding to a vast array of ECM proteins such as collagens, laminin, fibronectin, and vitronectin. The binding of the ECM to integrins activates downstream signaling cascades that can regulate various cellular behaviors such as survival and proliferation [129].

Laminin

Laminins are a family of cell adhesion molecules with a cruciform structure and a molecular weight between 500 to 1000 kDa [130]. *In vivo*, they are predominantly found in the basement membranes which are the thin sheets of ECM that underlie epithelial cells [131]. Laminin is one of the major components of the

brain basement membrane (basal lamina) and plays a key role in regulating NSC proliferation and differentiation behavior [132]. For instance, laminin has been shown to promote the proliferation [133] and migration [134] of mouse NSCs as well as proliferation and differentiation of human NSCs[123]. The regulatory effects of laminin on NSCs is, to a significant extent, mediated by interactions with cell-surface receptors (integrins) [131]. NSCs have been shown to express high levels of $\alpha_6\beta_1$ integrin which binds to laminin [135]. Disruption of the integrin-laminin binding in embryonic mouse brain has been shown to result in abnormal NSC proliferation and impaired formation of neocortex [136].

Collagen I

Collagen I is a major component of the natural ECM accounting for %25-30 of the total protein in the human body [137]. Type I collagen is an attractive candidate to be utilized for tissue engineering applications due to its abundance in mammalian tissues and its biocompatibility [138, 139]. Collagen I is composed of three polypeptide chains that wrap around one another to form a three-stranded rope structure (i.e. triple α helices) [140]. Even though collagen I is not abundant in the central nervous system, it can be found in the SVZ niche [43]. *In vitro*, collagen I has been shown to promote neural cell attachment and neurite outgrowth[141]. Moreover, collagen I has been commonly utilized to construct 3D scaffolds to promote axon regeneration after spinal cord injury in rodents [142].

Fibronectin

Fibroenctins are high molecular weight (500 to 560 kDa) glycoproteins that mainly exist as insoluble proteins in the ECM and soluble molecules in plasma. Fibronectins consists of two similar but not necessarily identical monomoers [143]. Each monomer is composed of three protein domains known as type I, II, and III repeats that exhibit functionally distinctive properties. These domains may contain binding sites for the cell-surface integrins and other ECM molecules [144]. Interactions between fibronectin and cells occur through binding of arginine- glycine-aspartic acid (RGD)-containing protein domain to $\alpha_5\beta_1$ and $\alpha_v\beta_1$ integrins [145]. Fibronectin is expressed during early brain development and its expression declines at the approximate time that neurogenesis occurs at the superficial cortical layers [146]. Fibronectin has been shown to stimulate neurite outgrowth and support neuronal cell adhesion and survival [147].

Collagen IV

Collagen IV is a member of the collagen superfamily and unlike most collagens occurs only in the basement membranes [148]. Collagen IV comprises up to six distinct α-chains, α1 (IV) to α6 (IV), which assemble into three heterotrimers α1 α1 α2 (IV), α3 α4 α5 (IV), and α5 α5 α6 (IV) [148]. *In vitro,* collagen IV has been shown to promote the neuronal differentiation of embryonic rat NSCs [149]and support the neurite outgrowth of embryonic mouse neuronal cells [150]. The interactions between collagen IV and NSCs is mediated via $\alpha_1\beta_1$ and $\alpha_2\beta_1$ class of integrins [151]. Even though the presence of collagen IV *in vivo* is sparse [152] it is

expressed as early as E11 in rodent brains and is hypothesized to play a potential role in early neuronal differentiation [153].

Matrigel

Matrigel is a gelatinous soluble assortment of several ECM proteins extracted from Engelbreth-Holm-Swarm mouse tumors [154]. Matrigel is composed of laminin (a major component), collagen IV, heparan sulfate proteoglycans, entactin, and several growth factors such as EGF, FGF, and transforming growth factor-β (TGF-β) [155]. Since Matrigel contains the main protein components of the basement membrane, it provides a supportive substrate for stem cell attachment, proliferation, and differentiation [156]. For instance, Matrigel has been shown to promote the proliferation of human embryonic stem cells [135] and NSCs [123]. Additionally, enhanced survival and neuronal differentiation of mouse and human embryonic stem cells cultured on Matrigel has been reported [157, 158].

Summary of the Contributions to the Field

The present dissertation focused on the study of human NSC response to 3D microenvironments, hypoxia, growth factors, and various ECM protein substrates.

The major contributions of this work are:

- The characterization of human NSC temporal output with respect to culture dimensionality, oxygen concentration, and mitogenic factors as a requirement for generation of NSC transplants with well-defined cellular compositions.

- The identification of hypoxic preconditioning as an effective method to enhance the survival of human NSCs and stimulate their transition into terminally differentiated progenies.
- The delineation of the synergistic effect of hypoxia and laminin-rich substrates (Matrigel and laminin) on enhancement of human NSC growth.

The current understanding of human NSC interactions with the important components of their *in vivo* niche was advanced in this dissertation. In **Chapter 3**, I studied the regulatory role of culture dimensionality, oxygen concentration, and growth factors on human NSC survival, proliferation, and differentiation and clarified their independent as well as synergistic effects on human NSC cellular composition. These findings have significance in the development of stem cell transplants with well-defined cellular compositions. This work is submitted to Biotechnology and Bioengineering Journal. In **Chapter 4**, I studied the effect of *in vitro* hypoxic preconditioning on human NSC survival and differentiation capacity. This study clarifies the effect of hypoxia on human NSC differentiation and introduces *in vitro* hypoxic preconditioning as a safe and effective method to enhance the differentiation of stem cells towards neuronal progenies without decreasing their survival. This work is in preparation for submission to Stem Cell Reports Journal. In **Chapter 5**, I studied the role of cell-ECM interaction and hypoxia on human NSC growth. My findings suggest a synergistic relationship between laminin-rich substrates and hypoxia that stimulates the stem cell *in vitro* expansion. These findings have significance in the development of new biomaterial substrates with the capability of maintaining high levels of proliferation. This work is published in Journal of Materials Chemistry B.

Chapter 3: Characterizing the Effect of Culture Dimensionality, Oxygen Concentration, and Growth Factors on Human Neural Stem Cell Survival, Proliferation, and Differentiation

Introduction

Neurodegenerative diseases such as Parkinson's disease (PD), Alzheimer's disease (AD), and stroke result in the loss of neurons and glia, leading to sensory, motor, and cognitive impairments [1]. The human brain, due to its structural complexity and low cell turnover, has a limited capacity for self-repair. Currently available therapies provide modest relief of disease symptoms, but they cannot compensate for the cell degeneration and consequently none are able to halt or reverse the disease progression [2]. Neural stem cell (NSC) transplantation is a cell-mediated, disease-modifying therapy with a promising potential to restore the neurological deficits.

NSCs possess two cardinal characteristics: the ability to renew themselves through mitotic division (self-renewal) and the capability to transition into other cell types (multipotency), such as intermediate progenitor cells (IPCs). NSCs and IPCs have the potential to differentiate into terminally differentiated (TD) neurons, astrocytes, and oligodendrocytes [3, 35, 159]. Thus, they present a renewable source of promising therapeutic candidate. Preclinical studies of NSC transplantation in animal models of stroke [52, 53, 160], PD [54-57], and AD [58] have shown enhanced behavioral recovery.

However, several clinical trials of transplantation of human embryonic mesencephalic tissue in patients with PD exhibited major improvements in some cases and modest to no benefits in the others [59-62]. It is proposed that the lack of standardized protocols for cell preparation play a major role in causing variable

clinical benefits [161]. NSCs are plastic in nature [65, 66], and depending upon the preparation method, can result in substantial cell type heterogeneity. Without standardized protocols, the cellular composition of the transplants derived from *in vitro* cultures may differ significantly, yielding variable clinical outcomes. Therefore, there is a need for designing standardized protocols to obtain human neural stem cells (hNSCs) with well-defined temporal and biochemical parameters.

In this work, the effects of growth factors (GFs), oxygen concentration, and culture dimensionality were evaluated with respect to three key characteristics of hNSC *in vitro* culture: survival, renewal-potential, and terminal differentiation. Furthermore, we present kinetic models to generate predictions for the rate of hNSC growth (renewal-potential) and terminal differentiation. We aim to clarify whether the interplay among key environmental cues can individually or synergistically regulate the renewal-potential and terminal differentiation of hNSCs. Moreover, we test whether a mathematical kinetic model of hNSC growth and terminal differentiation can further our ability to generate hNSC cultures with well-defined cellular composition.

Materials and Methods

All materials were procured from Sigma Aldrich (St. Louis, MO), Millipore (Billerica, MA) or Thermo Fisher Scientific (Waltham, MA*)* unless otherwise noted.

Human neural stem cell (hNSC) maintenance and culture

RenCell-CX, an immortalized cell line derived from 14-week gestation human fetal cerebral cortex was purchased from Millipore (Billerica, MA) and was used as a

model hNSC in these experiments. The cells were cultured on laminin-coated (1.33 μg/cm^2) flasks and maintained in serum-free complete growth medium (DMEM: F12 supplemented with 1x B27 supplement, heparin (10 U/ml), L-glutamine (2 mM), gentamicin (30 μg/ml), epidermal growth factor (EGF, 20 ng/ml), and fibroblast growth factor-2 (FGF2, 20 ng/ml). The cells were passaged every 3 to 4 days using Accutase^{TM} and plated in freshly laminin-coated flasks at a density of ~7×10^3 cell/cm^2. All experiments were carried out using cells between passages 9 to 15.

The hNSCs were seeded at a density of 3×10^4 cells/cm^2 onto laminin-coated 96-well tissue culture plates for 1, 2, 4 and 10 d and the medium was changed every 2 d. Complete growth medium with growth factors (GF$^+$) was utilized to assess the growth kinetics of hNSCs. To induce differentiation, complete medium without growth factors (GF$^-$) was used. For 3D experiments, the hNSCs were seeded at a density of 6×10^5 cells/ml within 3D laminin-incorporated collagen hydrogels (2 mg/ml collagen, 100 μg/ml laminin, 25 μl gels) and then cultured for 1, 2, 4 and 10 d, with medium changes every 2 d.

For 3D hydrogels, cell encapsulation and staining methods were adapted from [80, 81] and used rat-tail type I collagen from Corning (Corning, NY). Ice cold 10x DMEM, 7.5% sodium bicarbonate, sterile deionized water, collagen, laminin, and growth factors (for the growth kinetic experiments) were combined with hNSCs to generate 3D substrates. The hydrogel solution (containing cells) was placed in a culture incubator for 30 to 45 min to allow for gelation and then the culture medium was added.

Both 2D and 3D normoxic cultures were carried out in a humidified, 5% CO_2, 37°C incubator. The hypoxic cultures were carried out in a portable, humidified, and isolated hypoxic chamber (COY Laboratory, Grass Lake, MI) with 3% O_2, 5% CO_2 and 92% N_2. The hypoxic chamber was housed in a 37°C incubator. The concentration of oxygen in air was measured using O_2-sensitive electrode system (Dwyer Instruments, Michigan City, IN).

Viability study

The hNSC viability was measured using mammalian cell LIVE/DEAD viability assay (Thermo Fisher Scientific). After 4 and 10 d, the culture medium was aspirated and the samples were incubated with a solution of calcein-AM (live cell marker, 2 μM) and ethidium homodimer-1 (dead cell marker, 4 μM) in Tris-buffered saline (TBS) for 30 min (2D) and 60 min (3D) cultures. The samples were immediately imaged under fluorescent microscopy (Olympus, Center Valley, PA) and the numbers of calcein-AM^+ and ethidium homodimer-1^+ cells were counted.

Proliferation study

To detect hNSC proliferation during culture, the Click-iT EdU proliferation assay (Thermo Fisher Scientific) was performed. The hNSCs were incubated with EdU for 4 and 10 d with EdU being replenished every 2 d to prevent depletion. The cells were then fixed in 4% buffered formaldehyde for 20 min, permeabilized with TBS containing 0.1% Triton-X-100, and incubated with EdU reaction cocktail for 30 min (2D) and overnight (3D) followed by 4',6-diamidino-2-phenylindole (DAPI, 300

nM) nuclear stain. The samples were then imaged under fluorescent microscopy to measure the number of cells that proliferated during EdU incubation. The nuclei of EdU^+ cells fluoresced green because of Alexa Fluor 488 azide fluorescent dye detection. DAPI (blue) stains all nuclei. The numbers of EdU^+ and $DAPI^+$ cells were counted.

Immunofluorescence study

Samples after 10 d were fixed, permeabilized, and incubated with 10% goat serum in phosphate-buffered saline (PBS) for 30 min (2D) and 2 h (3D) in room temperature. The hNSCs were incubated with primary antibodies SOX-2 (1:1000, Millipore), nestin (1:2000, Millipore), GFAP (1:1000, Abcam, Cambridge, MA), and TUJ-1 (1:2000, Covance, Princeton, NJ) overnight, followed by fluorescently-conjugated secondary antibodies (Abcam) for 2 h (2D) and overnight (3D). The incubation of both primary and secondary antibodies was performed at 4°C. The samples were then stained with DAPI and imaged using fluorescent microscopy. Methods to perform the immunofluorescence procedure including washing steps, permeabilization, and antibody incubation were adapted from [80, 81].

Statistical Analysis

Experimental results are represented as mean ± SD ($n \geq 3$). Analysis of variance (ANOVA) tests were performed to determine statistical significance. The results derived from non-linear regression fitting are included only if the correlation coefficient $R^2 > 0.95$. The rate constants acquired from non-linear regression analysis

are presented without standard deviation. Model errors are expressed as confidence intervals in **Table 3.1**.

Model Description

The temporal output of NSC culture can be distributed into three cellular populations: daughter NSCs which are identical to the mother cell, multipotent IPCs, and TD neurons and glia. The daughter NSCs can either self-renew to populate the stem cell pool, or transition into IPCs, or terminally differentiate into mature neurons and glia. The IPCs are transient cells that will eventually generate mature neurons, astrocytes, and oligodendrocytes (**Fig.3.1**). Due to transient nature of IPCs, we assumed that the eventual composition of the NSC culture will consist of undifferentiated NSCs and TD neural and glial progenies, as well as dead cells. It is important to note that the final cellular composition of the NSC culture is dependent upon the culture conditions, in particular, the presence of mitogenic factors (GFs). Mathematical models should be able to predict the growth rate of NSCs (renewal-potential) as well as encompass the generation rate of fully differentiated progenies.

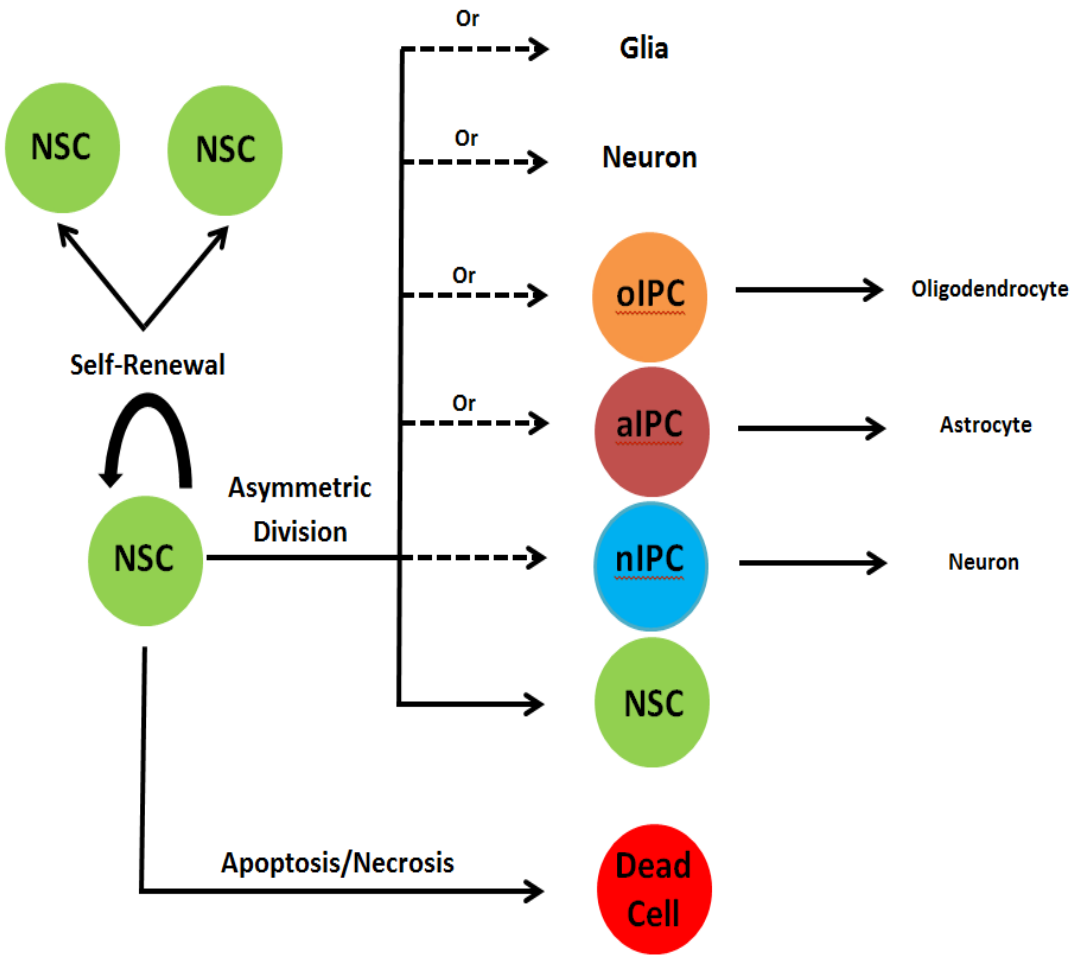

Figure 3.1. The predicted scenarios for NSC temporal output. NSCs, depending upon the culture conditions, can either self-renew in order to maintain their renewal-potential or differentiate into both postmitotic and intermediate progenitor neural and glial cells. Both self-renewal and differentiation processes can be associated with cell death. The heterogeneity of NSC culture stems from co-existence of postmitotic neurons and glia, IPCs, and undifferentiated NSCs. Mathematical models should be tailored to temporally predict the growth/decay rate of NSCs as well the rate of terminal differentiation into neural and glial progenies.

In this paper, we have defined two general culture conditions: self-renewal conditions (for cultures in the presence of growth factors) and differentiation conditions (for cultures in the absence of growth factors).

Self-renewal conditions

The established culture techniques require specific growth factors for the NSCs to undergo continuous proliferation and renewal [3]. A simple ordinary differential equation (ODE) for describing this continuous growth is:

$$\frac{dN_{Stem}}{dt} = AN_{Stem}(t) \quad (1)$$

In **Equation 1**, N_{Stem}, denotes the number of stem cells. A, with the unit $(\frac{1}{h})$, is the growth constant and consists of three sub-terms: the self-renewal constant $A_{Self\text{-}renewal}$, the differentiation constant $A_{Differentiation}$, and the cell death constant A_{Death}. The unit of all three sub-terms is $(\frac{1}{h})$ and they are all positive real numbers (i.e., $A_{Self\text{-}renewal}$, $A_{Differentiation}$, and $A_{Death}>0$). The mathematical formula for A is:

$$A = A_{Self\text{-}renewal} - A_{Differentiation} - A_{Death} \quad (2)$$

The self-renewing NSCs populate the stem cell pool. The differentiation process, on the other hand, derives IPCs and fully differentiated neural and glial progenies from stem cells and therefore decreases the number of NSCs. Similarly, cell death decreases NSC numbers. **Equation 1** has a solution of the form:

$$N_{Stem}(t) = n_0 \times e^{At} \quad (3)$$

which (if A > 0) describes an exponential increase in the NSC number.

In this model, time is the only contributing factor to the cell growth and more time translates to exponentially more cells. This unhindered exponential growth is biologically unrealistic even for tumorigenic cells due to restraints on nutrients and tissue-size [162, 163]. NSC proliferation *in vivo* is tightly regulated until a target niche-size is achieved and then is maintained at equilibrium [164, 165]. For instance, the proliferation of stem cells in the vertebrate nervous system (i.e., mouse neocortex) gradually decelerates and eventually ceases toward the end of embryonic development, due to two mechanisms: decreased fraction of mitotic daughter cells (NSCs) and increased cell cycle length [166]. Therefore, we hypothesize that a regulating feedback mechanism is required to maintain the rate of NSC growth within a certain limit. Here, a possible feedback mechanism is suggested [167] that has the ability to account for limitations on cell growth and represent a more relevant prediction of NSC expansion.

The following ODE denotes the NSC growth in a feedback-regulated system:

$$\frac{dN_{Stem}}{dt} = AN_{Stem}(t) - k \times {N_{Stem}}^2(t) \qquad (4)$$

The term $k \times N^2_{Stem}$ ($k > 0$) is the incorporated negative feedback and k ($\frac{1}{\text{cell number} \times \text{h}}$) is the feedback constant. The number of stem cells is defined by N_{Stem} (t) and the term A ($\frac{1}{\text{h}}$) is described by **Equation 2**. Cell-cell interactions play a crucial role in regulating the proliferation of NSCs. These interactions can take place either through cellular homeostatic pathways [168] or secretion of neurotransmitters [169, 170]. The number of interactions between N cells in a homogenously mixed population with

random encounters is equal to N×N or N^2 interactions. Consequently, we concluded that the magnitude of the regulatory feedback term should be proportional to the number of cells squared (hence $k \times N^2_{Stem}$).

Equation 4 has a solution of the form:

$$N_{Stem}(t) = \frac{A}{k + (A/n_0 - k) \times e^{-A \times t}} \qquad (5)$$

If $A_{Self\text{-}renewal}$ is larger than the sum of $A_{Differentiation}$ and A_{Death} (i.e., $A_{Self\text{-}renewal} > A_{Differentiation} + A_{Death}$) the term A will have a positive numerical value ($A > 0$). Consequently, NSCs will expand in number and the rate of their expansion is regulated by the incorporated feedback term. If $t \rightarrow \infty$ then $N_{Stem}(t) = \frac{A}{k}$. The term $\frac{A}{k}$ is the carrying capacity (CC) or the upper limit of NSC growth. In other words, the number of NSCs, in a feedback regulated system, will always be between the initial cell numbers and the carrying capacity (i.e., $n_0 < N_{Stem}(t) < \frac{A}{k}$). The constants A and k were determined by performing non-linear regression analysis of experimental data using the Minitab (State College, PA) non-linear regression module.

Differentiation conditions

The removal of growth factors from the NSC culture is associated with cell death or differentiation into IPCs and postmitotic cell types and consequently a decrease in NSC number. Thus, in the absence of growth factors, the NSC culture becomes a heterogeneous population of cells consisting of undifferentiated NSCs, IPCs, TD cell types, and dead cells (**Fig.3.1**). Because IPCs are transient cells, we assumed the hNSC culture will eventually consist of undifferentiated NSCs,

postmitotic neural and glial cell types and dead cells. Here, we suggest a mathematical model capable of encompassing the rate of NSC decay and terminal differentiation. The model includes three ODEs:

$$\frac{dN_{Stem}}{dt} = AN_{Stem}(t) \tag{6}$$

$$\frac{dN_{TD-Cells}}{dt} = A_{Differentiation}N_{Stem}(t) - d_{Death}N_{TD-Cells}(t) \tag{7}$$

$$N_{Total} = N_{Stem} + N_{TD-Cells} \tag{8}$$

Equation 6 describes the number of undifferentiated stem cells in the population. Since the growth factor removal is associated with reduction in stem cell numbers, we expect the numerical value of A to be less than zero ($A < 0$). The negative value for A indicates that the sum of $A_{Differentiation}$ and A_{Death} constants is larger than $A_{Self\text{-}renewal}$ (i.e., $A_{Self\text{-}renewal} < A_{Differentiation} + A_{Death}$). Due to temporal decrease in NSC numbers, designating a feedback mechanism to regulate the cell proliferation is unnecessary. We, instead, designed an independent ODE that describes the generation rate of TD cells from stem cells. **Equation 7** states that the number of TD cells, at any time, is dependent upon the number NSCs that undergo differentiation and TD cell death. Overall, the total number of cells in culture will be equal to undifferentiated NSC number plus the number of TD cells derived from stem cells (**Equation 8**). The mathematical terms for either NSC or TD cell death are incorporated in **Equation 6 and Equation 7** respectively (A_{Death} and d_{Death}). The analytical solutions of the **Equations 6-8** are as follows:

$$N_{Stem}(t) = n_0 \times e^{At} \quad (9)$$

$$N_{TD-Cells} = \left(\frac{A_{Differentiation} n_0}{A + d_{Death}}\right)\left[e^{At} - e^{-d_{Death}t}\right] \quad (10)$$

$$N_{Total} = N_{Stem} + N_{TD-Cells} = (n_0 \times e^{At}) + \left(\frac{A_{Differentiation} n_0}{A + d_{Death}}\right)\left[e^{At} - e^{-d_{Death}t}\right] \quad (11)$$

By performing non-linear regression analysis on **Equation 11** we determined the numerical values of A, $A_{Differentiation}$, and d_{Death}, and in turn, the number of NSCs, TD cells, and dead cells, and thus, the percentage of each cell type in the total population.

Results

Analysis of NSC growth rate in a 2D microenvironment in the presence of GFs for both normoxic and hypoxic conditions

Standard culture conditions for hNSCs include normal oxygen concentrations and supplementation with growth factors (FGF-2 and EGF). We tested the effect of growth factors and oxygen concentration on hNSC proliferation and differentiation rate by measuring the total number of hNSCs (**Fig.3.2A**). The main effects of both oxygen concentration and time yielded F-ratios of $F(1, 64) = 29.38$, $p < 0.001$ and $F(1, 64) = 94.54$, $p < 0.001$ respectively indicating significant effect of oxygen concentration and time on hNSC total number, and an interaction between time and oxygen concentration, $F(1, 64) = 4.59$, $p = 0.006$.

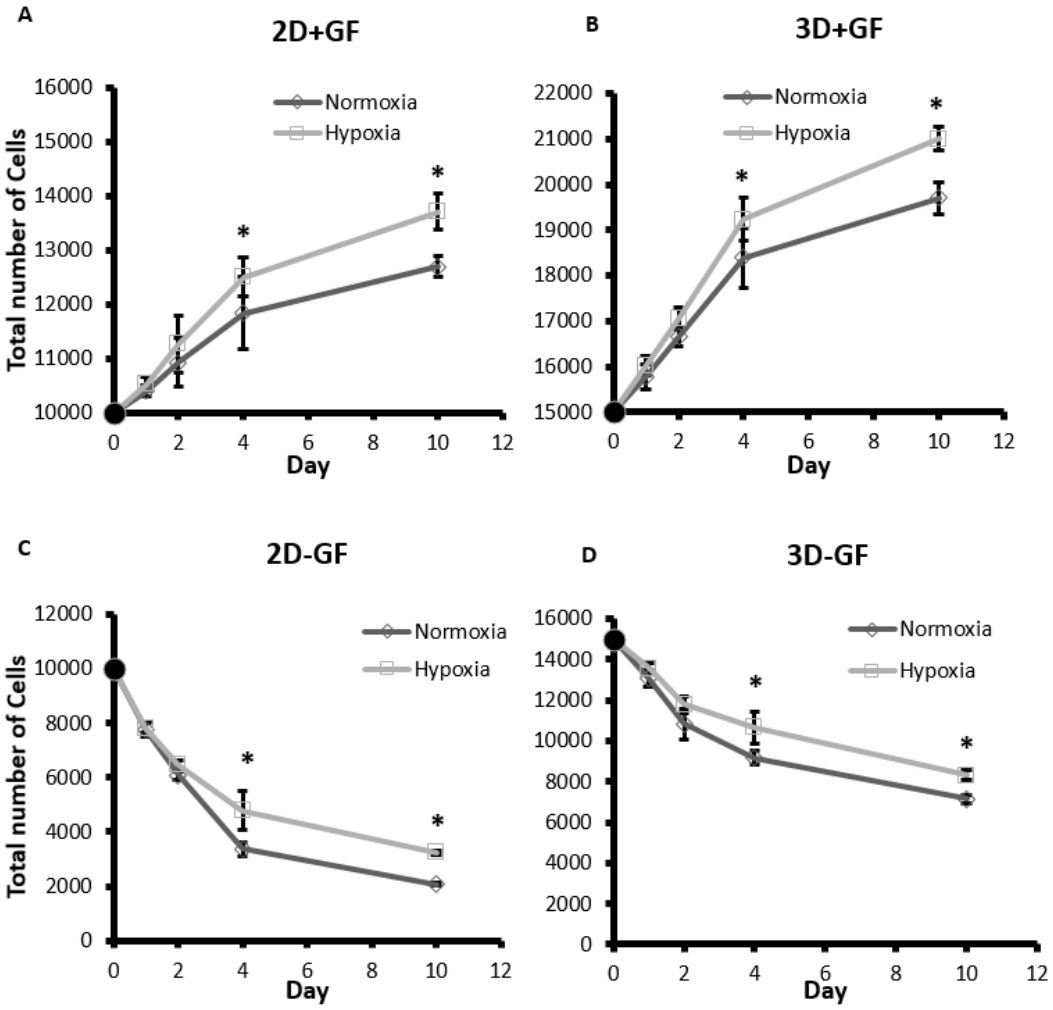

Figure 3.2. Number of total cells (DAPI+) at day 1, 2, 4 and 10 in 2D+GF, 2D-GF, 3D+GF, and 3D-GF cultures. After 4 and 10 d, in all of the experimental groups (**A, B, C, and D**), the total number of cells was significantly higher under hypoxia in comparison with normoxia. Symbol (*) denotes significant differences ($p < 0.001$) between normoxic and hypoxic groups. $n > 9$ samples; one representative set of experimental data is shown. $n > 50$ hNSCs/sample.

We investigated the cellular composition of the cultures by performing a viability assay and immunocytochemistry for cell-type specific biomarkers. After 10 d with GF, 94 ± 1% and 93 ± 1% of cells were viable (calcein^{+}) under normoxic and hypoxic conditions, respectively (**Fig.3.3A**). A two-way ANOVA analysis showed no statistical difference in hNSC viability between normoxia and hypoxia ($p = 0.65$) and no time-oxygen interaction ($p = 0.634$).

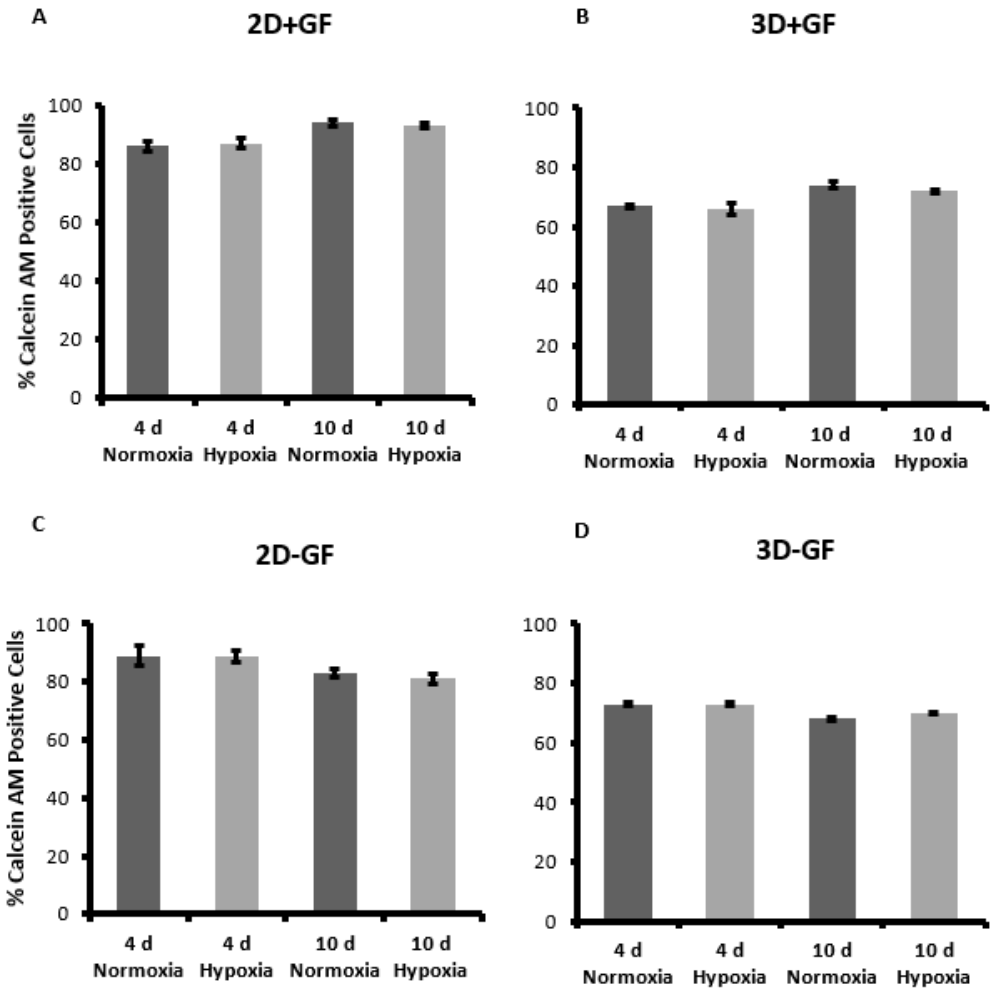

Figure 3. 3. The hNSC viability in 2D+GF, 2D-GF, 3D+GF, and 3D-GF cultures. In both 2D+GF (**A**) and 3D+GF (**B**) there was no significant effect of oxygen concentration on hNSC viability. Similarly, oxygen concentration did not show a significant effect on hNSC viability

in 2D-GF (**C**) and 3D-GF (**D**) groups. Bars represent mean ± SD. n > 9 independent experiments; n >50 NSCs/sample.

The molecular markers nestin and SOX-2 were utilized to detect the hNSCs that maintained their stemness. In both normoxic and hypoxic cultures, the majority of cells were both nestin and SOX-2 positive (**Fig.3.4A-D**) with no statistically significant differences with respect to oxygen concentration (one-way ANOVA, $p = 0.74$). No neuronal differentiation ($TUJ\text{-}1^+$ cells) was detected and limited (<5%) astrocytic differentiation was observed (**Fig.3.4E, F**). We concluded that the hNSC population after 10 d in culture in the presence of GFs consists of viable and undifferentiated stem cells under both normoxic and hypoxic conditions and the number of TD cells is negligible.

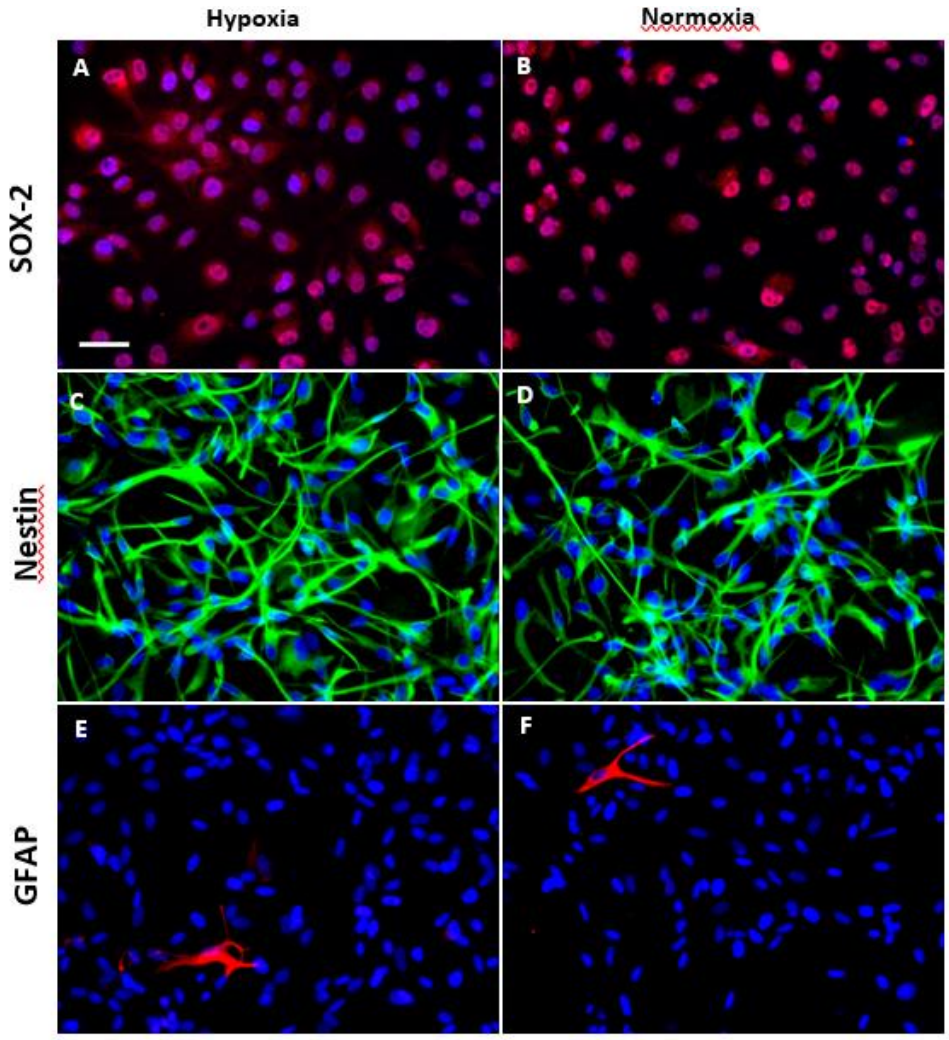

Figure 3.4. Expression of stemness markers in 2D cultures. Representative fluorescent images of hNSCs cultured on 2D laminin-coated 96-well plates. The hNSCs were labeled for SOX-2 **(A and B**), nestin (**C and D**), and GFAP (**E and F**). No neuronal (Tuj-1^{+}) cells were detected. Scale bar, 50 μm.

Since there was not any statistical difference between the conditions of normoxia and hypoxia in terms of viability and differentiation, we hypothesized that the larger population of cells under hypoxia may occur as a result of higher proliferation. To test our hypothesis, we performed EdU proliferation assay [171]. Our study showed a higher degree of proliferation for the hNSCs cultured under

hypoxia (**Fig. 3.5A, C, and E**). The percentage of EdU^+ cells was 11 ± 1% (4 d) and 16 ± 0.5% (10 d) under normoxia and 14 ± 1% (4 d) and 20 ± 1% (10 d) under hypoxia. Two-way ANOVA showed significant main effects of oxygen $F(1, 32) = 47.69$, $p < 0.001$ and time $F(1, 32) = 36.49$, $p < 0.001$ on hNSC proliferation with no significant interaction ($p = 0.291$).

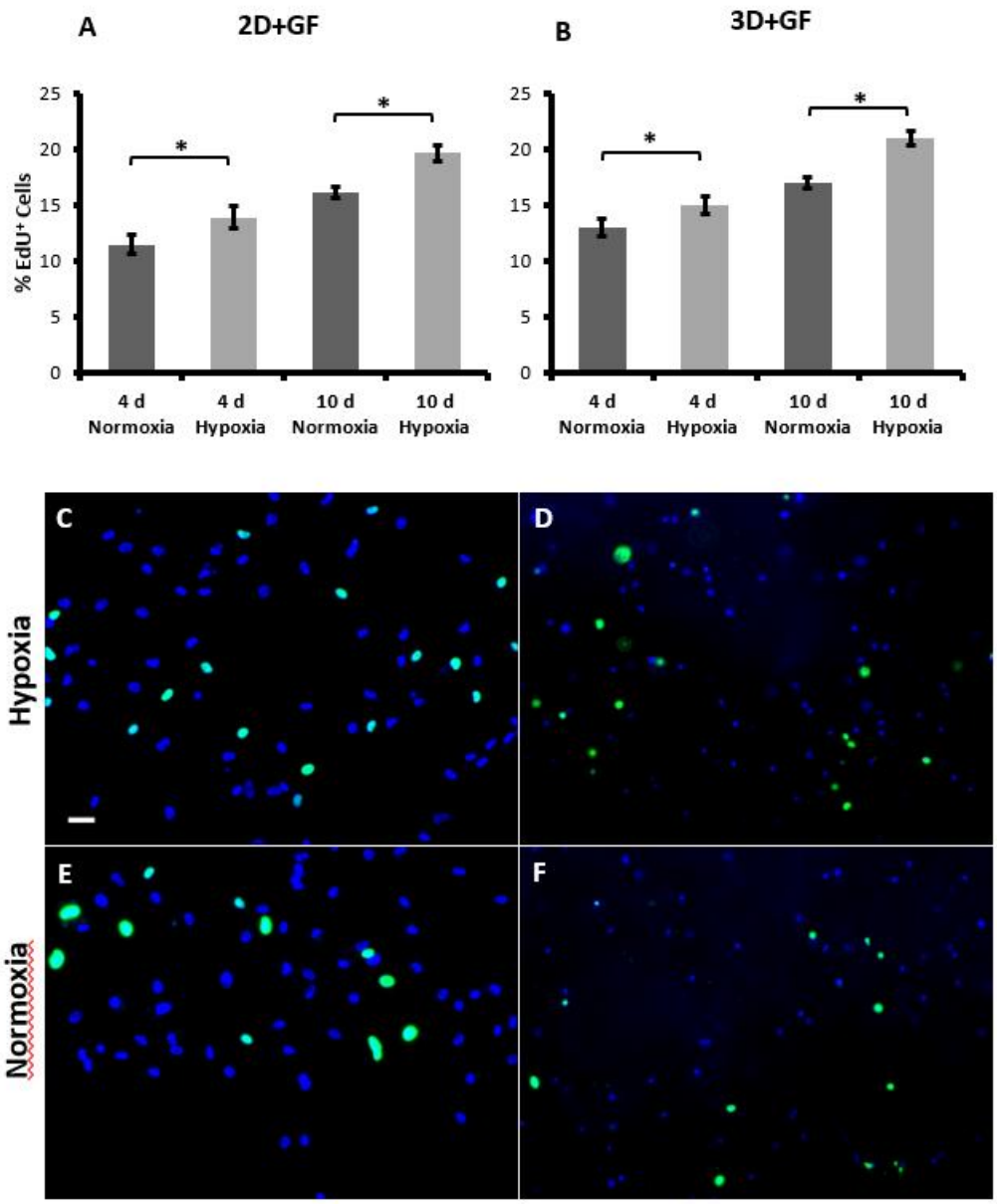

Figure 3.5. The hNSCs proliferation in 2D+GF (A) and 3D+GF (B) cultures.

Representative fluorescent images of hNSCs cultured on 2D laminin-coated 96-well plates and within 3D hydrogels under hypoxic (**C, D**) and normoxic (**E,F**) conditions. At both 4 and 10 d, the number of actively proliferating (EdU^+; green) cells was higher under hypoxic condition in comparison with normoxia in 2D+GF (**A**) and 3D+GF (**B**). Symbol (*) denotes significant difference ($p < 0.001$). The three-way ANOVA analysis test, exhibited a significant effect of culture dimensionality on hNSC proliferation ($p=0.009$). Bars represent

mean ± SD. n>9 independent experiments; n>50 NSCs/sample. Cell nuclei were labeled with DAPI (blue). Scale bar, 50 μm.

We then calculated the rate of hNSC growth by fitting the experimental values of the total cell number (**Fig.3.2A**) into **Equation 5**. Both A_{Death} and $A_{Differentiation}$, are approximately equal to zero and consequently the term A obtained from non-linear regression analysis is approximately equal to $A_{Self\text{-}renewal}$ (i.e., $A \approx A_{Self\text{-}renewal}$). The numerical values of A and k for the normoxic condition were 0.012 $\left(\frac{1}{\text{h}}\right)$ and 9.5×10^{-7} $\left(\frac{1}{\text{cell number} \times \text{h}}\right)$ and for the hypoxic condition were 0.012 $\left(\frac{1}{\text{h}}\right)$ and 8.9×10^{-7} $\left(\frac{1}{\text{cell number} \times \text{h}}\right)$. We calculated the hNSC division time by the following equation:

$$\tau = \frac{\ln 2}{A_{Self-renewal}} \qquad (12)$$

The hNSC division time was 58 h for 2D cultures.

Analysis of NSC growth rate in a 3D microenvironment in the presence of GFs for both normoxic and hypoxic conditions

The main effects on the total number of hNSCs within 3D cultures were found for oxygen concentration $F(1, 64) = 87.57$, $p < 0.001$, time $F(1, 64) = 819.91$, $p < 0.001$, along with a significant oxygen-time interaction $F(1, 64) = 13.05$, $p < 0.001$ (**Fig.3.2B**). Similar to 2D, in 3D cultures the majority of cells were also calcein^{+} after 10 d, the calcein^{+} cells constituted 74 ± 1% and 72 ± 0.5% of the total population under normoxia and hypoxia (**Fig.3.3B**) with no significant main effects of oxygen ($p = 0.065$) and time ($p = 0.32$) and no interaction ($p = 0.406$) on cell viability. Similar

to 2D, the hNSC terminal differentiation was also negligible (<5%, data not shown) under both normoxic and hypoxic 3D cultures and there was no statistical difference with respect to oxygen concentration (one-way ANOVA, $p = 0.572$). However, the EdU proliferation analysis showed that hNSCs exhibited greater proliferation under hypoxia (**Fig.3.5B, D, and F**). The percentage of EdU^+ cells after 4 and 10 d was 13 ± 1% and 17 ± 0.5% under normoxia and 15 ± 1% and 21 ± 1% under hypoxia. The two-way ANOVA showed a significant main effects of oxygen concentration $F(1, 32) = 305.71$, $p < 0.001$ and time $F(1, 32) = 664.88$, $p < 0.001$ on hNSC proliferation, and an interaction between time and oxygen concentration, $F(1, 32) = 46.69$, $p < 0.001$.

To test the effect of culture dimensionality on hNSC proliferation we performed a three-way ANOVA, which showed significant main effects of culture dimensionality $F(1, 64) = 7.27$, $p = 0.009$, oxygen concentration $F(1, 64) = 179.99$, $p < 0.001$, and time $F(1, 64) = 255.99$, $p < 0.001$. We did not find an interaction between oxygen concentration and time ($p = 0.077$) or between oxygen concentration and dimensionality ($p = 0.428$). However, significant interactions were found between dimensionality and time ($F(1, 64) = 24.61$, $p < 0.001$) and dimensionality and oxygen and time ($F(1, 64) = 14.13$, $p < 0.001$). The extent of this increase in proliferation was tested by the kinetic growth model. Based upon viability assay and immunofluorescence results both A_{Death} and $A_{Differentiation}$ are ≈ 0 for 3D cultures in the presence of GFs. By non-linear regression analysis, A and k were found to be 0.015 $\left(\frac{1}{\text{h}}\right)$ and 7.5×10^{-7} $\left(\frac{1}{\text{cell number} \times \text{h}}\right)$ under normoxia and 0.015 $\left(\frac{1}{\text{h}}\right)$ and 7×10^{-7} $\left(\frac{1}{\text{cell number} \times \text{h}}\right)$ under hypoxia. The cell division time (τ) was equal to 46 h under both normoxia and hypoxia.

Validation of feedback regulated growth model

The growth rate of fetal rat NSCs in 2D adherent culture was utilized to validate the feedback regulated growth model. The cell density data was kindly provided by Thermo Fisher Scientific (personal communication). Rat NSCs were cultured for 3, 7, and 10 d on a 2D poly-L-ornithine coated culture flask with an initial density of 5×10^4 cell/cm^2. The numerical values of A and k were obtained by performing non-linear regression analysis and the division time (τ) was calculated. The numerical values of A and k were found to be 0.03 $\left(\frac{1}{\text{h}}\right)$ and 5.5×10^{-11} $\left(\frac{1}{\text{cell number} \times \text{h}}\right)$. The cell division time for rat NSCs was equal to 23 ± 3 h.

Analysis of NSC decay and differentiation rate in 2D and 3D microenvironment

In both 2D and 3D cultures after growth factor removal and under both normoxic and hypoxic conditions, we observed a decrease in the total cell population (**Fig.3.2C, D**). At both 4 and 10 d the numbers of cells on 2D surfaces and within 3D hydrogels were significantly higher under hypoxia in comparison with normoxia. The two-way ANOVA analysis for 2D cultures found significant main effects of oxygen concentration $F(1, 64) = 61.43$, $p < 0.001$ and time $F(1, 64) = 610.54$, $p < 0.001$, with a significant interaction $F(1, 64) = 11.87$, $p < 0.001$. In 3D cultures, the main effects of oxygen concentration $F(1, 64) = 25.94$, $p < 0.001$, time $F(1, 64) = 275.58$, $p < 0.001$, and an interaction $F(1, 64) = 3.19$, $p = 0.031$ were calculated.

The hNSC culture in the absence of GFs initiates the differentiation phase and becomes a heterogeneous population consisting of undifferentiated hNSCs, TD

neurons and glia, and dead cells. We fitted **Equation 11** into the total cell number and uncovered the numerical values of $A_{Differentiation}$ as well as A_{Death} and d_{Death} constants. By substituting these constants in **Equation 10** we calculated the number of TD cells for both 2D and 3D cultures and under normoxic and hypoxic conditions (**Fig.3.6A, B**). The number of undifferentiated cells was found by subtracting the total number of cells from the number of TD cells (data not shown). The numerical values of $A_{Differentiation}$ in 2D cultures were 0.004 $\left(\frac{1}{h}\right)$ and 0.007 $\left(\frac{1}{h}\right)$ under normoxia and hypoxia, respectively. In 3D cultures the numerical value of $A_{Differentiation}$ was 0.008 $\left(\frac{1}{h}\right)$ under the normoxic condition and 0.01 $\left(\frac{1}{h}\right)$ under hypoxia.

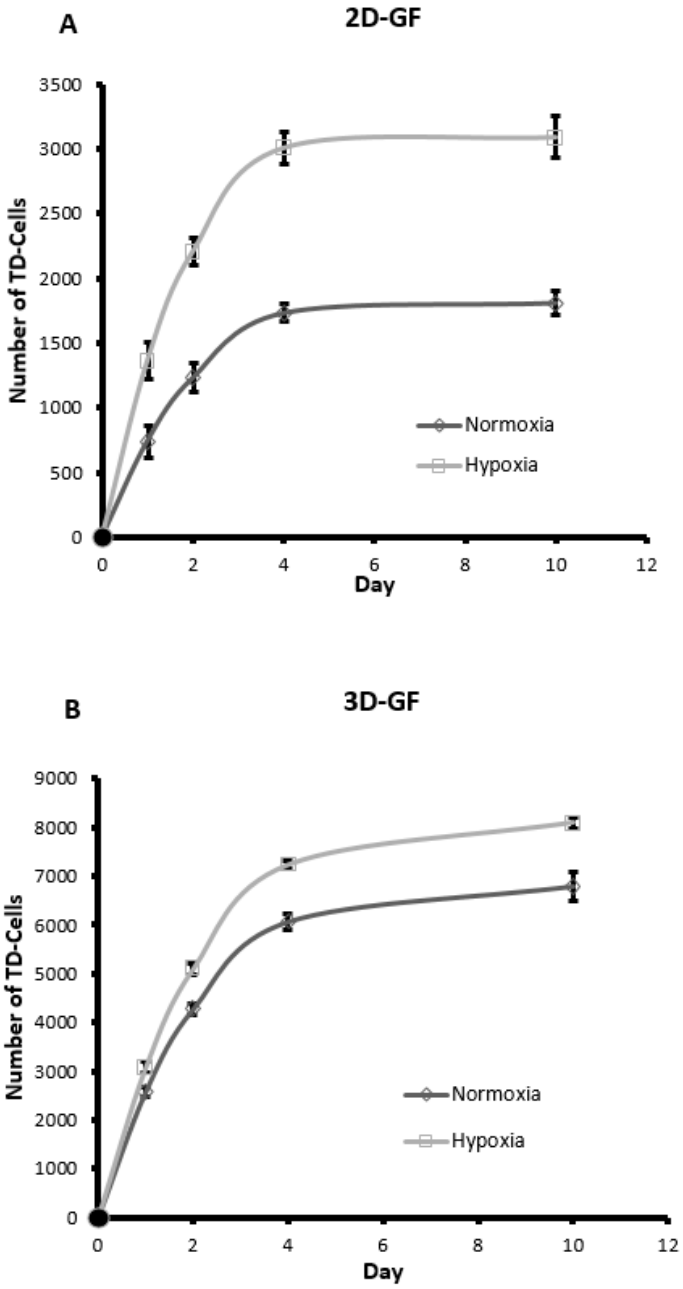

Figure 3.6. The number of TD cells generated in 2D-GF (A) and 3D-GF (B) cultures predicted by Equation 10

.

The percentages of dead cells in 2D culture after 10 d were 17 ± 1.5% and 19 ± 1.8% (**Fig.3.3C**) under normoxic and hypoxic cultures, respectively. For 3D cultures the percentages of dead cells were 32 ± 1% under nomoxia and 30 ± 0.5% under the hypoxic condition (**Fig.3.3D**). The two-way ANOVA analysis showed no significant effect of oxygen concentration ($p = 0.508$) and oxygen-time interaction ($p = 0.464$) on the viability of hNSCs in 2D cultures. Similarly, in 3D cultures no significant effects of oxygen concentration ($p = 0.093$) and interaction ($p = 0.324$) were calculated. It is important to note that the percentage of dead cells found by performing viability assay is cumulative of both undifferentiated and differentiated cells.

Discussion

The temporal output of hNSCs is influenced by a number of factors that need to be robustly controlled to achieve a safe and effective cell-replacement therapy. Matrix dimensionality, GFs, and oxygen concentration are among these important factors [47]. In this paper, the stemness of hNSCs under two general conditions has been studied: the hNSC cultures in the presence and absence of EGF and FGF-2. Under each general condition, the effects of normoxia and hypoxia (21% vs. 3%) and culture dimensionality (2D vs. 3D) on hNSC viability, proliferation and the expression of neuroprogenitor markers were investigated. We designed distinct mathematical models for each of the general conditions and have anticipated the rate of growth and differentiation of hNSCs.

The presence of mitogenic growth factors has been shown to promote NSC proliferation and inhibit lineage-commitment [3, 31]. Our results also confirm an

increase in the numbers of NSCs in both 2D and 3D cultures in the GF-containing medium for up to 10 d (**Fig.3.2A, B**). The cellular composition of the both 2D and 3D cultures in the presence of growth factors and under normoxic and hypoxic conditions consists of viable (**Fig.3.3A, B**) and undifferentiated (SOX-2^+ and nestin$^+$) stem cells (**Fig.3.4A-D**) with no statistical differences between normoxia-hypoxia and 2D-3D conditions. Therefore, we conclude that in the presence of mitogenic factors, the oxygen availability and culture dimensionality have negligible influence on the survival and differentiation of hNSCs. However, in both 2D and 3D cultures, the number of actively proliferating (EdU^+) cells is statistically higher under hypoxia vs normoxia (**Fig.3.5A-F**). This finding is in agreement with previous literature showing enhanced proliferation of rat [92] and human [93] NSCs under hypoxia in comparison with normoxia. Moreover, three-way ANOVA reveals a main effect of culture dimensionality on hNSC proliferation. Overall, lowered oxygen concentration and culture dimensionality positively influence the proliferation rate of viable and undifferentiated hNSCs in the presence of GFs.

To mathematically model the hNSC growth in the presence of GFs, we hypothesized that a growing population of NSCs requires a negative feedback mechanism to maintain the cell population size within a certain limit. Previous studies also confirm the existence of factors that regulate the proliferation of various mammalian stem cell types such as hematopoietic stem cells [172], retinal stem cells [173], and hair stem cells [174, 175]. The feedback regulatory mechanisms are necessary to maintain tissue homeostasis and prevent tumor formation. Based upon this understanding, we incorporated a negative feedback term in the exponential

growth model (**Equation 1**). The feedback term transforms the exponential curve into a logistic one (**Equation 4**). The logistic model assumes that a stable cell population will ultimately reach a saturation level or its carrying capacity. This assumption necessitates the rate of cell proliferation to decelerate and then cease when the target-tissue-size is achieved. Previous *in vivo* studies on the proliferation of stem cells in mice neocortex provide evidence for such growth behavior [166].

Our non-linear regression analysis shows that the growth behavior of NSCs in the presence of GFs in both 2D and 3D cultures follows a logistic curve over the course of 10 d. In the presence of GFs, both $A_{Differentiation}$ and A_{Death} are approximately equal to 0 and the hNSC self-renewal is the dominating scenario (i.e., $A \approx A_{Self\text{-}renewal}$). By comparing the 2D cultures with 3D, we realize that the numerical values of $A_{Self\text{-}renewal}$ for 3D cultures are greater than 2D under both normoxic and hypoxic cultures ($0.015\left(\frac{1}{h}\right)$ vs. $0.012\left(\frac{1}{h}\right)$). Based upon **Equation 12** the larger $A_{Self\text{-}renewal}$ translates into faster division time. The hNSC division time in 3D and 2D cultures is calculated to be ~46 h and ~58 h, respectively. Therefore, the higher proliferation rate in 3D cultures compared to 2D is probably due to shorter cell cycles. The numerical values of $A_{Self\text{-}renewal}$ for normoxic and hypoxic conditions and in both 2D and 3D cultures are similar (**Table 3.1**). However, the feedback constants under hypoxia are lower compared to the normoxic condition, indicating that proliferation under normoxia is restricted vs hypoxia.

Table 3.1. The numerical values of the growth, feedback, and differentiation constants derived from **Equations 5** and **11**. The constants are accompanied by the appropriate confidence intervals (CIs). The unit of A and $A_{Differentiation}$ constants is $(\frac{\mathbf{1}}{\mathbf{h}})$ and the unit of k is $(\frac{\mathbf{1}}{\mathbf{cell\ number} \times \mathbf{h}})$.

With GFs	**Normoxic 2D**	**Hypoxic 2D**	**Normoxic 3D**	**Hypoxic 3D**
A	0.012	0.012	0.015	0.015
95% **CI**	4×10^{-6}	4×10^{-8}	6×10^{-5}	2×10^{-5}
K	9.5×10^{-7}	8.9×10^{-7}	7.5×10^{-7}	7×10^{-7}
95% **CI**	3×10^{-10}	3×10^{-12}	3×10^{-9}	10^{-9}
Without GFs	**Normoxic 2D**	**Hypoxic 2D**	**Normoxic 3D**	**Hypoxic 3D**
$A_{Differentiation}$	0.004	0.007	0.008	0.01
95% **CI**	4×10^{-5}	2×10^{-4}	2×10^{-4}	3×10^{-4}

Fetal rat NSCs exhibit a similar logistic growth with the $A_{Self\text{-}renewal}$ equal to 0.03 $\left(\frac{1}{\mathrm{h}}\right)$ and the cell division time (τ) of ~23 h. The estimated NSC cycle length is estimated to be between 18 to 25 h for rodents [176-178] which is in agreement with the time anticipated by our model. The NSC cycle length of primates, depending upon the region of brain they reside, is estimated to be 20 to 40 h longer than rodents at a comparable developmental stage [179, 180]. This means that for a primate the NSC cycle length ranges from 38 to 65 h. Human brain in terms of size and number of neurogenic intervals is better represented by primate models. The cycle length of

hNSCs found by our model for both 2D and 3D cultures is located in the range between 38 to 65 h.

Upon the removal of growth factors, hNSCs differentiate into neurons and glia [3, 5]. By **Equation 10**, we predicted the number of TD cells for both 2D and 3D cultures and normoxic and hypoxic conditions (**Fig.3.6A, B**). The $A_{Differentiation}$ constants found by our model indicate that more TD cells are generated from hNSCs under hypoxia in both 2D and 3D cultures. Lowered oxygen levels have been shown to enhance the differentiation of hNSCs into neurons [181] and both neurons and oligodendrocytes [93]. Since the process of neurogenesis in human brain lasts for more than 70 d [166], a culture period of 10 days may not provide a sufficient amount of time for hNSCs to terminally differentiate into neurons and glia. We acknowledge, therefore, a comprehensive characterization of hNSC differentiation in a protracted culture period is a possible future direction of this work.

In summary, in this work by coupling *in vitro* hNSC culture results with mathematical modeling we attempted to clarify the effect of three important environmental cues on hNSC temporal output. These finding may contribute to generation of transplantable cellular grafts with well-defined cellular compositions.

Chapter 4: *In Vitro* Hypoxic Preconditioning for the Enhancement of Human Neural Stem Cell Survival and Differentiation

Introduction

Neural stem cell (NSC) transplantation has emerged as a novel treatment modality with potential clinical benefits for patients with neurological disorders or injuries [182]. This is primarily due to the unique characteristics of NSCs (i.e. self-renewal and multipotency). The NSCs possess the capacity of both generating more neuroprogenitors (self-renewal) as well as differentiating into neurons, astrocytes, and oligodendrocytes (multipotency) [3, 35, 159]. Thus, transplantation of NSCs, aiming at replacing damaged neurons and glia, presents a promising cell-mediated therapeutic approach to regenerate the damaged neural tissue. Preclinical studies, in stroke-induced rat models, showed that implanted NSCs yielded modest functional improvements by migrating towards the lesion site, differentiating into neurons [183], and partially integrating into the host neural circuitries [160, 184].

However, one of the major impediments in achieving efficacious and efficient NSC-based therapies is the limited survival of transplanted NSCs. Past studies indicate that only 10% to 40% of the total implanted cells survive following transplantation [8, 160]. The low survival of the cellular grafts is not unique to NSCs. In fact, stem cell regenerative therapies of cardiac [185], pancreatic [186], and muscular tissues [187] have also exhibited substantial cell loss post-transplantation. Thus, increasing the retention time of transplanted stem cells will result in enhanced therapeutic potential. Recently, it has been shown that the survival of stem cell transplants can be increased through genetic modification of cells aiming to overexpress anti-apoptotic and growth factors in the engrafted cells [188-190]. Even though this method resulted in a decreased cell loss after transplantation it may be

associated with an increased risk of tumor formation due to gene transfection [191]. Therefore, there is a need for development of safer and simpler pro-survival strategies that can enhance post-transplant cell survival.

Previously published work suggests that *in vitro* exposure of stem cells to hypoxic oxygen concentrations (hypoxic preconditioning; HP) prior to transplantation enhances the survival and tissue-repair capacity of stem cells [192]. For instance, transplantation of hypoxic preconditioned murine mesenchymal stem cells (MSCs) into rat infarcted heart tissues resulted in improved survival of the implanted cells, reduced infarct size, and enhanced cardiac function in comparison with MSCs that were cultured under atmospheric oxygen concentration (normoxia) prior to transplantation [10]. Additionally, hypoxic pretreatment of rodent MSCs and embryonic stem cells (ESCs) before transplantation into ischemic rat brain resulted in enhanced cell survival, extensive neuronal differentiation, and accelerated functional recovery [11, 193]. Based upon these findings, our goal is to define the effects of HP on the survival and differentiation potential of human neural stem cell (hNSCs).

Enhancing the survival of human NSCs (hNSCs) and promoting their transition into terminally differentiated neurons and glia are two key steps to increase the efficacy of the cell-replacement therapy. In the work herein presented, we assayed the viability, proliferation, and differentiation of human embryonic cortical NSCs cultured under hypoxic (3% oxygen) and normoxic conditions. The hNSCs were cultured in the absence of growth factors (GFs) under short-term (up to 10 d) and long-term (up to 60 d) HP and their survival as well as differentiation potential were

assessed. Our results indicate that short-term HP enhances the survival of hNSCs and that long-term HP promotes their differentiation into neural progenies.

Materials and Methods

All materials were procured from Sigma Aldrich (St. Louis, MO), Millipore (Billerica, MA) or Thermo Fisher Scientific (Waltham, MA*)* unless otherwise noted.

Human neural stem cell (hNSC) maintenance and culture

RenCell-CX, an immortalized cell line derived from 14-week gestation human fetal cerebral cortex was purchased from Millipore (Billerica, MA) and was used as a model hNSC in these experiments. The cells were cultured on laminin-coated (1.33 $\mu g/cm^2$) flasks and maintained in serum-free complete growth medium (DMEM: F12 supplemented with 1x B27 supplement, heparin (10 U/ml), L-glutamine (2 mM), gentamicin (30 μg/ml), epidermal growth factor (EGF, 20 ng/ml), and fibroblast growth factor-2 (FGF2, 20 ng/ml). The cells were passaged every 3 to 4 days using Accutase™ and plated in freshly laminin-coated flasks at a density of $\sim 7\times10^3$ cell/cm^2. All experiments were carried out using cells between passages 9 to 17.

To induce differentiation, the hNSCs were cultured in complete growth medium without growth factors (GF^-) referred to as the differentiation medium. The normoxic cultures were carried out in a humidified, 5% CO_2, 37°C incubator. The hypoxic cultures were carried out in a portable, humidified, and isolated hypoxic chamber (COY Laboratory, Grass Lake, MI) with 3% O_2**,** 5% CO_2 and 92% N_2. The hypoxic chamber was housed in a 37°C incubator. The concentration of oxygen in air

was measured using O_2-sensitive electrode system (Dwyer Instruments, Michigan City, IN).

Short-term HP was performed by seeding hNSCs at a density of 3×10^4 cells/cm^2 for 1, 2, 4, and 10 d and long-term HP was performed by seeding hNSCs at a density of 9×10^4 cells/cm^2 for 30 and 60 d. Both short-term and long-term cultures were conducted on laminin-coated 96-well tissue culture plates in differentiation medium (GF^-). The medium was changed every 2 d.

Viability study

The hNSC viability was measured using mammalian cell LIVE/DEAD viability assay (Thermo Fisher Scientific). After 4, 10, and 30 d the culture medium was aspirated and the samples were incubated with a solution of calcein-AM (live cell marker, 2 μM) and ethidium homodimer-1 (dead cell marker, 4 μM) in Tris-buffered saline (TBS) for 30 min. The samples were immediately imaged under fluorescent microscopy (Olympus, Center Valley, PA) and the numbers of calcein-AM^+ and ethidium homodimer-1^+ cells were counted.

Proliferation study

To detect hNSC proliferation during culture, the Click-iT EdU proliferation assay (Thermo Fisher Scientific) was performed. The hNSCs were incubated with EdU for 4 and 10 d with EdU being replenished every 2 d to prevent depletion. The cells were then fixed in 4% buffered formaldehyde for 20 min, permeabilized with TBS containing 0.1% Triton-X-100, and incubated with EdU reaction cocktail for 30

min followed by 4',6-diamidino-2-phenylindole (DAPI, 300 nM) nuclear stain. The samples were then imaged under fluorescent microscopy to measure the number of cells that proliferated during EdU incubation. The nuclei of EdU^+ cells fluoresced green because of Alexa Fluor 488 azide fluorescent dye detection. DAPI (blue) stains all nuclei. The numbers of EdU^+ and $DAPI^+$ cells were counted.

Immunofluorescence study

The immunofluorescence staining methods were adapted from lab protocols previously published in [80, 81]. In brief, the hNSCs cultured onto 96-well tissue culture plates after 10 d, 30 d, and 60 d were fixed with 4% buffered paraformaldehyde, washed with Tris-buffered saline (TBS, pH 8.0), and incubated with 10% goat serum in phosphate buffered saline (PBS) for 30 min in room temperature. The hNSCs were then incubated with primary antibodies SOX-2 (1:1000, Millipore), nestin (1:2000, Millipore), TUJ-1 (1:2000, Covance, Princeton, NJ), MAP-2 (1:2000, Abcam, Cambridge, MA), DCX (1:2000, Millipore), GFAP (1:1000, Abcam), S100β (1:500, Abcam), and GalC (1:1000, Millipore) diluted in 10% goat serum PBS overnight followed by washing steps and then incubation with fluorescently-conjugated secondary antibodies (Abcam) for 2 h and washing. The incubation of both primary and secondary antibodies was performed at 4°C. The samples were then stained with DAPI and imaged using fluorescent microscopy.

Statistical Analysis

Experimental results are represented as mean ± SD (n≥3). Student's t-test and analysis of variance (ANOVA) tests were performed to determine statistical significance.

Results

Effect of short-term hypoxic preconditioning on hNSC viability, proliferation, and differentiation potential

The standard culture method to induce hNSC differentiation into neurons, astrocytes, and oligodendrocytes is by withdrawing growth factors (FGF-2 and EGF) from the culture media (**Fig.4.1**).

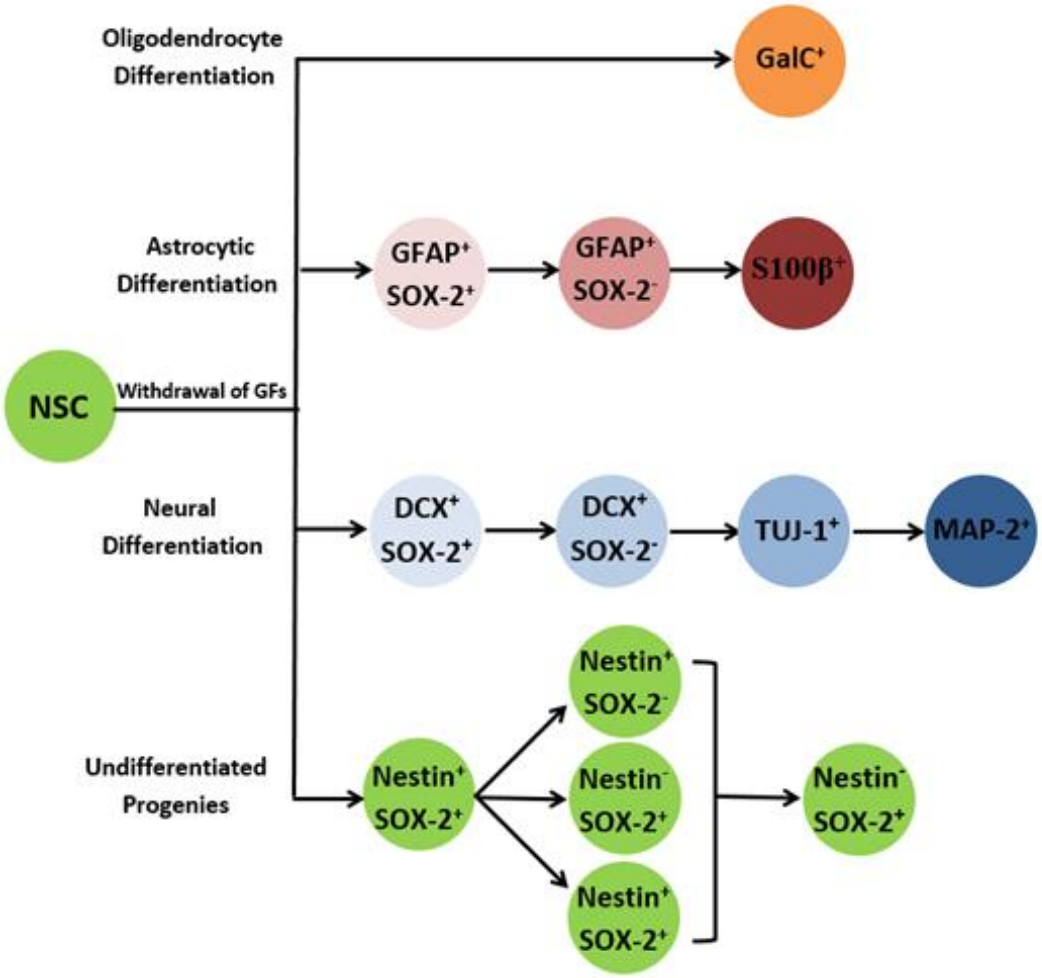

Figure 4.1. The withdrawal of growth factors from the hNSC culture initiates the differentiation of stem cells into neural and glial progenies. The proposed differentiation model in this work suggest that the neural lineage-commitment transitions from $DCX^+/SOX\text{-}2^+$ and $DCX^+/SOX2^-$ precursors to $TUJ\text{-}1^+$ immature neurons and eventually to $MAP\text{-}2^+$ mature neuronal cells. The astrocytic differentiated cells temporally transition from $GFAP^+/SOX\text{-}2^+$ progenies to terminally differentiated $GFAP^+/SOX2^-$ and $S100\beta^+$ astrocytes. The terminally differentiated oligodendrocytes ($GalC^+$) are generated over the course of 60 d from stem cells. The undifferentiated hNSCs persist through the entire culture period of 60 d and consist of

$Nestin^+/SOX\text{-}2^+$ cells at day 10, $Nestin^+/SOX2^-$, $Nestin^-/SOX\text{-}2^+$, and $Nestin^+/SOX\text{-}2^+$ populations at day 30, and $Nestin^-/SOX\text{-}2^+$ cells at day 60.

We grew hNSC cultures for 1, 2, 4, and 10 d in differentiation medium (GF^-) under both hypoxic and normoxic (control) conditions. To test the effect of short-term HP on hNSC survival, we first measured the total number of cells in both hypoxic and control groups (**Fig.4.2A**). After 4 and 10 d, the number of hNSCs cultured under hypoxia was significantly higher in comparison with normoxia. A two-way ANOVA showed significant main effects of time $F(1, 64) = 610.54$, $p < 0.001$ and oxygen concentration $F(1, 64) = 61.43$, $p < 0.001$ on hNSC total number, and an interaction between time and oxygen concentration, $F(1, 64) = 11.87$, $p < 0.001$. We investigated whether the increased number of cells under hypoxia was due to enhanced viability. Our viability analysis results at 4 and 10 d showed that the viable cells ($calcein^+$) constituted 89 ± 2% (hypoxia) vs 89 ± 4% (control) and 83 ± 2% (hypoxia) vs 81 ± 2% (control) of total cells, respectively (**Fig.4.2B**). A two-way ANOVA analysis indicated a significant main effect of time $F(1, 32) = 66.98$, $p < 0.001$ with no significant main effect of oxygen concentration $F(1, 32) = 0.45$, $p = 0.508$ and time x oxygen interaction $F(1, 32) = 0.55$, $p = 0.464$ on hNSC viability. We hypothesized that the larger population of cells under hypoxia may occur as a result of higher proliferation. To test this hypothesis, we performed EdU pulse-labeling [171] to detect the cells in the S-phase of division. The percentage of EdU^+ cells was 8 ± 0.3% (4d) and 7 ± 0.6% (10 d) under hypoxia and 6 ± 0.8% (4 d) and 5 ± 0.4% (10 d) under normoxia (**Fig.4.2C-E**). A two-way ANOVA showed a significant main effect of oxygen $F(1, 32) = 26.85$, $p < 0.001$ with no effect of time $F(1, 32) = 2.35$, p

= 0.135 and time x oxygen interaction $F(1, 32) = 1.66$, $p = 0.206$ on hNSC proliferation.

To clarify whether the generation of differentiated progenies contributed to enhanced cell number under hypoxia, we performed immunocytochemistry for cell-type specific biomarkers. Nestin and SOX-2 stem cell markers, GFAP astrocytic marker, and TUJ-1 neuronal marker were utilized to detect the undifferentiated stem cells as well as astrocytes and neurons, respectively. After 10 d, the majority of cells were $Nestin^+/SOX\text{-}2^+$ (**Fig.4.2F, G**) with very limited (<5%) $GFAP^+$ cells and no $TUJ\text{-}1^+$ cells. A Student's t-test did not show any statistical difference $t(16) = 0.34$, $p = 0.74$ in percentage of $Nestin^+/SOX\text{-}2^+$ cells with respect to oxygen concentration.

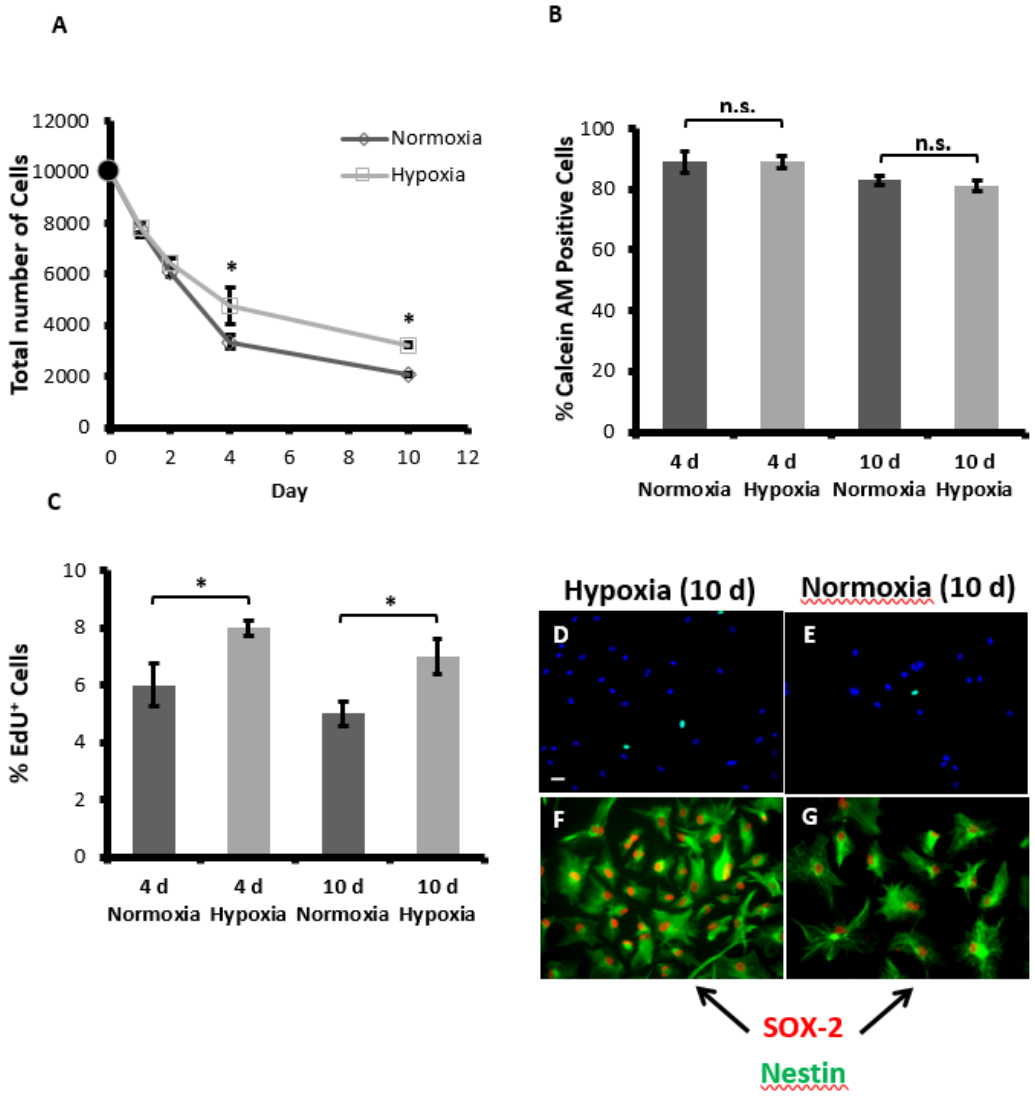

Figure 4.2. The effect of short-term HP on the survival and differentiation potential of hNSCs. Number of total cells (DAPI$^+$) at day 1, 2, 4 and 10 in differentiation medium (**A**). After 4 and 10 d the total number of cells was significantly higher under hypoxia in comparison with normoxia. There was no significant effect of oxygen concentration on hNSC viability (**B**). However, at both 4 and 10 d, the number of actively proliferating (EdU$^+$) cells was higher under the hypoxic condition in comparison with normoxia (**C**). Representative fluorescent images of EdU$^+$ (green) and DAPI$^+$ (blue) hNSCs cultured under hypoxic (**D**) and normoxic (**E**) conditions. After 10 d, the majority of hNSCs (>95%) expressed both SOX-2 (red) and Nestin (green) stem cells markers (Nestin$^+$/SOX-2$^+$) under both hypoxic (**F**) and

normoxic (**G**) conditions with no statistical difference with resepect to oxygen concenteation. Symbol (*) denotes significant differences ($p < 0.001$) between hypoxic and normoxic groups. $n > 9$ samples; one representative set of experimental data is shown. Bars represent mean ± SD. $n > 50$ hNSCs/sample.

These results yielded in two outcomes. First, short-term HP enhances hNSC survival by increasing the proliferation of undifferentiated hNSCs without reducing cell viability. Secondly, a culture period of 10 days without GFs, regardless of oxygen concentration, does not provide a sufficient amount of time for hNSCs to differentiate into neurons and glia. Therefore, short-term HP does not influence the differentiation potential of hNSCs.

Effect of long-term hypoxic preconditioning on hNSC viability and proliferation

Since the majority of hNSCs (>95%) maintained their undifferentiated state after 10 d we extended the culture period of both hypoxic and normoxic groups to 30 and 60 d in growth factor-free medium and counted the total numbers of cells (**Fig.4.3A**). A two way ANOVA analysis showed a significant main effect of time $F(1, 32) = 774.05$, $p < 0.001$ but no main effect of oxygen $F(1, 32) = 1.61$, $p = 0.214$ or a time x oxygen interaction $F(1, 32) = 0$, $p = 0.982$ on hNSC number. Our cell viability analysis at 30 d indicated that 71 ± 1% (hypoxia) and 70 ± 1% (control) of total cells were viable (**Fig.4.3B**) with no statistical difference between hypoxia and normoxia (Student's t-test, $t (16) = 0.18$, $p = 0.861$). We concluded that long-term exposure of hNSCs to hypoxia does not reduce cell survival.

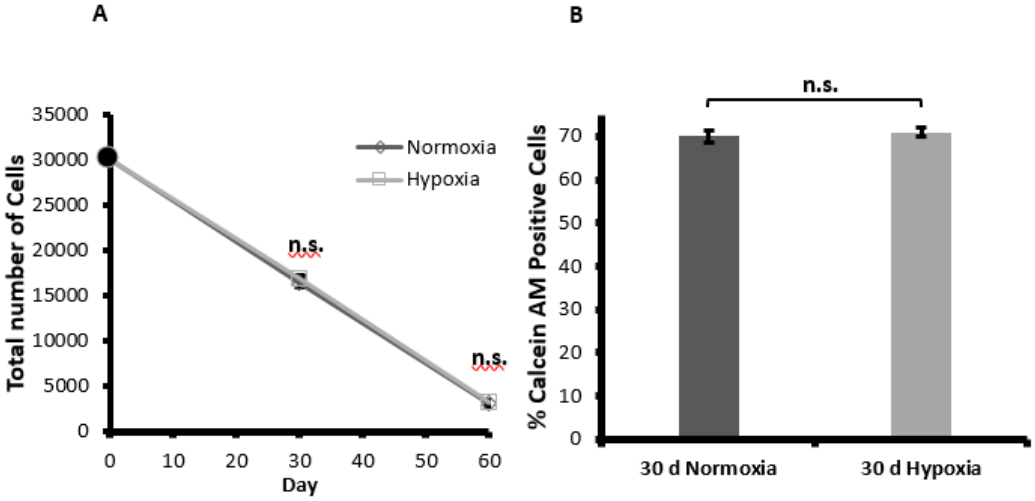

Figure 4.3. The effect of long-term HP on the survival of hNSCs. Number of total cells ($DAPI^+$) at day 30 and 60 in differentiation medium (**A**). There was not any statistical difference in total number of cells between the conditions of hypoxia and normoxia. Moreover, oxygen concentration did not influence the viability of the cells after 30 d of culture in differentiation medium (**B**).

Effect of long-term hypoxic preconditioning on hNSC differentiation potential

Next, we tested whether the long-term HP influences the differentiation potential of hNSCs. The extent of differentiation was evaluated by performing immunocytochemistry utilizing neural (DCX, TUJ-1, and MAP-2), astrocytic (GFAP and S100β), oligodendrocyte (GalC), and undifferentiated stem cell (Nestin and SOX-2) specific biomarkers. The cells that were immunoreactive for DCX consisted of $DCX^+/SOX\text{-}2^+$ and $DCX^+/SOX2^-$ cells. After 30 d, the percentage of $DCX^+/SOX\text{-}2^+$ cells under hypoxia and normoxia was 5 ± 1% and 2 ± 1%, respectively (**Fig.4.4A**). The $DCX^+/SOX2^-$ cells constituted 4 ± 1% (hypoxia) and 1 ± 0.5% (normoxia) of the total cell number (**Fig.4.4A**). A student's t-test analysis yielded t-values of $t(16) = 4.03$, $p = 0.001$ and $t(16) = 5.83$, $p < 0.001$ indicating a significant effect of oxygen concentration on hNSC differentiation to $DCX^+/SOX\text{-}2^+$ and $DCX^+/SOX2^-$ cells. The $TUJ\text{-}1^+$ neurons constituted 2 ± 0.5% of total cells under hypoxia and there were not any $TUJ\text{-}1^+$ cells in the control group (**Fig.4.4A**). A student's t-test analysis indicated a significant effect of oxygen concentration $t(16) = 7.77$, $p < 0.001$ on the number of $TUJ\text{-}1^+$ cells.

After 30 d, we detected two populations of differentiated astrocytic progenies: $GFAP^+/SOX\text{-}2^+$ and $GFAP^+/SOX2^-$ cells. The $GFAP^+/SOX\text{-}2^+$ and $GFAP^+/SOX2^-$ cells constituted 13 ± 1% (hypoxia), 17 ± 1% (control), 16 ± 1% (hypoxia), and 11 ± 1% (control) of the total cell number (**Fig.4.4B**). A student's t-test statistical analysis yielded t-values of $t(16) = 3.06$, $p = 0.007$ and $t(16) = 5.61$, $p < 0.001$ indicating a significant effect of oxygen concentration on the number of $GFAP^+/SOX\text{-}2^+$ and $GFAP^+/SOX2^-$ astrocytic progenies.

We identified three populations of undifferentiated hNSCs: $Nestin^{+}/SOX\text{-}2^{-}$, $Nestin^{+}/SOX2^{+}$, and $Nestin^{-}/SOX\text{-}2^{+}$ cells. After 30 d, the hypoxic cultures had 11 ± 1% $Nestin^{+}/SOX2^{-}$, 11 ± 1% $Nestin^{+}/SOX\text{-}2^{+}$, and 24 ± 2% $Nestin^{-}/SOX\text{-}2^{+}$ cells and the control groups consisted of 10 ± 1% $Nestin^{+}/SOX2^{-}$, 16 ± 1% $Nestin^{+}/SOX\text{-}2^{+}$, and 35 ± 2% $Nestin^{-}/SOX\text{-}2^{+}$ stem cells (**Fig.4.4C**). A student's t-test did not indicate any significant effect of oxygen concentration on the number of $Nestin^{+}/SOX2^{-}$ cells ($t(16) = 0.99$, $p = 0.338$). However, it yielded in t-values of $t(16) = 7.38$, $p < 0.001$ and $t(16) = 7.41$, $p < 0.001$, indicating a significant effect of oxygen concentration on the amount of $Nestin^{+}/SOX\text{-}2^{+}$ and $Nestin^{-}/SOX\text{-}2^{+}$ undifferentiated stem cells.

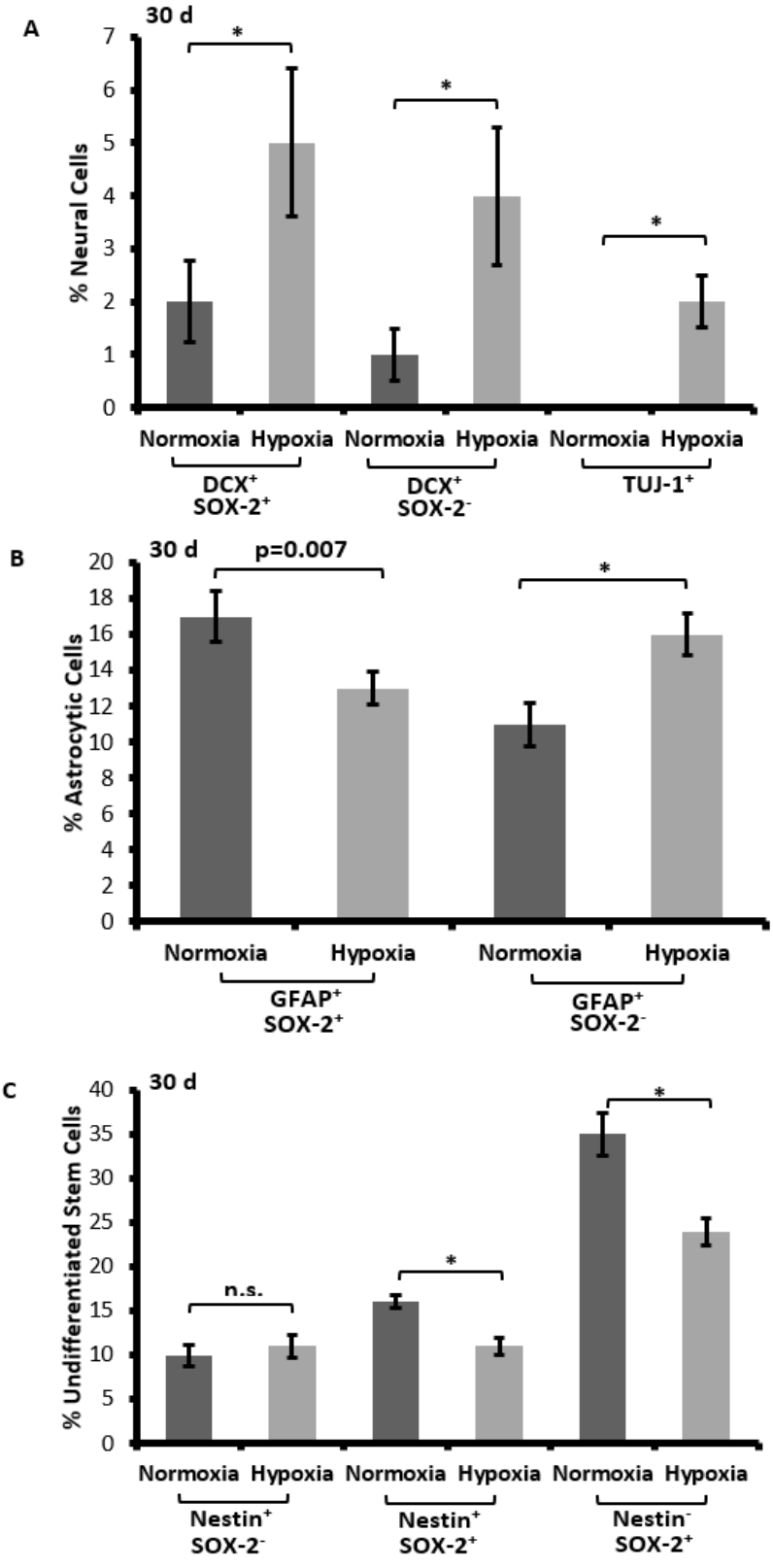
A
30 d
% Neural Cells
Normoxia Hypoxia Normoxia Hypoxia Normoxia Hypoxia
DCX+ SOX-2+
DCX+ SOX-2-
TUJ-1+
B
30 d
p=0.007
% Astrocytic Cells
Normoxia Hypoxia Normoxia Hypoxia
GFAP+ SOX-2+
GFAP+ SOX-2-
C
30 d
% Undifferentiated Stem Cells
n.s.
Normoxia Hypoxia Normoxia Hypoxia Normoxia Hypoxia
Nestin+ SOX-2-
Nestin+ SOX-2+
Nestin- SOX-2+

Figure 4.4. The effect of long-term (30 d) HP on the differentiation potential of hNSCs. The hNSCs were cultured in differentiation medium (GF^-) for 30 d under hypoxic and normoxic conditions and the extent of their differentiation was measured by performing immunocytochemistry utilizing neural, glial, and stem cell specific biomarkers. The neural differentiated progenies consisted of $DCX^+/SOX\text{-}2^+$, $DCX^+/SOX2^-$, and $TUJ\text{-}1^+$ populations. The numbers of all neural differentiated populations were statistically higher under hypoxia vs normoxia (**A**). The astrocytic progenies constituted two distinct populations: $GFAP^+/SOX\text{-}2^+$ astrocytic precursors and $GFAP^+/SOX2^-$ astrocytes. The numbers of $GFAP^+/SOX\text{-}2^+$ cells were statistically lower under hypoxia while the numbers of $GFAP^+/SOX2^-$ astrocytes was statistically higher (**B**). There was no statistical difference in the number of $Nestin^+/SOX\text{-}2^-$ undifferentiated hNSCs between the conditions of hypoxia and normoxia. However, the numbers of $Nestin^+/SOX\text{-}2^+$ and $Nestin^-/SOX\text{-}2^+$ hNSCs were statistically lower under hypoxia vs normoxia (**C**). Symbol (*) denotes significant differences ($p < 0.001$) between hypoxic and normoxic groups. $n > 9$ samples; one representative set of experimental data is shown. Bars represent mean ± SD. $n > 50$ cells/sample.

Even though these results indicate that, after 30 d, hypoxia promotes the transition of hNSCs into differentiated progenies, yet, ~46% (hypoxia) and 61% (normoxia) of the total hNSCs maintain their undifferentiated state. Moreover, we did not detect any $GalC^+$ oligodendrocytes after 30 d. Therefore, we attempted to further measure the extent of hNSC differentiation by prolonging the culture period to 60 d. **Figures 4.5A-D** and **4.5E-F** represent the immunofluorescence expression of neural and astrocytic progenies after 30 d.

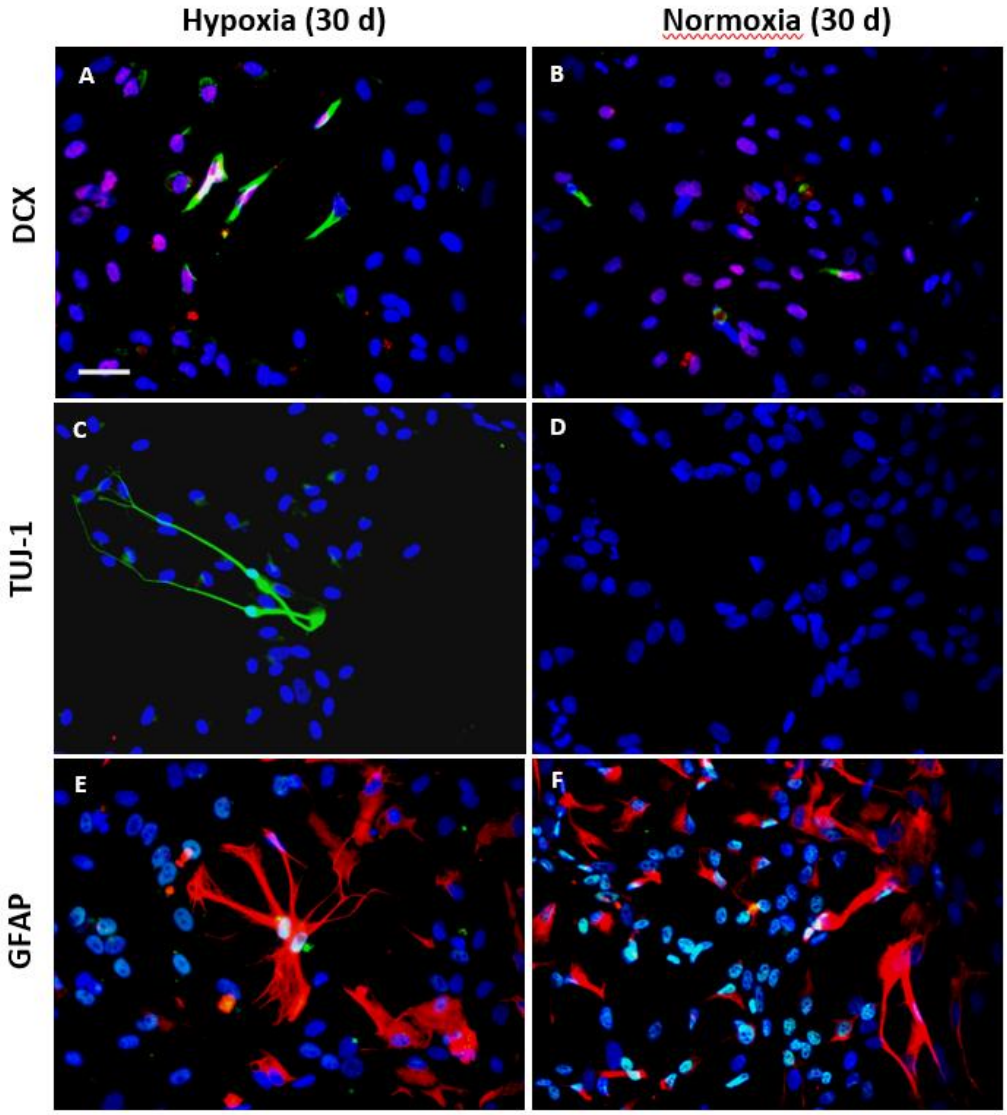

Figure 4.5. Expression of neural and astrocytic cell markers after 30 d. The neural progenies stained $DCX^{+}/SOX\text{-}2^{+}$ (green-red), $DCX^{+}/SOX2^{-}$ (green) neural precursor markers (**A and B**) and $TUJ\text{-}1^{+}$ (green) immature neural markers (**C and D**). The cells with astrocytic lineage were $GFAP^{+}/SOX\text{-}2^{+}$ (red-green) precursors and $GFAP^{+}/SOX2^{-}$ (red) astrocytic differentiated cells (**E and F**). Scale bar, 50 µm.

After 60 d, we identified two groups of neural populations: DCX^+ and MAP-2^+ cells. The hypoxic cultures contained 12 ± 1% DCX^+ and 15 ± 1% MAP-2^+ cells vs 9 ± 1% DCX^+ and 9 ± 1% MAP-2^+ cells in the controls (**Fig.4.6A**). A student's t-test analysis indicated a significant effect of oxygen concentration on the number of DCX^+ cells ($t(16) = 5.3$, $p < 0.001$) and MAP-2^+ cells ($t(16) = 12.51$, $p < 0.001$). The astrocytic differentiated cells consisted of $GFAP^+$ and $S100\beta^+$ populations. The $GFAP^+$ and $S100\beta^+$ astrocytes constituted 18 ± 1% (hypoxia), 17 ± 1% (control), 12 ± 2% (hypoxia), and 12 ± 1% (control) of the total cells, respectively (**Fig.4.6B**). A student's t-test analysis did not show any statistical difference between the number of $GFAP^+$ ($t(16) = 0.46$, $p = 0.649$) and $S100\beta^+$ astrocytes ($t(16) = 0.41$, $p = 0.689$) with respect to oxygen concentration. We detected $GalC^+$ oligodendrocyte differentiated progenies in the cultures after 60 d. The hypoxic and control groups contained 10 ± 1% and 8 ± 1% of $GalC^+$ cells, respectively (**Fig.4.6C**). A student's t-test analysis yielded in a t-value of $t(16) = 4.89$, $p < 0.001$ indicating a significant effect of oxygen concentration on hNSC differentiation to $GalC^+$ oligodendrocytes. The undifferentiated hNSCs, after 60 d, consisted of $Nestin^-/SOX\text{-}2^+$ cells that constituted 20 ± 1% and 35 ± 1% of the total cells under hypoxia and normoxia, respectively (**Fig.4.6D**). A student's t-test analysis showed a significant effect of oxygen concentration on the number $Nestin^-/SOX\text{-}2^+$ cells after 60 d ($t(16) = 17.48$, $p < 0.001$).

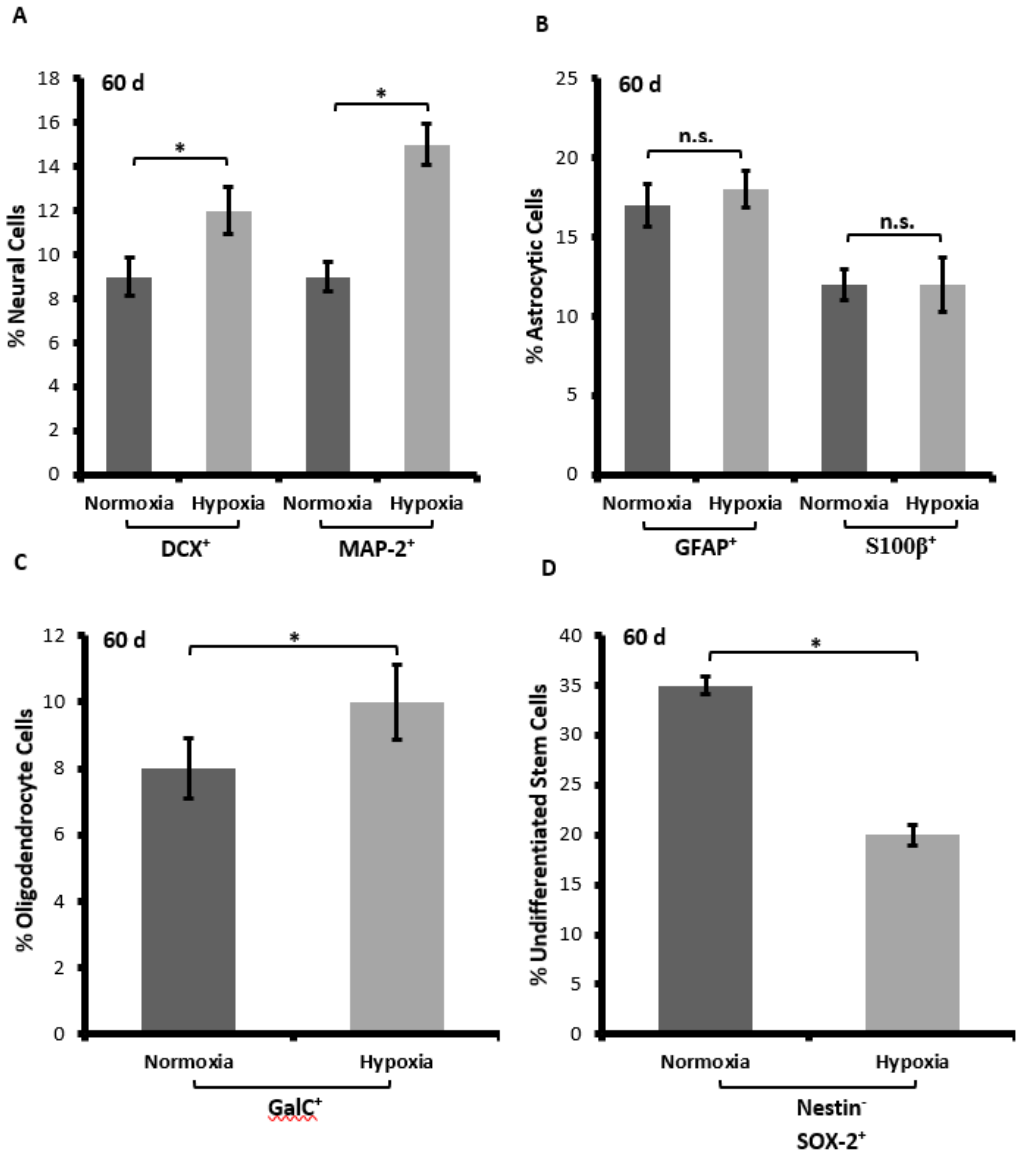

Figure 4.6. The effect of long-term (60 d) HP on the differentiation potential of hNSCs. The hNSCs were cultured in differentiation medium (GF^-) for 60 d under hypoxic and normoxic conditions and were labeled for neural, glial, and stem cell specific biomarkers. The numbers of neural differentiated cells, consisting of DCX^+ and $MAP\text{-}2^+$ progenies, were statistically higher under hypoxia vs normoxia (**A**). There was no statistical difference in numbers of $GFAP^+$ and $S100\beta^+$ differentiated astrocytes between hypoxia and normoxia (**B**). The number of $GalC^+$ oligodendrocytes was statistically higher under hypoxia compared to normoxia (**C**) and the number of $Nestin^-/SOX\text{-}2^+$ undifferentiated hNSCs was statistically lower under the

hypoxic condition vs normoxia (**D**). Symbol (*) denotes significant differences ($p < 0.001$) between hypoxic and normoxic groups. $n > 9$ samples; one representative set of experimental data is shown. Bars represent mean ± SD. $n > 50$ cells/sample.

The immunofluorescence expression of neural (**Fig.4.7A-D**), astrocytic (**Fig.4.7E-H**), and oligodendrocytes (**Fig.4.7I, J**) after 60 d are presented.

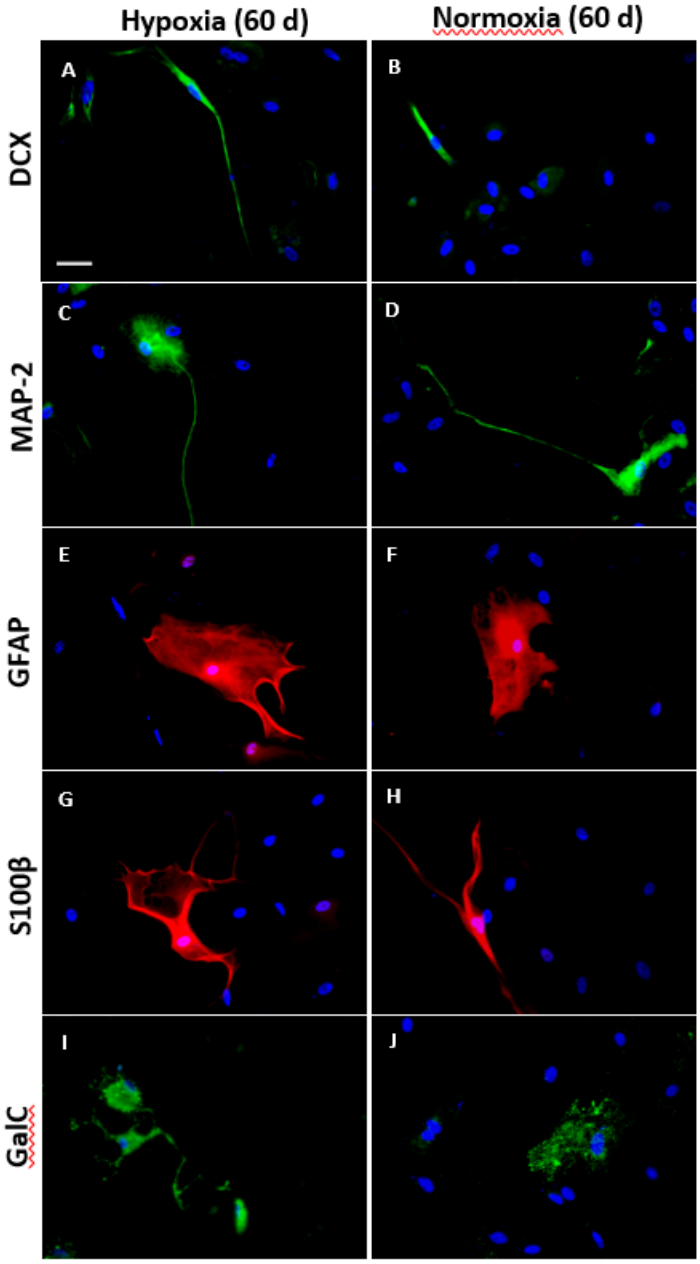

Figure 4.7. Expression of neural and glial cell markers after 60 d. The neural progenies stained positive for DCX (green; **A and B**) and MAP-2 (green) neural markers (**C and D**). The cells with astrocytic lineage stained positive for GFAP (red) and S100β (red) astrocytic markers (**E-H**). The differentiated oligodenrrocytes were labeled for the GalC (green) marker (**I and J**). Scale bar, 50 µm.

Discussion

The capability of human brain to repair after a neurological disorder or injury is limited due to its highly complex structure and low cell turnover. Stem cell transplantation utilizing multipotent NSCs with tissue-specific differentiation capacity holds great promise for the repair and restoration of brain tissue and function. However, the substantial loss of engrafted NSCs, which can be as much as much 90% [8] of the total transplanted cell number, limits the translational potential of NSC-mediated therapy. To achieve efficacious regenerative therapeutics, there is a need to enhance the survival of transplanted NSCs as well as their differentiation towards functional neural and glial differentiated cells.

The human brain is a hypoxic environment with an oxygen concentration between 3% to 4% [15, 194]. However, the hNSC *in vitro* cultures have been conventionally performed under normoxic O_2 concentration (21%) which is 5 to 7 times higher than that of natural brain tissue. This significant discrepancy in O_2 concentration between *in vitro* cultures and the *in vivo* environment may stress the NSCs and cause cell death post transplantation. Since hNSCs are exposed to hypoxia in their native niche, we hypothesized that an *in vitro* hypoxic culture may provide a permissive environment for the hNSC survival and differentiation. Manipulation of O_2 concentration, *in vitro*, provides a scalable, cost-effective, and xeno-free tool for the production of differentiated neurons and glia. Moreover, it may reduce the risk of oxidative stress on hNSCs and their differentiated progenies after being implanted in the hypoxic brain environment.

To test our hypothesis, we investigated the effect of oxygen concentration on the survival and differentiation behavior of hNSCs in short-term (up to10 d) and long-term (up to 60 d) cultures in the absence of mitogenic factors (i.e. FGF2 and EGF). The hNSCs, upon withdrawal of GFs, begin to differentiate into neural and glial progenies and resulting in a heterogeneous population of cells consisting of undifferentiated hNSCs, terminally differentiated neurons and glia as well as dead cells (**Fig.4.1**) [96, 195]. The process of hNSC differentiation in the human brain lasts as long as 70 d [166, 196]. Based upon this initial understanding from the *in vivo* scenario, we did not expect to detect extensive neural and glial differentiation in our short-term (10 d) cultures. However, it was crucial to perform short-term HP to assess the effect of lowered oxygen concentration on the survival of hNSCs. We, then, extended the culture periods to 30 and 60 d to measure the extent of hNSC differentiation.

In both hypoxic and normoxic cultures we observed a temporal decrease in cell density during the course of 10 d (**Fig.4.2A**). However, after 4 and 10 days the total number of cells under hypoxia was significantly higher than normoxia (**Fig.4.2A**). Our cell viability analysis indicated no statistical difference in the number of viable cells between the hypoxic and normoxic groups (**Fig.4.2B**). However, the number of actively proliferating (EdU^+) cells under hypoxia was statistically higher vs normoxia (**Fig.4.2C**). This finding is in agreement with previously published studies showing a positive effect of hypoxia on mouse [91] and rat [92] NSC proliferation in the absence of growth factors. Under both hypoxia and normoxia, the majority of cells (>95%) expressed both Nestin and SOX-2 stem cell markers

(Nestin^{+}/SOX-2^{+}) (**Fig.4.2F, G**). Therefore, we concluded that short-term HP enhances the survival of undifferentiated hNSCs by increasing the proliferation of the cells without influencing their viability and differentiation.

Long-term HP did not reduce the survival of hNSCs or their differentiated progenies. After 30 d, there was no statistical difference in the total cell number (**Fig.4.3A**) and the number of viable cells between the hypoxic and normoxic groups (**Fig.4.3B**). We measured the extent of differentiation by performing immunocytochemistry for neural, glial, and stem cells specific markers. After 30 d, the neural differentiated progenies consisted of three populations: DCX^{+}/SOX-2^{+}, DCX^{+}/SOX2^{-}, and TUJ-1^{+} cells. The DCX is a marker for neuroblasts which are neuronal precursors that will eventually differentiate into neurons [197, 198]. Our immunocytochemistry analysis shows a significant effect of hypoxia on the number of DCX^{+}/SOX-2^{+} (5% vs 2%), DCX^{+}/SOX2^{-} (4% vs 1%), and TUJ-1^{+} (2% vs 0%) cells (**Fig.4.4A**) meaning that hypoxia significantly enhanced the neural differentiation capacity of hNSCs. These results are in agreement with previous studies showing the positive effect of hypoxia on rat [92] and human [93] NSC as well as human ESC [199] differentiation potential towards neural progenies.

The astrocytic progenies, after 30 d, consisted of astrocytic precursors (GFAP^{+}/SOX-2^{+}) and terminally differentiated astrocytes (GFAP^{+}/SOX2^{-}). The number of GFAP^{+}/SOX-2^{+} cells was statistically lower under hypoxia (13% vs 17%) while the number of GFAP^{+}/SOX2^{-} cells was higher (16% vs 11%, **Fig.4.4B**). However, the sum of GFAP^{+}/SOX-2^{+} and GFAP^{+}/SOX2^{-} cells was similar in both hypoxic and normoxic cultures (29% vs 28%) indicating that, after 30 d, hypoxia did

not influence the extent of hNSC differentiation into astrocytic progenies. Previously published studies on hNSC [93] and hESC [199] differentiation also indicate no significant differences in the extent of astrocytic differentiation with respect to oxygen concentration. However, our results indicate that hypoxia enhances the transition from precursor state to terminal differentiation. This is evident by the higher number of $GFAP^{+}/SOX2^{-}$ and lower number of $GFAP^{+}/SOX\text{-}2^{+}$ cells under hypoxia (**Fig.4.4B**).

The population of undifferentiated stem cells which consisted of $Nestin^{+}/SOX\text{-}2^{-}$, $Nestin^{+}/SOX2^{+}$, and $Nestin^{-}/SOX\text{-}2^{+}$ cells constituted ~46% (hypoxia) and ~61% (normoxia) of the total cells (**Fig.4.4C**). There was no statistical difference in the number of $Nestin^{+}/SOX\text{-}2^{-}$ cells between hypoxia and normoxia (11% vs 10%). However, the number of $Nestin^{+}/SOX\text{-}2^{+}$ (11% vs 16%) and $Nestin^{-}/SOX\text{-}2^{+}$ (24% vs 35%) cells was statistically lower under hypoxia vs normoxia (**Fig.4.4C**). Previously published works on mouse [200] and human [201] NSCs indicate that SOX-2 expression temporally decreases when NSCs are cultured in differentiation medium (GF^{-}). In our cultures >95% of hNSCs expressed SOX-2 at day 10 which decreased to 35% (hypoxia) and 51% (normoxia) at day 30 which is in agreement with these findings. Moreover, hypoxia has been shown to reduce the expression of SOX-2 in murine MSCs [202] and human ESCs [203] in the differentiation phase which also agrees with our results.

Our differentiation analysis after 60 d shows that the hypoxic cultures contained a higher number of neural progenies compared to the normoxic groups. The number of both DCX^{+} (12% vs 9%) and $MAP\text{-}2^{+}$ (15% vs 9%) cells was statistically

higher under hypoxia and yielded a total of 27% differentiated neural progenies vs 18% under normoxia (**Fig.4.6A**). There was no statistical difference in the number of astrocytic progenies with respect to O_2 concentration. The $GFAP^+$ astrocytes, after 60 d, constituted 18% of the total cell number under hypoxia vs 17% under normoxia (**Fig.4.6B**). Both hypoxic and normoxic cultures contained 12% of $S100\beta^+$ astrocytes and the sum of $GFAP^+$ and $S100\beta^+$ astrocytes was 30% under hypoxia vs 29% under normoxia (**Fig.4.6B**). We detected $GalC^+$ oligodendrocytes after 60 d of differentiation. The number of $GalC^+$ cells was statistically higher under hypoxia (10%) vs normoxia (8%) which is in agreement with previously published work showing that hypoxia favors the differentiation of hNSCs to neurons and oligodendrocytes (**Fig.4.6C**) [93]. The undifferentiated stem cells, after 60 d, only consisted of $Nestin^-/SOX\text{-}2^+$ cells and were statistically lower under hypoxia (20%) vs normoxia (35%, **Fig.4.6D**).

In summary, our results show that hypoxia promotes the survival of hNSCs in short-term cultures by increasing the proliferation of hNSCs without reducing their viability. In long-term cultures hypoxia promotes the transition of hNSCs into terminally differentiated cells, possibly through decreased expression of SOX-2 transcription factor, and enhances the hNSC differentiation towards neural progenies. These results may introduce HP as a pro-survival pre-conditioning strategy, for *in vitro* culture of hNSCs, with the potential to improve the tissue-regenerative capacity of hNSCs.

Chapter 5: Synergistic Effect of Hypoxia and Laminin-rich Substrates on the Enhancement of Human Neural Stem Cell Growth

Introduction

Neural stem cells (NSCs) are a self-renewing somatic cell type with the capacity to generate the major neural and glial cell types in the brain [3, 35, 159]. Due to their ability to self-renew and their multipotency, NSCs are promising candidates to be utilized in cell-replacement therapy in patients with neurological disorders or injury. Preclinical studies have shown that the transplantation of NSCs in animal experimental models such as stroke [52, 53, 160], Parkinson's disease [54-57], and Alzheimer's disease [58] has resulted in enhanced behavioral recovery. However, the application of stem cells in clinical trials may require as many as 10^{10} cells per patient [204] and therefore a need exists for cost-effective and scalable methods of producing large quantities of hNSCs *in vitro*.

Neural stem cells, *in vivo*, reside within a specialized anatomical compartment known as the NSC niche [41, 205]. The NSC niche provides extrinsic cues that influence cell survival and regulate stem cell proliferation and differentiation [206, 207]. The interaction between NSCs and the extracellular matrix (ECM) [47, 208] as well as the gradient of important cues such as oxygen [15] are among the important regulators of NSC proliferation. For instance, the proliferative behaviors of mouse neuroepithelial cells [133], as well as mouse and human NSCs [123] have been shown to be influenced by ECM molecules (e.g., laminin). NSC adhesion to ECM is mediated via several cell-surface receptors, of which the major class is integrins [128]. The upregulation of β1 integrin expression, in particular, has been linked to the effect of cell-ECM interaction on NSC proliferation [209-211]. Additionally, the NSC niche is a hypoxic environment with an oxygen concentration between 3% to 4% as

opposed to the atmospheric oxygen concentration (normoxia, 21%) [15, 194] conventionally utilized in *in vitro* NSC culture. Further, hypoxia has been shown to enhance the proliferation of both rat and human NSCs [92, 93]. Due to ease of scalability, availability, and no risk of pathogen transmission, manipulation of oxygen concentration in NSC cultures can provide a powerful tool for improving production strategies for NSCs.

In the NSC niche, the ECM varies in composition [121, 212], where laminin [211], collagen I [43, 213], collagen IV [149], and low levels of fibronectin [214] are among its protein constituents. Yet, the relationship between NSC proliferation, substrate composition and the concentration of oxygen in culture has not yet been examined. Herein, we test the hypothesis that the synergistic effect of a lowered oxygen concentration across various substrates can enhance the *in vitro* expansion of NSCs.

We assayed the proliferation of human embryonic cortical NSCs cultured on six different substrates and under both normoxic and hypoxic conditions (3% oxygen). Four purified ECM proteins (i.e. laminin, collagen I, collagen IV, and fibronectin), a positively charged non-ECM polymer (i.e. poly-L-ornithine or PLO), and a cell-adhesive matrix for NSCs which is a tissue-derived ECM (Matrigel, reduced-growth factor) were utilized. The proliferation and apoptosis of NSCs when cultured on these substrates and under both normoxia and hypoxia were assessed. In this work, we have shown that the laminin-rich substrates in synergy with low oxygen concentration can significantly contribute to *in vitro* expansion of NSCs.

Materials and Methods

All materials were procured from Sigma Aldrich (St. Louis, MO), Millipore (Billerica, MA), Life Technologies (Grand Island, NY), or Trevigen (Gaithersburg, MD) unless otherwise noted.

Human neural stem cell (hNSC) maintenance and culture

Rencell-CX, an immortalized cell line derived from 14-week gestation human fetal cortex was purchased from Millipore (Billerica, MA) and was used as a model hNSC in these experiments. Cell culture flasks were coated with natural mouse laminin (Life Technologies; 20 μg/ml) and used to maintain cells in serum-free complete growth medium composed of DMEM: F12 supplemented with 1x B27 supplement, heparin (10 U/ml), L-glutamine (2 mM), gentamicin (30 μg/ml), epidermal growth factor (EGF, 20 ng/ml), and fibroblast growth factor-2 (FGF-2, 20 ng/ml). The cells were passaged every 3 to 4 days using Accutase™ and plated in freshly laminin-coated flasks at a density of ~7×10^3 cell/cm^2. All experiments were carried out using cells between passages 10 to 14.

To assess hNSC proliferation, the cells were seeded at a density of 3×10^4 cells/cm^2 onto 96-well tissue culture plates coated with the various substrates; cultures were carried out for 2 and 4 d and the medium was changed every 2 d. All the proliferation experiments were carried out using complete growth medium containing growth factors.

The normoxic cultures were carried out in a humidified, 5% CO_2, 37 C incubator. The hypoxic cultures were carried out in a portable, humidified, and isolated hypoxic chamber (COY Laboratory, Grass Lake, MI) with 3% O_2, 5% CO_2 and 92% N_2. The hypoxic chamber was housed in a 37 C incubator. The concentration of oxygen in air was measured using O_2-sensitive electrode system (Dwyer Instruments, Michigan City, IN).

Substrates

Solutions of human fibronectin, laminin, reduced-growth factor Matrigel, and poly-L-ornithine (30000-70000 MW) in DMEM: F12 as well as collagen I (Corning, Corning, NY) in 0.02 N acetic acid and collagen IV (Santa Cruz Biotechnology, Dallas, TX) in 0.05 N hydrochloric acid were prepared for coating 96-well tissue plates. Fibronectin, laminin and poly-L-ornithine solutions were incubated in the 96-well plates overnight in a 37 C, 5% CO_2, humidified incubator and then the wells were rinsed with phosphate-buffered saline (PBS) before plating the cells. Matrigel was incubated in the wells at room temperature for 2 h and subsequently the wells were rinsed and incubated in DMEM: F12 overnight in a humidified 37 C, 5% CO_2 incubator. Collagen I and collagen IV solutions were incubated in the wells at room temperature for 2 h and then the wells were rinsed with sterile water, PBS, and DMEM: F12 before plating the cells. The final concentration of all protein substrates and PLO in the wells was assumed to be 3 $\mu g/cm^2$.

Proliferation assay

To detect hNSC proliferation during culture, the Click-iT EdU proliferation assay (Life Technologies) was performed. The hNSCs were incubated with EdU for 2 and 4 d with EdU being replenished every 2 d to prevent depletion. The cells were then fixed in 4% buffered formaldehyde (Thermo Fisher Scientific, Pittsburgh, PA) for 20 min, permeabilized with Tris-buffered saline (TBS) containing 0.1% Triton-X-100, and incubated with EdU reaction cocktail for 30 min followed by 4',6-diamidino-2-phenylindole (DAPI, 300 nM) nuclear stain. The samples were then imaged under fluorescence microscopy (Olympus, Center Valley, PA) to measure the number of cells that proliferated during EdU incubation. The nuclei of EdU^+ cells fluoresced green because of Alexa Fluor 488 azide fluorescent dye detection. DAPI (blue) stained all nuclei. The numbers of EdU^+ and $DAPI^+$ cells were counted.

Apoptosis assay

To detect cell apoptosis, the terminal deoxynucleotidyl transferase-mediated nick end labeling (TUNEL) assay (Life Technologies) was performed. After 4 d in culture, hNSCs were fixed in 4% buffered formaldehyde, permeabilized, and incubated with terminal deoxynucleotidyl transferase (TdT) buffer for 10 min. The cells were then incubated for 1 h at 37 C with TdT reaction cocktail (according to the manufacturer's instructions) and were subsequently washed two times with 3% goat serum in PBS for 5 min followed by incubation with TUNEL Click-iT reaction cocktail for 30 min. The samples were then stained with DAPI and imaged under fluorescence microscopy. All nuclei fluoresced blue because of the DAPI nuclear

stain; also, the nuclei of TUNEL$^+$ cells fluoresced green due to Alexa Fluor 488 dye detection. The numbers of TUNEL$^+$ and DAPI$^+$ cells were counted.

Statistical Analysis

Experimental results are represented as mean ± SD ($n \geq 3$). Student's t-test and analysis of variance (ANOVA) tests were performed to analyze statistical significance among groups.

Results

To test the effect of substrate type and oxygen concentration on hNSC proliferation, we first determined the total number of cells in culture after 2 and 4 d. Identical numbers of cells were seeded on 96-well plates coated with PLO, collagen I, collagen IV, fibronectin, laminin, and reduced-growth factor Matrigel, and cultured under both normoxic and hypoxic conditions. The hNSCs were subsequently fixed, stained with DAPI nuclear stain, and imaged using fluorescent microscopy. After 2 d and 4 d, we did not detect any DAPI$^+$ hNSCs on collagen I and PLO coated wells (results not shown), suggesting that the hNSCs did not adhere to these two substrates and were washed away during medium replacement or fixation.

The total number of hNSCs cultured on fibronectin and collagen IV substrates decreased over time (**Fig. 5.1**). After 4 d, the hNSCs cultured on collagen IV and fibronectin, under both normoxic and hypoxic conditions, exhibited ~65% and ~20% decreases in cell density, respectively.

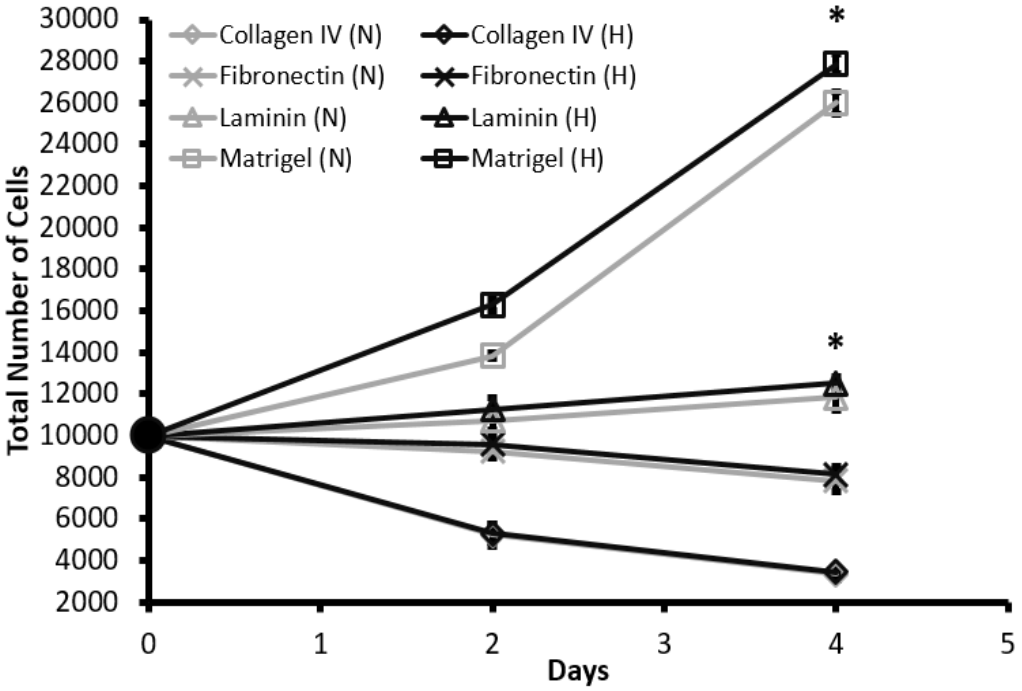

Figure 5.1. Number of total cells (DAPI+) at days 2 and 4 cultured on fibronectin, collagen IV, laminin, and Matrigel substrates. After 4 d, there were no statistical differences in cell number between normoxia and hypoxia for the cells cultured on fibronectin and collagen IV. The total number of cells was significantly higher under hypoxia in comparison with normoxia at day 4 for the cells cultured on laminin and Matrigel ($p<0.05$). The total number of cells cultured on Matrigel are significantly higher than laminin under both normoxic and hypoxic conditions ($p<0.001$). Symbol (*) denotes significant differences ($p<0.05$) between normoxic and hypoxic groups. n>9 samples; one representative set of experimental data is shown. n>50 hNSCs/sample.

To determine whether the decrease in the total cell number is due to cell death or a lack of proliferation, we used EdU pulse-labeling [171] to label the cells in the S-phase of division. After 4 d, the EdU^+ cells constituted 16±1% and 16±0.9% of hNSCs cultured on collagen IV under normoxic and hypoxic conditions, respectively (**Fig.5.2A**). The hNSCs cultured on fibronectin, after 4 d, consisted of 31±1% and 32±1.1% of EdU^+ cells under normoxia and hypoxia, respectively (**Fig.5.2A**). A student's t-test analysis showed no statistical difference in cell density between normoxia and hypoxia for both fibronectin ($t(16) = 0.13$, $p = 0.899$) and collagen IV substrates ($t(16) = 0.37$, $p = 0.72$) after 4 d. In addition, no statistical difference in percentage of EdU^+ cells with respect to oxygen concentration was found for both fibronectin (Student's t-test, $t(16) = 1.28$, $p = 0.219$) and collagen IV ($t(16) = 0.6$, $p = 0.554$). This suggests that oxygen concentration did not influence the proliferation of hNSCs cultured on fibronectin and collagen IV.

The total number of hNSCs cultured on laminin and laminin-rich Matrigel substrates increased over time (**Fig.5.1**). The hNSCs cultured on laminin, after 4 d, exhibited ~18% and ~25% increases in number under normoxia and hypoxia, respectively. The hNSCs cultured on reduced-growth factor Matrigel represent ~160% and ~179% increases in number, after 4 d in normoxic and hypoxic conditions. A two-way ANOVA analysis indicates significant effects of oxygen ($F(1, 32) = 6.81$, $p = 0.014$) and substrate ($F(1, 32) = 145.87$, $p < 0.001$) on hNSC total number after 4 d of culture on laminin and Matrigel with no oxygen-substrate interaction ($F(1, 32) = 0.4$, $p = 0.532$). The EdU proliferation assay for laminin, after 4 d, determined that 11±1% and 14±1% of cells were EdU^+ under normoxia and

hypoxia, respectively (**Fig.5.2B**). For reduced-growth factor Matrigel, 24±1.1% and 31±0.9% of stem cells under normoxia and hypoxia, respectively, were actively proliferating after 4d (**Fig.5.2B**). Similar to cell density, a two-way ANOVA analysis indicates significant effect of oxygen ($F(1, 32) = 8.55$, $p = 0.006$) and substrate ($F(1, 32) = 129.76$, $p < 0.001$) on hNSC proliferation with no interaction ($F(1, 32) = 0.14$, $p = 0.707$).

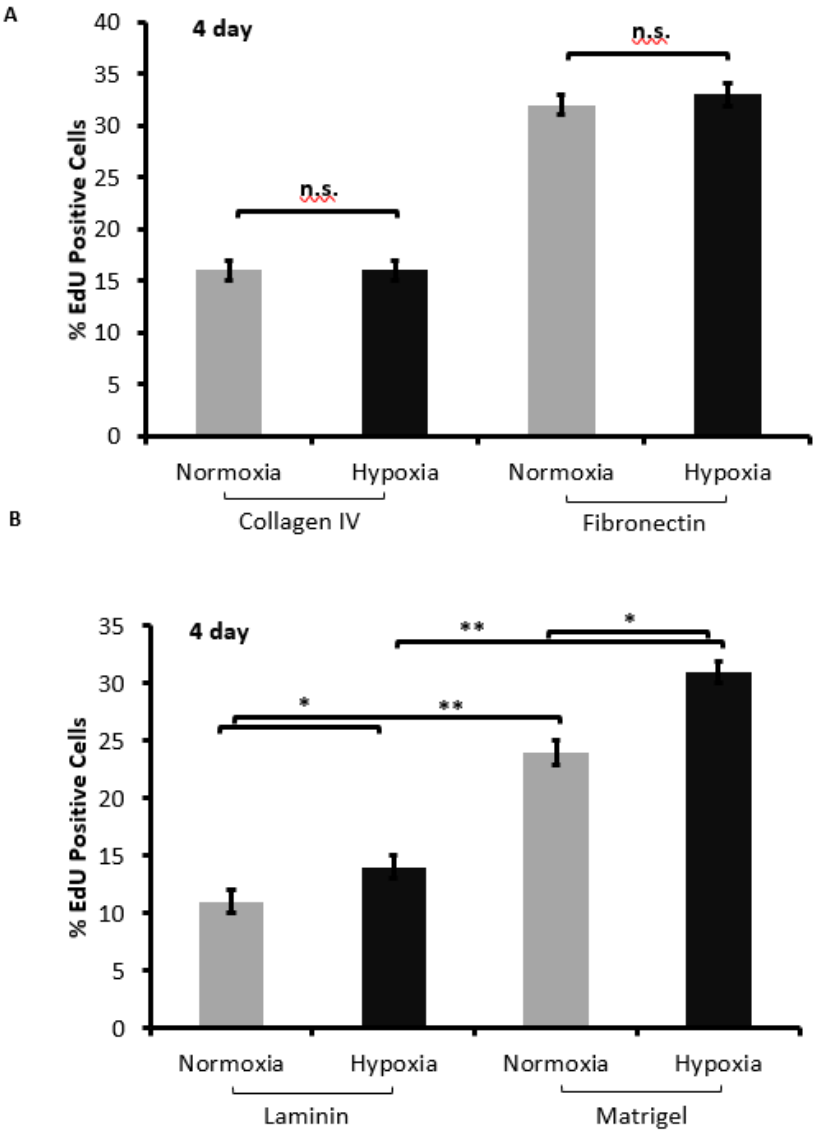

Figure 5.2. The proliferation of hNSCs on fibronectin and collagen IV (A) and laminin and Matrigel (B) substrates.The cells cultured on fibronectin and collagen IV did not exhibit a significant difference in number of actively proliferating cells (EdU^+) between normoxia and hypoxia. The cells cultured on laminin and Matrigel had a higher proliferation under hypoxia in comparison with normoxia ($p < 0.01$). The percentage of EdU^+ cells was significantly higher for the cells cultured on Matrigel compared to laminin under both

normoxic and hypoxic conditions. Symbols denote significant differences (*, $p < 0.01$ and **, $p < 0.001$). A two-way ANOVA analysis indicated significant effects of substrate type and oxygen concentration on hNSC proliferation. Bars represent mean ± SD. n>9 independent experiments; n>50 NSCs/sample.

To clarify whether the temporal decrease in cell numbers in collagen IV and fibronectin cultures is due to cell death, we performed a TUNEL assay to detect the apoptotic hNSCs in culture.[215] After 4 d, in collagen IV cultures, 32±0.6% (normoxia) and 33±0.87% (hypoxia) of hNSCs were apoptotic $TUNEL^+$ cells (**Fig.5.3A**). The hNSCs cultured on fibronectin consisted of 19±0.99% and 20±0.64% of $TUNEL^+$ cells under normoxia and hypoxia, respectively (**Fig.5.3A**). The hNSCs cultured on laminin-rich substrates (i.e., laminin and reduced-growth factor Matrigel) were associated with less apoptosis vs fibronectin and collagen IV substrates. The hNSCs cultured on laminin had 8±0.24% (normoxia) and 7±0.95% (hypoxia) apoptotic cells (**Fig.5.3B**). Similarly, in reduced-growth factor Matrigel cultures, 8±0.71% and 8±0.44% of hNSCs were apoptotic under normoxia and hypoxia, respectively (**Fig.5.3B**). A two-way ANOVA indicates a significant effect of substrate ($F(3, 64) = 1750.30$, $p < 0.001$) on hNSC apoptosis and no effect of oxygen concentration ($F(1, 64) = 1.42$, $p = 0.238$) and oxygen-substrate interaction ($F(3, 64) = 2.02$, $p = 0.121$). Therefore, we concluded that the relatively lower cell density in collagen IV and fibronectin cultures may be due to increased apoptosis vs cells cultured on laminin-rich substrates.

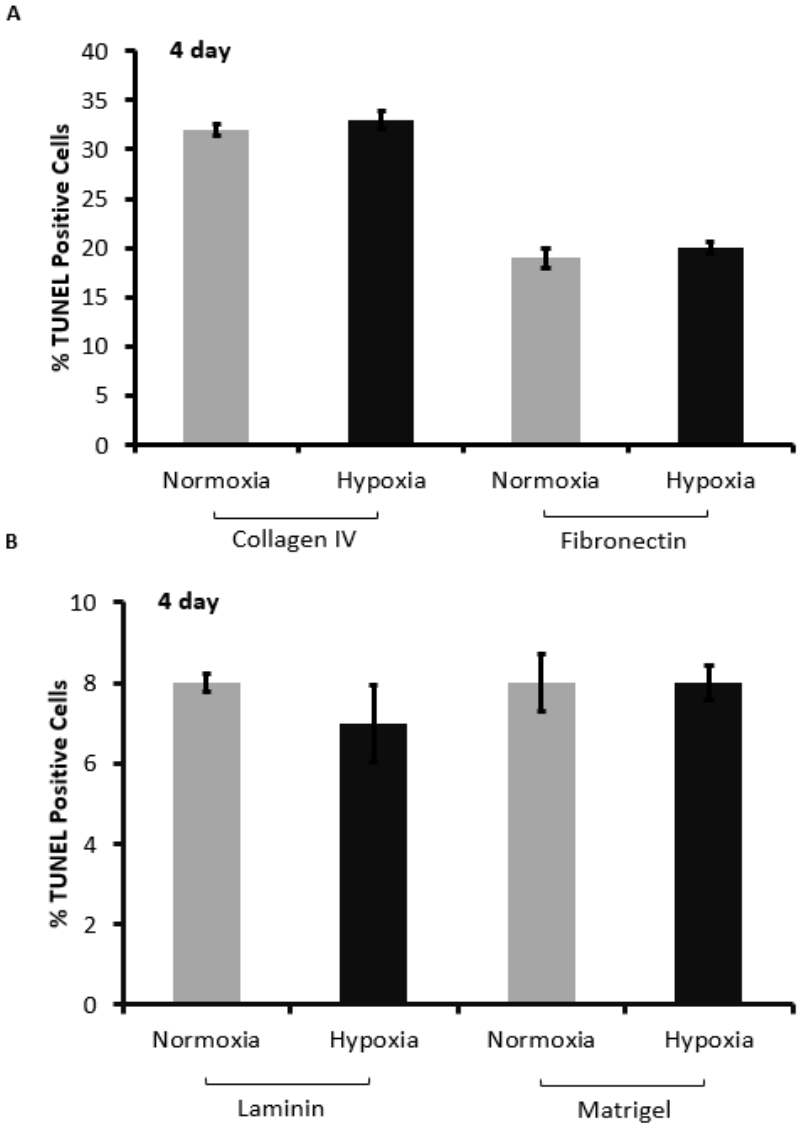

Figure 5.3. The apoptosis of hNSCs cultured for 4 days on fibronectin and collagen IV (A) and on laminin and Matrigel (B) substrates. The cells cultured on collagen IV and fibronectin exhibited ~4 fold and ~2.5 fold higher percentages of apoptotic cells ($TUNEL^{+}$) compared to laminin-rich substrates, respectively. A two-way ANOVA analysis indicated a significant effect of substrate ($p<0.001$) on hNSC apoptosis with no significant effect of oxygen concentration. Bars represent mean ± SD. n>9 independent experiments; n>50 NSCs/sample.

I previously showed in **Chapter 3** that, in the presence of growth factors, hNSCs maintain their undifferentiated state and exhibit negligible differentiation. Based upon this and the EdU proliferation and TUNEL apoptosis results, the hypoxic culture on Matrigel supports the expansion of undifferentiated hNSCs *in vitro*.

Discussion

Our results demonstrate a synergistic effect of laminin-rich substrates (i.e., reduced-growth factor Matrigel) and oxygen concentration on the expansion of hNSCs. These results are consistent with published works [123, 133, 216] showing that laminin-rich substrates promote the proliferation of mouse and human NSCs. We observed that the stem cells exhibit a temporal increase in density when cultured on laminin and laminin-rich Matrigel substrates (**Fig.5.1**). However, the numbers of hNSCs cultured on fibronectin and collagen IV decreased over time (**Fig.5.1**). To start to understand this distinction, we considered the three possible scenarios for the fate of a population of hNSCs: self-renewal, differentiation, or death [3]. The immunofluorescence analysis using stemness markers (i.e., nestin and SOX-2) showed that the majority (>95%) of cells in culture maintained their stemness and did not differentiate into neural or glial progenies (**Chapter 3**). In the absence of differentiation, the total cell number in culture is regulated via two cellular behaviors (i.e., proliferation and death). The EdU assay confirmed that hNSC proliferate regardless of substrate type and oxygen concentration (**Fig.5.2A, B**). Therefore, the relative differences in total cell numbers under different conditions could be explained by differing extents of cell death.

We thus investigated hNSC apoptosis when cultured under all conditions by performing the TUNEL apoptosis assay (**Fig.5.3A, B**). Our results indicate that the substrate composition had a significant effect ($p<0.001$) on the survival of hNSCs with no significant difference between normoxia and hypoxia ($p = 0.238$). Percentages of apoptotic ($TUNEL^+$) cells were greatest for collagen IV (~32%) and fibronectin (20%, **Fig.5.3A**) whereas in laminin and Matrigel cultures the percentages of apoptotic cells were lower (~8%, **Fig.5.3B**). Therefore, the higher percentage of apoptotic cells in collagen IV and fibronectin cultures may explain the lower density of hNSCs on these two substrates.

The binding of cells to ECM is mediated via cell-surface receptors such as integrins [129]. The hNSCs express high levels of $\alpha_6\beta_1$ integrin [217], which binds to laminin. However, hNSCs express only low levels of fibronectin-binding receptors ($\alpha_5\beta_1$ and $\alpha_V\beta_1$) and collagen IV receptors ($\alpha_1\beta_1$ and $\alpha_2\beta_1$) [128, 151, 217]. For instance, it has been shown that $\leq$2% of hNSCs express α_1 and α_2 integrin subunits [123] which are required for adhesion to collagen I and collagen IV. For a variety of cells, proper integrin-mediated binding to ECM plays a crucial role in cell survival [218, 219]. Thus, the lower survival of hNSCs cultured on fibronectin and collagen IV may be due to low expression of appropriate integrin receptors and consequently insufficient cell-ECM adhesion.

The hNSCs cultured for 4 d on Matrigel had a ~2 fold greater increase in total cell numbers in comparison with the cells cultured on laminin regardless of oxygen concentration (**Fig.5.1**). The number of actively proliferating cells, as determined by an EdU assay, is also ~2 fold higher on Matrigel versus laminin at 4 d regardless of

oxygen concentration (**Fig.5.2B**). Matrigel is a secreted ECM extracted from Engelbreth-Holm-Swarm mouse tumor and is a complex mixture of laminin, collagen IV, entactin, and heparin sulfate proteoglycans [220]. Since laminin is one of many constituents of Matrigel, the concentration of laminin in Matrigel-coated substrates is expected to be lower than on laminin-coated substrates. Therefore, other components of Matrigel are likely responsible for the enhanced cell numbers vs laminin alone. Growth factor signaling in synergy with β_1 integrin signaling play a regulatory role in hNSC maintenance [221]. Therefore, the enhanced proliferation of hNSCs on Matrigel may be due to the presence of heparin sulfate proteoglycans, which stabilize heparin-binding growth factors such as FGF, providing protection from degradation [222-224], and allowing upregulation of growth factor signaling processes involved in adhesion and survival.

For the hNSCs cultured on laminin and Matrigel, hypoxic conditions are associated with significant increases both the stem cell density (**Fig.5.1**) and the percentage of actively proliferating (EdU^+) cells over time (**Fig.5.2B**). However, for hNSCs cultured on fibronectin and collagen IV, the lowered oxygen concentration does not affect hNSC density and proliferation (**Fig.5.1 and Fig.5.2A**). Thus in summary, we report that the synergistic effect of the laminin-rich substrate (i.e. Matrigel) and lowered oxygen concentration increases the rate of hNSC *in vitro* expansion. Manipulation of oxygen concentration in culture provides a scalable and a xeno-free alternative to enhance *in vitro* hNSC growth. We acknowledge that Matrigel and laminin are both animal-derived and hence xenogeneic. However, this result may inform the development of new xeno-free biomaterial substrates with the

capability of binding to $\alpha_6\beta_1$ integrins, stabilizing growth factors, and maintaining high levels of proliferation.

Chapter 6: Conclusions and Future Directions

The progressive neural and glial cell degeneration in neurodegenerative disorders cause debilitating difficulties in movement (ataxia) and mental functioning (dementia) of the patients. To date, there is no disease modifying therapy with the capability of halting the disease progression and regenerating the damaged neural tissue. Transplantation of neural stem cells (NSCs) with tissue-specific differentiation capacity provides a promising therapeutic modality for the treatment of these diseases. A proof of principle for the effectiveness of cell-replacement therapy was obtained from the transplantation of human NSCs in patients with Parkinson's disease. However, the variability in functional outcome, poor cell survival, and the limited availability of NSCs are among the major challenges that need to be resolved to achieve effective and efficient therapies.

The current dissertation assumes that the key to enhance the functional efficacy of NSC grafts relies on the improvement of the *in vitro* culture methods utilized for generation of NSCs transplants. A prerequisite for designing modified culture methods is to investigate how the essential components and interactions of the *in vivo* microenvironment influence the NSC fate. Therefore, herein, the effects of culture dimensionality, reduced oxygen concentration (hypoxia), growth factors as well as the interactions between cells and the extracellular matrix (ECM) on the survival, growth, and differentiation behavior of human NSCs have been examined. Overall, this dissertation, provides a foundation for designing improved strategies for *in vitro* characterization, expansion, and differentiation of human NSCs.

Characterizing the Effect of Culture Dimensionality, Oxygen Concentration, and Growth Factors on Human Neural Stem Cell Survival, Proliferation, and Differentiation

NSCs, *in vivo*, reside within a local niche that regulates stem cell maintenance in a three dimensional (3D) microenvironment under hypoxic oxygen concentrations and in the presence of soluble factors. However, *in vitro*, NSCs have been traditionally studied on two dimensional (2D) surfaces under normoxia. This discrepancy between the *in vivo* scenario and the conventional *in vitro* 2D normoxic cultures may be an underlying reason for the heterogeneous outcomes observed in clinical trials. Therefore, the first project in the current dissertation was inspired by the need to characterize the regulatory effects of culture dimensionality, oxygen concentration, and growth factors on the survival, proliferation, and differentiation behavior of NSCs. The results of this characterization will aid in delineating the individual and synergistic effects of these important culture parameters on human NSC behavior and will further our ability in generating cellular transplants with well-defined compositions.

Contributions of the current dissertation

In **Chapter 3**, I demonstrated a synergy between hypoxia and three dimensionality of the culture that positively regulates the proliferation and differentiation behavior of human NSCs. I cultured human NSCs in the presence and absence of growth factors, under both normoxic and hypoxic conditions, as well as in 2D and 3D cultures. In the presence of growth factors, regardless of hypoxia and

dimensionality, the cellular composition of the cultures consisted of viable undifferentiated NSCs. However, hypoxia and dimensionality individually and synergistically enhanced the proliferation of the cells resulting in NSC expansion in number. The largest population of NSCs was detected in 3D hypoxic cultures, indicating a positive synergistic regulatory effect of dimensionality-hypoxia on the cell growth. The synergistic cooperation of culture dimensionality and hypoxia, in the absence of growth factors, yielded the most number of differentiated progenies. Thus, I report that the niche-derived environmental cues play an important role in regulating human NSC temporal output and that the 3D hypoxic cultures may provide a more physiologically relevant *in vitro* culture method for human NSCs.

Future Directions

- Performing growth factor dose-dependent studies under both hypoxia and normoxia and in 2D and 3D cultures to discover the optimum growth factor concentration that in synergy with hypoxia and dimensionality provides the maximum number of viable undifferentiated cells.
- Investigating the signaling pathways that may be responsible for less restricted proliferation of NSCs under hypoxia. Measuring the expression of hypoxia-inducible factor-1α (HIF-1α) as well as FGFR-1 and EGFR growth factor receptor expression under both normoxic and hypoxic conditions and examining their possible synergy with notch signaling pathway can be a viable starting point for this project.

- Measuring the expression of cyclin D1 protein in 2D and 3D cultures to determine whether the overexpression of cyclin D1 protein plays a role in shorter NSC cycle lengths in 3D cultures.

In Vitro Hypoxic Preconditioning for the Enhancement of Human Neural Stem Cell Survival and Differentiation

A major challenge limiting the effectiveness of NSC-mediated therapy is the low survival of the transplanted cells which can be as low as 10% of the total cell number. The extensive NSC death after implantation results in limited generation of terminally differentiated neurons and glia and overall reduces the efficacy of the therapy. Therefore, the second project (**Chapter 4**) in the current dissertation was inspired by the need for the development of novel strategies that can enhance the survival and differentiation of NSCs after transplantation. Even though the pro-survival strategies based upon permanent gene alteration have shown to enhance the survival of the engrafted NSCs, these methods may have an increased risk of tumorigenicity. On the other hand, *in vitro* hypoxic preconditioning (HP) of mesenchymal and embryonic stem cells prior to transplantation has resulted in enhanced survival and regenerative capacity of the stem cells after implantation. HP provides a simpler and safer non-genetic pro-survival strategy. However, to this date, the effect of HP on the survival and differentiation behavior of human NSCs is not well understood. Therefore, I sought to investigate whether an *in vitro* hypoxic culture could provide a permissive environment for enhanced survival and differentiation of human NSCs.

Contributions of the current dissertation

In **Chapter 4**, I demonstrated that short-term HP enhances the survival of human NSCs and long-term HP promotes the differentiation of human NSCs towards neural progenies without reducing their survival. Human NSC differentiation into neurons and glia, *in vivo*, lasts as long as 70 d. Based upon this initial understanding from the *in vivo* situation, I defined four culture periods in my experimental design: 4 and 10 d (short-term HP) and 30 and 60 d (long-term HP). I, first, sought to assess whether short-term HP influences the NSC survival and, then, extended the culture periods to 30 and 60 d to assess both the long-term survival and the extent of differentiation into neurons and glia. The short-term HP preconditioning yielded more number of NSCs over the course of 10 d due to higher proliferation of the cells and no difference in cell viability. After 30 and 60 d, even though there was no difference in cell number and viability between hypoxic vs normoxic cultures, long-term HP promoted the differentiation of NSCs towards neural progenies. These results introduce HP as a promising method for enhancing human NSC survival and differentiation.

Future Directions

- Investigating the long-term (30 and 60 d) differentiation potential of human NSCs cultured within 3D hydrogels.
- Measuring the expression of vascular endothelial growth factor (VEGF) and erythropoietin (EPO) in both normoxic and hypoxic long-term differentiation cultures. This may be a viable starting point to explain the enhanced generation of neural progenies under hypoxia.

Synergistic Effect of Hypoxia and Laminin-rich Substrates on the Enhancement of Human Neural Stem Cell Growth

The number of stem cells required for clinical therapies falls in the range of a few tens of millions to a few billion per patient. The production of such quantities of stem cells in a cost-effective and scalable manner is a prerequisite for exploiting the therapeutic potential of stem cells. Currently, the *in vitro* expansion of NSCs is accomplished by utilizing proliferative factors which are costly and, hence, have a limited ability for scalability. In the NSC niche, the oxygen concentration and the interactions between cells and the ECM are the two important regulators of NSC proliferation. Yet, the synergistic relationship between hypoxia and the ECM composition on human NSC proliferation is not well understood. Compared to growth factors, oxygen is more easily scalable and widely available. Therefore, manipulation of oxygen concentration in NSC cultures provides a powerful strategy for *in vitro* expansion of these cells. Therefore, the third project in this dissertation (**Chapter 5**) was inspired by the need for the development of cost-effective methods for rapid and scalable *in vitro* production of human NSCs.

Contributions of the current dissertation

In **Chapter 5**, I analyzed the growth of human NSCs on six different substrates (collagen I, poly-L-ornithine, fibronectin, collagen IV, laminin, and Matrigel) under normoxia and hypoxia. The cells, regardless of oxygen concentration, did not adhere to collagen I and poly-L-ornithine and the cells cultured on collagen

IV and fibronectin decreased in number over time due to insufficient cell-ECM binding and apoptosis. The NSCs that had been cultured on Matrigel and laminin exhibited a temporal increase in cell density which indicates the individual positive effect of laminin-rich substrates on human NSC growth. The hypoxic Matrigel cultures had the highest cell density and number of actively proliferating cells followed by normoxic Matrigel, hypoxic laminin, and normoxic laminin cultures. This suggests an individual positive effect of oxygen concentration and a synergistic effect of substrate-oxygen on human NSC growth. Thus, I report that laminin rich substrates as well as hypoxia positively regulate the proliferation of human NSCs and the synergistic effect of Matrigel-hypoxia yields the highest growth.

Future Directions

- Comparing and contrasting the expansion of human NSCs derived from other sources such as adult brain and induced pluripotent stem cells (iPSCs) cultured on Matrigel under normoxia and hypoxia to test whether the Matrigel-hypoxia synergy provides a generalizable cell expansion strategy.

Chapter 7: Appendix

Culture and Immunofluorescence Staining of Human Neural Stem Cells in Two Dimensional Platforms and Three Dimensional Hydrogels

The human neural stem cell (NSC) model utilized in this dissertation (RenCell-CX, Millipore, SCC007) is a commercially available immortalized cell line derived from 14-week gestation human fetal cerebral cortex. In this chapter, I provide methods for two dimensional (2D) and three dimensional (3D) culture of these cells as well as the protocols for immunofluorescence staining and assessing viability of these cells.

Reagents and Supplies Required for 2D Culture, Passaging, and Freezing of NSCs

1. 1×10^6 vial of viable RenCell-CX cells (Millipore, SCC007)
    a) **Note**: Many thanks to Dr. Elizabeth M. Powell for generously providing the NSCs for the experiments performed in the current dissertation.
2. DMEM/F12 culture medium without HEPES and with L-Glutamine (Millipore, DF-042-B)
3. 50x B27 supplement (ThermoFisher, 17504044)
4. Heparin sodium salt (Sigma Aldrich, H3149)
5. Fibroblasts growth factor-2 (FGF-2, Millipore, GF003)
6. Epidermal Growth Factor (EGF, Millipore, GF001)
7. Accutase™ (Millipore, SCR005)
8. Laminin mouse protein (ThermoFisher, 23017015)
9. Gentamicin (ThermoFisher, 15750060)

10. Phosphate-buffered saline (PBS), sterile
11. Fetal Bovine Serum (ThermoFisher, 10437-028)
    b) **Note**: This serum in only used for freezing the cells.
12. Dimethyl sulfoxide (DMSO)
    c) **Note**: DMSO is only used for freezing the cells.
13. Sterile water
14. Tissue culture-ware

Methods

Preparation of coated flasks

1. After receiving the frozen vial of the cells, immediately store the vial in a liquid nitrogen tank.
    a) **Note**: Please keep in mind that RenCell-CX is a very sensitive cell line and it is absolutely necessary to store the cells in a liquid nitrogen tank and not the -80 C freezer.
2. Thaw the laminin at a 4 C fridge.
    b) **Note 1**: The concentration of laminin varies from batch to batch (1 to 1.2 mg/ml). Please note the concentration listed in the product catalog in your lab notebook.

    Note 2: Please avoid performing repeated freeze-thaw cycles of laminin. Definitely make aliquots of laminin in autoclaved Eppendorf tubes.

3. Dilute laminin in DMEM/F12 to the final concentration of 20 µg/ml and add the diluted solution to cover the entire surface of a T-75 tissue culture-ware (5 ml of the solution is enough for a T-75 culture flask).
4. Incubate the tissue culture-ware in a 37 C, 5% CO_2 regular incubator for at least 4 h.
5. Before plating cells in the coated tissue culture-ware, aspirate the laminin solution and rinse the flask once with 1x PBS.

Preparation of the NSC medium

1. Add 5 ml of DMEM/F12 to the heparin sodium salt container and pipette up and down multiple times to ascertain a well-mixed solution
2. Filter-sterilize the heparin solution by using a syringe filter and subsequently add 2.5 ml of the heparin solution to a 500 ml bottle of DMEM/F12
3. Add the 50x B27 supplement to a 500 bottle of DMEM/F12
4. Add sterile water to the vials of FGF-2 and EGF and prepare multiple growth factor aliquots with a final concentration of 0.5 µg/µl
    a) **Note**: Store the aliquots in a -20 C freezer and do not add them to the medium at this point. The EGF and FGF-2 should be freshly added to the medium when the cell culture is being performed.

Thawing the vial of NSCs (RenCells)

1. Before thawing the cells, please ascertain that the laminin coated T75 tissue culture-ware and the culture medium is ready.

2. Make an aliquot of the culture medium and warm it in a 37 C water bath and then add gentamicin to the pre-warmed culture medium (containing heparin and B-27) at a final concentration of 30 µg/ml.
3. Remove the RenCell vial from the liquid nitrogen tank and thaw the vial of the cells immediately in a 37 C water bath. Please carefully monitor the vial and make sure that the vial is entirely thawed and as soon as the vial is thawed proceed to the next step. Please keep in mind that acquiring the maximum viability is a function of complete and rapid thawing.
4. Immediately transfer the cell suspension into a 15 ml centrifuge Conical tube and avoid introducing any bubbles during the transfer process.
5. Very slowly (dropwise) add 9 ml of the pre-warmed cell culture medium to the 15 ml tube and avoid creating any bubbles.
6. Very gently mix the cell suspension by slow pipetting up and down.
7. Centrifuge the tube at 300 × g for 5 minutes to pellet the cells.
8. In the meantime, prepare the complete growth medium by adding FGF-2 and EGF at a final concentration of 20 ng/ml to the culture medium.
    a) **Note**: FGF-2 and EGF should always be added fresh to the culture medium.
9. Discard the supernatant.
10. Gently, resuspend the cells in 5 ml of the complete growth medium by pipetting up and down.

11. Plate the cell suspension onto a laminin coated T-75 tissue culture-ware and add an extra 5 ml of the complete growth medium to the flask and place the flask in a regular incubator for 24 h.
12. Replace the medium with a fresh complete growth medium the next day.

Passaging the NSCs

1. At least, 4 h before passaging, prepare a freshly laminin coated tissue culture-ware (a T-75 or a T-25 flask and a 96- or 48- or a 24-well tissue culture plate if you are initiating an experiment).
2. Aspirate the old complete growth medium in the T-75 flask and gently rinse the flask with 1x PBS.
3. Add 5 ml of Accutase™ to the flask and place the flask in a regular incubator for 5 min.
4. Add 10 ml of pre-warmed complete growth medium to the flask and gently pipette up and down twice to make sure the cells are detached.
5. Transfer the cell suspension into a 15 ml centrifuge Conical tube.
6. Centrifuge the tube at 300 × g for 5 minutes to pellet the cells.
7. Discard the supernatant.
8. Resuspned the cells in 5 ml of complete growth medium.
9. Count the number of cells by using hemocytometer.
10. Plate the cells into a pre-warmed freshly laminin coated tissue culture-ware at a density of 7×10^{3} cell/cm^2

a) **Note**: At this point, if you are trying to initiate an experiment, you can culture the cells in laminin coated 96- or 48- or 24-well tissue culture plates at a desired cell density (depending upon the experiment).
b) Always make sure that you have enough cells for starting an experiment as well as maintaining a population of NSCs for future experiments. Do not use all your cells for one experiment. In this case, you will not have any cells for the future experiments and will have to thaw a new vial.
c) If your experiments require continuous growth of NSCs you need to make sure that the culture medium is supplemented with FGF-2 and EGF (the complete growth medium).
d) If you are intending to study the differentiation of RenCells, allow the cells to attach to the 96- or 48- or 24-well tissue culture plates in the complete growth medium for 3 h after plating and then replace the complete growth medium with a culture medium that does not contain FGF-2 and EGF

Freezing the NSCs

1) Ascertain that you have cryovial tubes available.
2) Prepare two 15 ml Styrofoam tube trays. You will need to sandwich the cryovials between these Styrofoam trays at step 8. The Styrofoam trays will allow the cells to freeze over time (ideally -1 C/min) and not abruptly. This will result in enhanced viability of the cells.
3) Follow the passaging protocol up to step 7.

4) Resuspend the cells in a complete growth medium containing 20% FBS (v/v).
5) Count the number of cells.
    a) **Note**: The optimum density for freezing is 1-5 $\times 10^6$ cell/ml in the cryovials.
6) Add 10% DMSO to the cell suspension and very gently pipette the suspension up and down three times to ensure a homogeneous mixture.
7) Immediately, transfer the cell suspension that contains DMSO to the cryovials.
8) Immediately, sandwich the vials between the Styrofoam trays and immediately transfer the trays to a -80 C freezer.

    Note: Please keep in mind that the time between adding DMSO and the time to transfer the vials to the -80 C freezer should be minimized (this is very important).
9) After 24 h, transfer the vials to a liquid nitrogen tank. This step is absolutely necessary.

    Note: Do not freezer the cells in a –20 C freezer, it is too warm!!!

Reagents and Supplies Required for 3D Encapsulation of NSCs in 3D Collagen Hydrogels

1. Collagen stock solution: Collagen, type I from rat tail, concentration range 3-4 mg/ml in 0.02 N acetic acid, (Corning, 354236), sterile, store at 4°C
2. Dulbecco's modified Eagle's medium (10x DMEM, Sigma Aldrich, D2429), sterile, store at 4 C

3. 7.5% (w/v) sodium bicarbonate solution, sterile filtered, suitable for cell culture (Sigma Aldrich, S8761)
4. Laminin mouse protein (ThermoFisher, 23017015)
5. Phosphate-buffered saline (PBS), sterile
6. Sterile water
7. Coverslips, 12-mm diameter, glass
8. 24-well tissue culture plates, sterile

Methods

1. Please ascertain that you have autoclaved and appropriately sealed in-box Eppendorf tubes. Keep the box in a 4 C fridge.
2. Make sure that you have aliquots of laminin, FGF-2, and EGF.
3. Follow the passaging protocol up to step 9 and write down the number of available cells in your lab notebook.
4. Determine the final volume of your solution and the desired final concentration of collagen in the solution:

$$Volume\ of\ collagen = \frac{Final\ volume \times Final\ collagen\ concentration\ (\frac{mg}{ml})}{Stock\ collagen\ concentration\ (\frac{mg}{ml})}$$

For example, if you would like to make 30 gels (25 µl each in volume) then the final volume of your solution will be 750 µl. The final concentration of collagen varies depending upon the experiment and the stock concentration of collagen varies from batch to batch and it is labeled on the collagen container

procured from Corning. However, here, we assume the final concentration of collagen is 2 mg/ml and the stock concentration is 4 mg/ml. Therefore, the volume of collagen you need is:

$$\textit{Volume of collagen} = \frac{750 \times 2\ (\frac{mg}{ml})}{4\ (\frac{mg}{ml})} = 375\ \mu l$$

5. In the laminar flow hood:
   a) Add the following volume of 10x DMEM and sodium bicarbonate solution to a cold empty tube:

$$\textit{Volume of 10x DMEM} = \frac{Final\ volume}{10} = \frac{750}{10} = 75\ \mu l$$

$$\textit{Volume of sodium bicarbonate} = \frac{Final\ volume}{10} = \frac{750}{10} = 75\ \mu l$$

   b) Calculate the volume of laminin, FGF-2, and EGF based upon the final concentration that you need. The final concentration of laminin, FGF-2, and EGF varies depending upon the experiment. Here, we assume the final concentration of laminin that we need is 20 µg/ ml and the final concentration of FGF-2 and EGF is 20 ng/ml. If the stock concentration of laminin is 1 (mg/ml) and the stock concentration of FGF-2 and EGF is 0.01 (mg/ml) then:

$$\textit{Volume of laminin} = 15\ \mu l$$

$$\textit{Volume of FGF-2 and EGF} = 1.5\ \mu l$$

c) Add to the 10x DMEM and bicarbonate solution the following volume of sterile water:

Volume of water = Final volume – final volume of collagen – volume of 10X DMEM – volume of sodium bicarbonate – volume of laminin - volume of FGF-2 - volume of EGF - volume of cell suspension (volume of cells is also equal to final volume divided by 10 or 75 µl in this case*)*

Volume of water = 750 – 375 – 75 – 75 – 15 – 1.5 – 1.5 – 75 = 132 µl

d) Add calculated volume of collagen.

e) Add cold sodium bicarbonate in 10 µl increments followed by mixing until the solution turns purple, indicating pH~8.

Note: It will be extremely helpful if you use PH papers before starting any experiments involving cells to exclusively observe the correlation between the color of the solution and the corresponding PH.

f) Add the calculated amount of laminin, FGF-2, and EGF.

g) Add the calculated amount of cell suspension.

h) By using a micropipette, pipette up and down a few time to ensure a homogeneous mixture.

i) Pipette 25 µL of the collagen/cell solution onto an untreated sterile coverslip in a 24-well plate.

j) Incubate the plate in a 37 C cell culture incubator for 30-40 minutes to allow the solution to form a soft solid gel. The sign of proper gelation is that gel will start floating in the medium.

k) Carefully add 500 µL medium to each well.

l) Incubate the plate in a 37°C cell culture incubator.

Reagents and Supplies Required for 2D and 3D Viability Analysis and Immunofluorescence of Human NSCs

1. LIVE/DEAD cell viability assay for mammalian cells (ThermoFisher, L3224)
2. Primary antibodies (**Table 6.1**)
3. Secondary Antibodies
4. Normal goat serum (ThermoFisher, 50062z)
5. 300 µM 4',6-diamidino-2-phenylindole dihydrochloride (DAPI; Life Technologies, D1306) in water. Prepare 1 ml aliquots in Eppendorf tubes and store at -80°C. Protect from light using aluminum foil.
6. 8% buffered formaldehyde in PBS
7. Fluoromount-G (SouthernBiotech, 010001)
8. Phosphate-buffered saline (PBS), sterile
9. Tris-buffered saline (TBS)
10. Multiwell chamber coverslip, 9 mm, 1 mm depth (ThermoFisher, C24778)
11. Parafilm
12. Aluminum foil

Table 7. 1. The list of primary antibodies and the corresponding suppliers

Primary Antibody	Supplier Company	Catalog Number
SOX-2	Millipore	AB5603
Nestin	Millipore	MAB5326
DCX	Millipore	MABN707
TUJ-1	Covance	801201
MAP-2	Abcam	Ab11267
GFAP	Abcam	Ab4674
S100β	Abcam	Ab52642
GalC	Millipore	MAB342

Abbreviations: DCX doublecortin (DCX), microtubule associated protein-2 (MAP-2), glial fibrillary acidic factor (GFAP), galactocerebroside (GalC).

Methods

Viability staining

1. At the end of the culture period, aspirate the medium and add the cell-permeant fluorescent green calcein AM dye at the concentration of 2 µM and the red nucleus stain ethidium homodimer-1 at the concentration of 4 µM to each well. Incubate 2D cultures for 30 minutes and 3D cultures for 45-60 minutes.

Note: The optimal concentration of calcein AM and ethidium homodimer-1 may vary depending upon the cell type. For both dyes, select concentrations that do not cause significant fluorescence in the cell cytoplasm.

2. For 2D cultures, aspirate the calcein AM-ethidium homodimer-1 solution after 30 minutes and add a sufficient amount of PBS to create a very thin film of liquid at the bottom of the well. This is necessary in order to prevent the cells from drying. Do not add to much PBS because that may create background noise when you are performing fluorescence microscopy.

   Note: For viability staining, it is absolutely necessary to perform the fluorescence microscopy immediately after adding PBS.

3. For 3D cultures, aspirate the calcein AM-ethidium homodimer-1 solution after 45-60 minutes and wash the gels once in PBS for 10 min.
4. Immediately mount the gels. For mounting, add one drop of mounting medium per well of the multiwell chamber coverslip. Very carefully, place the coverslip and gel on the drop of mounting medium. Be careful not to introduce any bubbles and not to fold the gel.
5. Perform fluorescence microscopy.
6. Count the number of live (calcein AM^+, green) and dead (ethidium homodimer-1^+, red) cells in 3 to 5 in 3 samples in each of 3 replicates (total n $\geq$ 18) and calculate the percentage of viability utilizing the following formula:

$$\% \text{ Viability} = \frac{Number\ of\ live\ cells\ (green)}{number\ of\ live\ cells\ (green) + number\ of\ dead\ cells\ (red)}$$

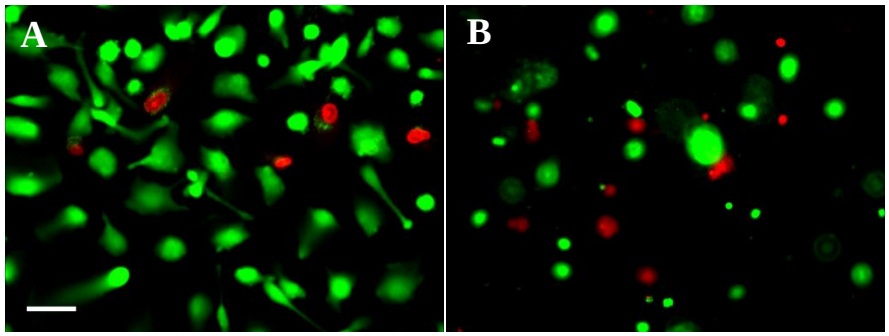

Figure 7.1. Viability staining sample images of 2D and 3D cultures. Human NSCs were cultured on 2D 96-well tissue culture plates (**A**) and within 3D collagen-laminin hydrogels (**B**) for 10 d in the presence of growth factors and were then stained with LIVE/DEAD viability assay and imaged using fluorescence microscopy.

2D Immunofluorescence

1. At the end of the culture period, add 100 µl of 8% formaldehyde to 100 µl of the culture medium. Therefore, the final concentration of formaldehyde will be 4% in each well. Allow to react at room temperature for 10 minutes.

   Note: The volumes mentioned here in the immunofluorescence section are for 2D cultures in a 96-well tissue culture plates.
2. Aspirate the formaldehyde-medium solution and add 100 µl of ice cold PBS buffer to each well and leave it in the well for 10 min. Perform two more washes with ice cold PBS (duration of each wash: 10 min). At this point, you can either initiate the staining process or add 100 µl of ice cold PBS to each well and wrap the tissue-culture ware with Parafilm and store the plate at a 4 C fridge for up to several weeks.

3. Wash the samples with PBS two times for 10 min each, then one time in 0.1% Triton X-100 in PBS for 10 min, then 3 times in PBS for 10 min each.

   Note: Early in your experiments, you can try and see whether PBS or TBS provides better results during the washing steps.

4. To block non-specific binding, add 100 µl of 10% goat serum to each well and incubate the serum for 30 min.
5. Add the desired primary antibodies diluted in 10% goat serum to each well. To save more antibody, you can add 50 µl of the antibody-serum solution to each well. See **Table 6.1** for the recommended antibodies. Incubate the plate overnight at a 4 C fridge.

   Note: For finding the appropriate dilution factors, search for the scientific papers that studied the similar cell line(s). This will help significantly with discovering the appropriate range of dilutions for each antibody.

6. Wash the samples with PBS two times for 10 min each, then one time in 0.1% Triton X-100 in PBS for 10 min, then 3 times in PBS for 10 min each.
7. Add 50 µl of fluorescently-tagged secondary antibody diluted in 10% goat serum and incubate for 2 h at 4 C.
8. Wash the samples with PBS two times for 10 min each, then one time in 0.1% Triton X-100 in PBS for 10 min, then 3 times in PBS for 10 min each.

9. To stain nuclei, prepare a solution of DAPI at 300 nM in water or PBS, which is a 1:1000 dilution of the 300 µM DAPI stock aliquots. Add 100 µL of 300 nM DAPI to each well and allow to react at room temperature for 10 minutes.
10. Wash the samples with PBS two times for 10 min each.
11. Wrap aluminum foil around the plates to prevent light exposure (keep in mind that the secondary antibodies are light sensitive) and store the plates in a 4 C fridge.
12. Perform fluorescence microscopy.

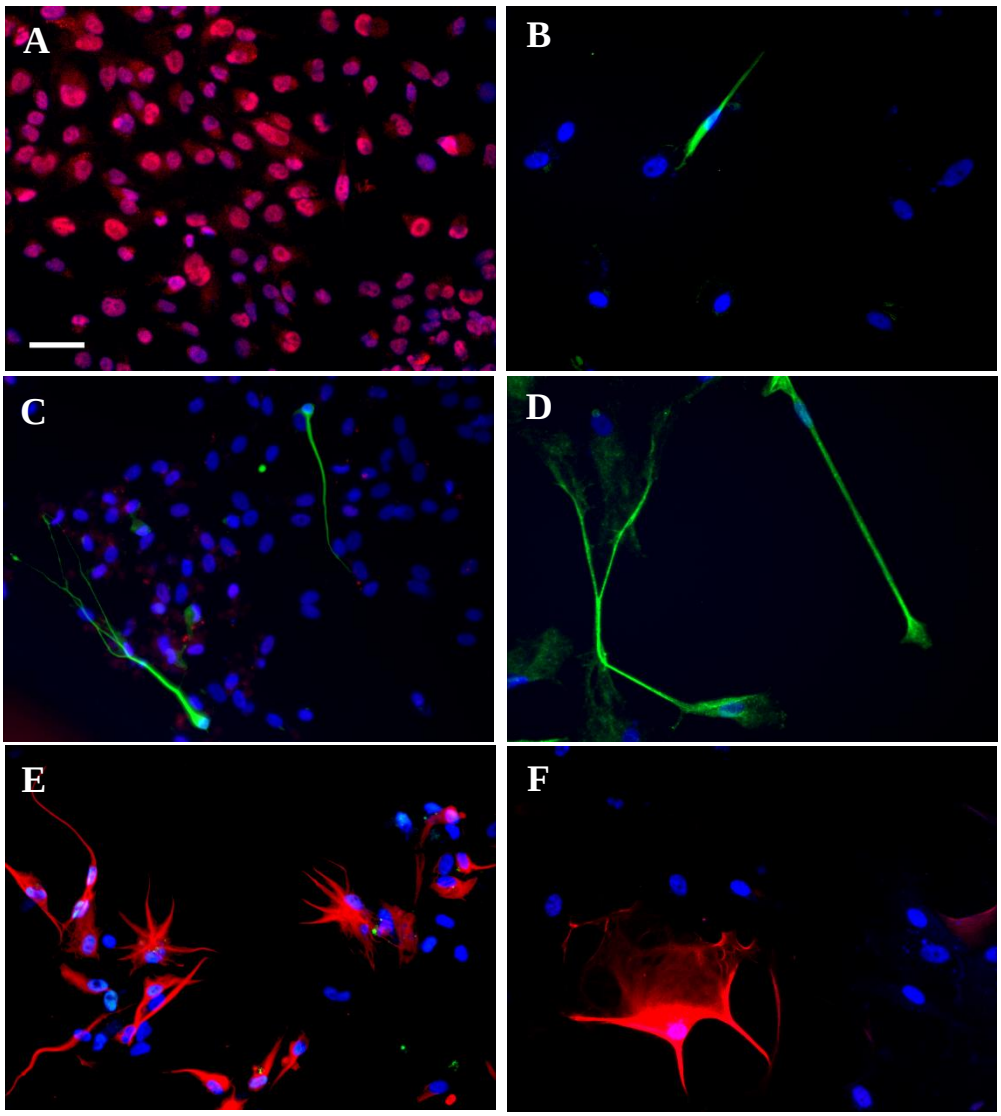

Figure 7.2. Immunofluorescence staining sample images. Human NSCs were cultured on 2D 96-well tissue culture plates and stained with SOX-2 (**A**), DCX (**B**), TUJ-1 (**C**), MAP-2 (**D)**, GFAP (**E**), and S100β (**F**). Scale bar 50 µm.

3D Immunofluorescence

1. At the end of the culture period, add 500 µl of 8% formaldehyde to 500 µl of the culture medium. Therefore, the final concentration of formaldehyde will be 4% in each well. Allow to react at room temperature for 30 minutes.
2. Aspirate the formaldehyde-medium solution and add 500 µl of ice cold PBS buffer to each well and leave it in the well for 10 min. Perform two more washes with ice cold PBS (duration of each wash: 10 min). At this point, you can either initiate the staining process or add 500 µl of ice cold PBS to each well and wrap the tissue-culture ware with Parafilm and store the plate at a 4 C fridge for up to several weeks.
3. Wash the samples with PBS for 25 min, then two times in 0.1% Triton X-100 in PBS for 25 min each, then two times in PBS for 20 min each.
4. To block non-specific binding, add 300 µl of 10% goat serum to each well and incubate the serum for 2 h.
5. Add the desired primary antibodies diluted in 10% goat serum to each well (300 µl per well). See **Table 6.1** for the recommended antibodies. Incubate the plate overnight at a 4 C fridge.
6. Wash the samples two times with PBS for 25 min each, then two times in 0.1% Triton X-100 in PBS for 25 min each, then two times in PBS for 20 min each.
7. Add 300 µl of fluorescently-tagged secondary antibody diluted in 10% goat serum and incubate at 4 C overnight.

8. Wash the samples two times with PBS for 25 min each, then two times in 0.1% Triton X-100 in PBS for 25 min each, then two times in PBS for 20 min each.
9. To stain nuclei, prepare a solution of DAPI at 300 nM in water or PBS, which is a 1:1000 dilution of the 300 µM DAPI stock aliquots. Add 300 µL of 300 nM DAPI to each well and allow to react at room temperature for 30 minutes.
10. Wash for 30 minutes at room temperature in PBS. The gels may be mounted immediately or add 500 µL PBS to each well and store at 4ºC, wrapped in foil for up to several weeks.
11. For mounting the gels, add one drop of mounting medium per well of the multiwell chamber coverslip. Very carefully, place the coverslip and gel on the drop of mounting medium. Be careful not to introduce any bubbles and not to fold the gel.
12. Perform fluorescence microscopy.

Bibliography

1. Lindvall, O., Z. Kokaia, and A. Martinez-Serrano, Stem cell therapy for human neurodegenerative disorders-how to make it work. Nat Med, 2004. 10 Suppl: p. S42-50.
2. Lindvall, O. and Z. Kokaia, Stem cells for the treatment of neurological disorders. Nature, 2006. 441(7097): p. 1094-1096.
3. Gage, F.H., Mammalian Neural Stem Cells. Science, 2000. 287(5457): p. 1433-1438.
4. Lindvall, O., Clinical translation of stem cell transplantation in Parkinson's disease. Journal of internal medicine, 2016. 279(1): p. 30-40.
5. Kriegstein, A. and A. Alvarez-Buylla, The Glial Nature of Embryonic and Adult Neural Stem Cells. Annual review of neuroscience, 2009. 32: p. 149-184.
6. Bonaguidi, M.A., et al., A unifying hypothesis on mammalian neural stem cell properties in the adult hippocampus. Current opinion in neurobiology, 2012. 22(5): p. 754-761.
7. Daadi, M.M., A.L. Maag, and G.K. Steinberg, Adherent self-renewable human embryonic stem cell-derived neural stem cell line: functional engraftment in experimental stroke model. PLoS One, 2008. 3(2): p. e1644.
8. Kallur, T., et al., Human fetal cortical and striatal neural stem cells generate region-specific neurons in vitro and differentiate extensively to neurons after intrastriatal transplantation in neonatal rats. Journal of neuroscience research, 2006. 84(8): p. 1630-1644.

9. Muscari, C., et al., Priming adult stem cells by hypoxic pretreatments for applications in regenerative medicine. J Biomed Sci, 2013. 20(1): p. 63.

10. Hu, X., et al., Transplantation of hypoxia-preconditioned mesenchymal stem cells improves infarcted heart function via enhanced survival of implanted cells and angiogenesis. The Journal of thoracic and cardiovascular surgery, 2008. 135(4): p. 799-808.

11. Theus, M.H., et al., In vitro hypoxic preconditioning of embryonic stem cells as a strategy of promoting cell survival and functional benefits after transplantation into the ischemic rat brain. Experimental neurology, 2008. 210(2): p. 656-670.

12. Dings, J., et al., Clinical experience with 118 brain tissue oxygen partial pressure catheter probes. Neurosurgery, 1998. 43(5): p. 1082-1095.

13. Kirouac, D.C. and P.W. Zandstra, The systematic production of cells for cell therapies. Cell Stem Cell, 2008. 3(4): p. 369-381.

14. Gattazzo, F., A. Urciuolo, and P. Bonaldo, Extracellular matrix: a dynamic microenvironment for stem cell niche. Biochimica et Biophysica Acta (BBA)-General Subjects, 2014. 1840(8): p. 2506-2519.

15. Mohyeldin, A., T. Garzón-Muvdi, and A. Quiñones-Hinojosa, Oxygen in stem cell biology: a critical component of the stem cell niche. Cell stem cell, 2010. 7(2): p. 150-161.

16. Kolios, G. and Y. Moodley, Introduction to stem cells and regenerative medicine. Respiration, 2013. 85(1): p. 3-10.

17. Rossi, F. and E. Cattaneo, Neural stem cell therapy for neurological diseases: dreams and reality. Nat Rev Neurosci, 2002. 3(5): p. 401-409.

18. Jacobson, L.O., et al., Recovery from Radiation Injury. Science, 1951. 113(2940): p. 510-511.

19. Ford, C.E., et al., Cytological Identification of Radiation-Chimaeras. Nature, 1956. 177(4506): p. 452-454.

20. Nowell, P.C., et al., Growth and Continued Function of Rat Marrow Cells in X-radiated Mice. Cancer Research, 1956. 16(3): p. 258-261.

21. Gunsilius, E., G. Gastl, and A.L. Petzer, Hematopoietic stem cells. Biomedicine & pharmacotherapy, 2001. 55(4): p. 186-194.

22. Alison, M.R., et al., An introduction to stem cells. The Journal of pathology, 2002. 197(4): p. 419-423.

23. Lunn, J.S., et al., Stem cell technology for neurodegenerative diseases. Annals of neurology, 2011. 70(3): p. 353-361.

24. Khurana, V., et al., Toward stem cell-based phenotypic screens for neurodegenerative diseases. Nature Reviews Neurology, 2015. 11(6): p. 339-350.

25. Olesen, J., et al., The economic cost of brain disorders in Europe. European Journal of Neurology, 2012. 19(1): p. 155-162.

26. T, D., et al., Global Burden of Neurological Disorders: Estimates and Projections, in Neurological Disorders: Public Health Challenges. 2006, WHO Press: Geneva, Switzerland. p. 26-39.

27. Dutta, S., et al., Cell Therapy: The Final Frontier for Treatment of Neurological Diseases. CNS Neuroscience & Therapeutics, 2013. 19(1): p. 5-11.

28. Eriksson, M., et al., Functional Outcome 3 Months after Stroke Predicts Long-Term Survival. Cerebrovascular Diseases, 2008. 25(5): p. 423-429.

29. y Cajal, S.R., Degeneration & regeneration of the nervous system. Vol. 1. 1913: Oxford University Press.

30. Ma, D.K., et al., Adult neural stem cells in the mammalian central nervous system. Cell Res, 2009. 19(6): p. 672-82.

31. Reynolds, B.A. and S. Weiss, Generation of neurons and astrocytes from isolated cells of the adult mammalian central nervous system. science, 1992. 255(5052): p. 1707-1710.

32. Reynolds, B.A. and S. Weiss, Clonal and population analyses demonstrate that an EGF-responsive mammalian embryonic CNS precursor is a stem cell. Developmental biology, 1996. 175(1): p. 1-13.

33. Eriksson, P.S., et al., Neurogenesis in the adult human hippocampus. Nat Med, 1998. 4(11): p. 1313-1317.

34. Davis, A.A. and S. Temple, A self-renewing multipotential stem cell in embryonic rat cerebral cortex. Nature, 1994. 372(6503): p. 263-266.

35. Temple, S., The development of neural stem cells. Nature, 2001. 414(6859): p. 112-117.

36. Noctor, S.C., et al., Neurons derived from radial glial cells establish radial units in neocortex. Nature, 2001. 409(6821): p. 714-720.

37. Gotz, M. and W.B. Huttner, The cell biology of neurogenesis. Nat Rev Mol Cell Biol, 2005. 6(10): p. 777-788.

38. Egger, B., K.S. Gold, and A.H. Brand, Regulating the balance between symmetric and asymmetric stem cell division in the developing brain. Fly, 2011. 5(3): p. 237-241.

39. Morrison, S.J. and J. Kimble, Asymmetric and symmetric stem-cell divisions in development and cancer. Nature, 2006. 441(7097): p. 1068-1074.

40. Olynik, B.M. and M. Rastegar, The genetic and epigenetic journey of embryonic stem cells into mature neural cells. Front Genet, 2012. 3: p. 81.

41. Spradling, A., D. Drummond-Barbosa, and T. Kai, Stem cells find their niche. Nature, 2001. 414(6859): p. 98-104.

42. Scharffb, F.D.C., Challenges for brain repair: insights from adult neurogenesis in birds and mammals. Brain Behav Evol, 2001. 58: p. 306-322.

43. Alvarez-Buylla, A. and D.A. Lim, For the long run: maintaining germinal niches in the adult brain. Neuron, 2004. 41(5): p. 683-686.

44. Martino, G., et al., Brain regeneration in physiology and pathology: the immune signature driving therapeutic plasticity of neural stem cells. Physiological reviews, 2011. 91(4): p. 1281-1304.

45. Fuentealba, L.C., K. Obernier, and A. Alvarez-Buylla, Adult neural stem cells bridge their niche. Cell stem cell, 2012. 10(6): p. 698-708.

46. Wagers, A.J., The stem cell niche in regenerative medicine. Cell stem cell, 2012. 10(4): p. 362-369.

47. Discher, D.E., D.J. Mooney, and P.W. Zandstra, Growth factors, matrices, and forces combine and control stem cells. Science, 2009. 324(5935): p. 1673-1677.

48. Trounson, A. and C. McDonald, Stem cell therapies in clinical trials: progress and challenges. Cell stem cell, 2015. 17(1): p. 11-22.

49. Gage, F.H. and S. Temple, Neural stem cells: generating and regenerating the brain. Neuron, 2013. 80(3): p. 588-601.

50. Darsalia, V., T. Kallur, and Z. Kokaia, Survival, migration and neuronal differentiation of human fetal striatal and cortical neural stem cells grafted in stroke-damaged rat striatum. Eur J Neurosci, 2007. 26(3): p. 605-14.

51. Kelly, S., et al., Transplanted human fetal neural stem cells survive, migrate, and differentiate in ischemic rat cerebral cortex. Proc Natl Acad Sci U S A, 2004. 101(32): p. 11839-44.

52. Mine, Y., et al., Grafted human neural stem cells enhance several steps of endogenous neurogenesis and improve behavioral recovery after middle cerebral artery occlusion in rats. Neurobiology of disease, 2013. 52: p. 191-203.

53. Smith, E.J., et al., Implantation site and lesion topology determine efficacy of a human neural stem cell line in a rat model of chronic stroke. Stem cells, 2012. 30(4): p. 785-796.

54. Ben-Hur, T., et al., Transplantation of human embryonic stem cell–derived neural progenitors improves behavioral deficit in parkinsonian rats. Stem Cells, 2004. 22(7): p. 1246-1255.

55. Ebert, A.D., et al., Human neural progenitor cells over-expressing IGF-1 protect dopamine neurons and restore function in a rat model of Parkinson's disease. Experimental neurology, 2008. 209(1): p. 213-223.

56. Bjugstad, K.B., et al., Human neural stem cells migrate along the nigrostriatal pathway in a primate model of Parkinson's disease. Experimental neurology, 2008. 211(2): p. 362-369.

57. Redmond, D.E., et al., Behavioral improvement in a primate Parkinson's model is associated with multiple homeostatic effects of human neural stem cells. Proceedings of the National Academy of Sciences, 2007. 104(29): p. 12175-12180.

58. Park, D., et al., Human neural stem cells over-expressing choline acetyltransferase restore cognition in rat model of cognitive dysfunction. Experimental neurology, 2012. 234(2): p. 521-526.

59. Lindvall, O., et al., Human fetal dopamine neurons grafted into the striatum in two patients with severe Parkinson's disease: a detailed account of methodology and a 6-month follow-up. Archives of neurology, 1989. 46(6): p. 615-631.

60. Lindvall, O., et al., Evidence for long-term survival and function of dopaminergic grafts in progressive Parkinson's disease. Annals of neurology, 1994. 35(2): p. 172-180.

61. Spencer, D.D., et al., Unilateral transplantation of human fetal mesencephalic tissue into the caudate nucleus of patients with Parkinson's disease. New England Journal of Medicine, 1992. 327(22): p. 1541-1548.

62. Wenning, G.K., et al., Short-and long-term survival and function of unilateral intrastriatal dopaminergic grafts in Parkinson's disease. Annals of neurology, 1997. 42(1): p. 95-107.

63. Freed, C.R., et al., Transplantation of embryonic dopamine neurons for severe Parkinson's disease. New England Journal of Medicine, 2001. 344(10): p. 710-719.

64. Ma, Y., et al., Dyskinesia after fetal cell transplantation for parkinsonism: a PET study. Annals of neurology, 2002. 52(5): p. 628-634.

65. Dranovsky, A., et al., Experience dictates stem cell fate in the adult hippocampus. Neuron, 2011. 70(5): p. 908-923.

66. Vescovi, A.L. and E.Y. Snyder, Establishment and properties of neural stem cell clones: plasticity in vitro and in vivo. Brain pathology, 1999. 9(3): p. 569-598.

67. Dimmeler, S., et al., Translational strategies and challenges in regenerative medicine. Nature medicine, 2014. 20(8): p. 814-821.

68. Carpenter, M.K., et al., In vitro expansion of a multipotent population of human neural progenitor cells. Experimental neurology, 1999. 158(2): p. 265-278.

69. Johansson, C.B., et al., Neural stem cells in the adult human brain. Experimental cell research, 1999. 253(2): p. 733-736.

70. Vescovi, A.L., et al., Isolation and cloning of multipotential stem cells from the embryonic human CNS and establishment of transplantable human neural stem cell lines by epigenetic stimulation. Experimental neurology, 1999. 156(1): p. 71-83.

71. Villa, A., et al., Establishment and properties of a growth factor-dependent, perpetual neural stem cell line from the human CNS. Experimental neurology, 2000. 161(1): p. 67-84.

72. Tibbitt, M.W. and K.S. Anseth, Hydrogels as extracellular matrix mimics for 3D cell culture. Biotechnology and bioengineering, 2009. 103(4): p. 655-663.

73. Baker, B.M. and C.S. Chen, Deconstructing the third dimension–how 3D culture microenvironments alter cellular cues. Journal of cell science, 2012. 125(13): p. 3015-3024.

74. Mitragotri, S. and J. Lahann, Physical approaches to biomaterial design. Nature materials, 2009. 8(1): p. 15-23.

75. Seliktar, D., Designing cell-compatible hydrogels for biomedical applications. Science, 2012. 336(6085): p. 1124-1128.

76. Nguyen, K.T. and J.L. West, Photopolymerizable hydrogels for tissue engineering applications. Biomaterials, 2002. 23(22): p. 4307-4314.

77. Cukierman, E., et al., Taking cell-matrix adhesions to the third dimension. Science, 2001. 294(5547): p. 1708-1712.

78. Rhee, S. and F. Grinnell, Fibroblast mechanics in 3D collagen matrices. Advanced drug delivery reviews, 2007. 59(13): p. 1299-1305.

79. Semino, C.E., et al., Functional differentiation of hepatocyte-like spheroid structures from putative liver progenitor cells in three-dimensional peptide scaffolds. Differentiation, 2003. 71(4-5): p. 262-270.

80. Ribeiro, A., et al., β1-Integrin cytoskeletal signaling regulates sensory neuron response to matrix dimensionality. Neuroscience, 2013. 248: p. 67-78.

81. Ribeiro, A., et al., Substrate three-dimensionality induces elemental morphological transformation of sensory neurons on a physiologic timescale. Tissue Engineering Part A, 2011. 18(1-2): p. 93-102.

82. Rustad, K.C., et al., Enhancement of mesenchymal stem cell angiogenic capacity and stemness by a biomimetic hydrogel scaffold. Biomaterials, 2012. 33(1): p. 80-90.

83. Stenberg, J., et al., Sustained embryoid body formation and culture in a non-laborious three dimensional culture system for human embryonic stem cells. Cytotechnology, 2011. 63(3): p. 227-237.

84. Banerjee, A., et al., The influence of hydrogel modulus on the proliferation and differentiation of encapsulated neural stem cells. Biomaterials, 2009. 30(27): p. 4695-4699.

85. Simon, M.C. and B. Keith, The role of oxygen availability in embryonic development and stem cell function. Nature reviews Molecular cell biology, 2008. 9(4): p. 285-296.

86. De Filippis, L. and D. Delia, Hypoxia in the regulation of neural stem cells. Cellular and Molecular Life Sciences, 2011. 68(17): p. 2831-2844.

87. Panchision, D.M., The role of oxygen in regulating neural stem cells in development and disease. Journal of cellular physiology, 2009. 220(3): p. 562-568.

88. Erecińska, M. and I.A. Silver, Tissue oxygen tension and brain sensitivity to hypoxia. Respiration physiology, 2001. 128(3): p. 263-276.

89. Mitchell, J.A. and J.M. Yochim, Intrauterine oxygen tension during the estrous cycle in the rat: its relation to uterine respiration and vascular activity. Endocrinology, 1968. 83(4): p. 701-705.

90. Rodesch, F., et al., Oxygen measurements in endometrial and trophoblastic tissues during early pregnancy. Obstetrics & Gynecology, 1992. 80(2): p. 283-285.

91. Wakai, T., et al., Hypoxic preconditioning enhances neural stem cell transplantation therapy after intracerebral hemorrhage in mice. Journal of Cerebral Blood Flow & Metabolism, 2015: p. 0271678X15613798.

92. Studer, L., et al., Enhanced proliferation, survival, and dopaminergic differentiation of CNS precursors in lowered oxygen. The Journal of Neuroscience, 2000. 20(19): p. 7377-7383.

93. Santilli, G., et al., Mild hypoxia enhances proliferation and multipotency of human neural stem cells. PloS one, 2010. 5(1): p. e8575.

94. Gritti, A., et al., Multipotential stem cells from the adult mouse brain proliferate and self-renew in response to basic fibroblast growth factor. The Journal of Neuroscience, 1996. 16(3): p. 1091-1100.

95. Reynolds, B.A., W. Tetzlaff, and S. Weiss, A multipotent EGF-responsive striatal embryonic progenitor cell produces neurons and astrocytes. The Journal of neuroscience, 1992. 12(11): p. 4565-4574.

96. Vescovi, A.L., et al., bFGF regulates the proliferative fate of unipotent (neuronal) and bipotent (neuronal/astroglial) EGF-generated CNS progenitor cells. Neuron, 1993. 11(5): p. 951-966.

97. Kuhn, H.G., et al., Epidermal growth factor and fibroblast growth factor-2 have different effects on neural progenitors in the adult rat brain. The Journal of Neuroscience, 1997. 17(15): p. 5820-5829.

98. Palmer, T.D., J. Takahashi, and F.H. Gage, The adult rat hippocampus contains primordial neural stem cells. Molecular and Cellular Neuroscience, 1997. 8(6): p. 389-404.

99. Reubinoff, B.E., et al., Neural progenitors from human embryonic stem cells. Nature biotechnology, 2001. 19(12): p. 1134-1140.

100. Svendsen, C.N., et al., A new method for the rapid and long term growth of human neural precursor cells. Journal of neuroscience methods, 1998. 85(2): p. 141-152.

101. Zhang, S.-C., et al., In vitro differentiation of transplantable neural precursors from human embryonic stem cells. Nature biotechnology, 2001. 19(12): p. 1129-1133.

102. Holley, R.W. and J.A. Kiernan, Control of the initiation of DNA synthesis in 3T3 cells: serum factors. Proceedings of the National Academy of Sciences, 1974. 71(7): p. 2908-2911.

103. Grothe, C. and M. Timmer, The physiological and pharmacological role of basic fibroblast growth factor in the dopaminergic nigrostriatal system. Brain research reviews, 2007. 54(1): p. 80-91.

104. Turner, C.A., S.J. Watson, and H. Akil, The fibroblast growth factor family: neuromodulation of affective behavior. Neuron, 2012. 76(1): p. 160-174.

105. Vaccarino, F.M., et al., Changes in cerebral cortex size are governed by fibroblast growth factor during embryogenesis. Nature neuroscience, 1999. 2(3): p. 246-253.

106. Raballo, R., et al., Basic fibroblast growth factor (Fgf2) is necessary for cell proliferation and neurogenesis in the developing cerebral cortex. The Journal of Neuroscience, 2000. 20(13): p. 5012-5023.

107. Zheng, W., R.S. Nowakowski, and F.M. Vaccarino, Fibroblast growth factor 2 is required for maintaining the neural stem cell pool in the mouse brain subventricular zone. Developmental neuroscience, 2005. 26(2-4): p. 181-196.

108. Dono, R., et al., Impaired cerebral cortex development and blood pressure regulation in FGF-2-deficient mice. The EMBO journal, 1998. 17(15): p. 4213-4225.

109. Johnson, D.E. and L.T. Williams, Structural and functional diversity in the FGF receptor multigene family. Advances in cancer research, 1993. 60: p. 1.

110. Cohen, S., Isolation of a Mouse Submaxillary Gland Protein Accelerating Incisor Eruption and Eyelid Opening in the New-born Animal. Journal of Biological Chemistry, 1962. 237(5): p. 1555-1562.

111. Carpenter, G. and S. Cohen, Epidermal growth factor. Annual review of biochemistry, 1979. 48(1): p. 193-216.

112. Craig, C.G., et al., In vivo growth factor expansion of endogenous subependymal neural precursor cell populations in the adult mouse brain. The Journal of neuroscience, 1996. 16(8): p. 2649-2658.

113. Martens, D.J., R.M. Seaberg, and D. Van Der Kooy, In vivo infusions of exogenous growth factors into the fourth ventricle of the adult mouse brain increase the proliferation of neural progenitors around the fourth ventricle and the central canal of the spinal cord. European Journal of Neuroscience, 2002. 16(6): p. 1045-1057.

114. Schlessinger, J. and A. Ullrich, Growth factor signaling by receptor tyrosine kinases. Neuron, 1992. 9(3): p. 383-391.

115. Kornblum, H.I., et al., Prenatal ontogeny of the epidermal growth factor receptor and its ligand, transforming growth factor alpha, in the rat brain. Journal of Comparative Neurology, 1997. 380(2): p. 243-261.

116. Threadgill, D.W., et al., Targeted disruption of mouse EGF receptor: effect of genetic background on mutant phenotype. Science, 1995. 269(5221): p. 230-234.

117. Le Blanc, K., et al., Mesenchymal stem cells for treatment of steroid-resistant, severe, acute graft-versus-host disease: a phase II study. The Lancet, 2008. 371(9624): p. 1579-1586.

118. Weissman, I.L. and J.A. Shizuru, The origins of the identification and isolation of hematopoietic stem cells, and their capability to induce donor-specific transplantation tolerance and treat autoimmune diseases. Blood, 2008. 112(9): p. 3543-3553.

119. Gospodarowicz, D., D. Delgado, and I. Vlodavsky, Permissive effect of the extracellular matrix on cell proliferation in vitro. Proceedings of the National Academy of Sciences, 1980. 77(7): p. 4094-4098.

120. Kazanis, I., Extracellular matrix and the neural stem cell niche. Developmental neurobiology, 2011. 71(11): p. 1006-1017.

121. Hynes, R.O., The extracellular matrix: not just pretty fibrils. Science, 2009. 326(5957): p. 1216-1219.

122. Sharee Ghourichaee, S. and J.B. Leach, The effect of hypoxia and laminin-rich substrates on the proliferative behavior of human neural stem cells. Journal of Materials Chemistry B, 2016.

123. Flanagan, L.A., et al., Regulation of human neural precursor cells by laminin and integrins. Journal of neuroscience research, 2006. 83(5): p. 845-856.

124. Lu, P., V.M. Weaver, and Z. Werb, The extracellular matrix: a dynamic niche in cancer progression. The Journal of cell biology, 2012. 196(4): p. 395-406.

125. Brizzi, M.F., G. Tarone, and P. Defilippi, Extracellular matrix, integrins, and growth factors as tailors of the stem cell niche. Current opinion in cell biology, 2012. 24(5): p. 645-651.

126. Wade, A., A. McKinney, and J.J. Phillips, Matrix regulators in neural stem cell functions. Biochimica et Biophysica Acta (BBA)-General Subjects, 2014. 1840(8): p. 2520-2525.

127. Douet, V., et al., Fractone-heparan sulphates mediate FGF-2 stimulation of cell proliferation in the adult subventricular zone. Cell proliferation, 2013. 46(2): p. 137-145.

128. Hynes, R.O., Integrins: bidirectional, allosteric signaling machines. Cell, 2002. 110(6): p. 673-687.

129. Legate, K.R., S.A. Wickström, and R. Fässler, Genetic and cell biological analysis of integrin outside-in signaling. Genes & development, 2009. 23(4): p. 397-418.

130. Reichardt, L. and A. Prokop, Introduction: the role of extracellular matrix in nervous system development and maintenance. Developmental neurobiology, 2011. 71(11): p. 883-888.

131. Durbeej, M., Laminins. Cell and tissue research, 2010. 339(1): p. 259-268.

132. Barros, C.S., S.J. Franco, and U. Müller, Extracellular matrix: functions in the nervous system. Cold Spring Harbor perspectives in biology, 2011. 3(1): p. a005108.

133. Drago, J., V. Nurcombe, and P.F. Bartlett, Laminin through its long arm E8 fragment promotes the proliferation and differentiation of murine neuroepithelial cells in vitro. Experimental cell research, 1991. 192(1): p. 256-265.

134. Kearns, S.M., et al., Extracellular matrix effects on neurosphere cell motility. Experimental neurology, 2003. 182(1): p. 240-244.

135. Xu, C., et al., Feeder-free growth of undifferentiated human embryonic stem cells. Nature biotechnology, 2001. 19(10): p. 971-974.

136. Loulier, K., et al., β1 integrin maintains integrity of the embryonic neocortical stem cell niche. PLoS Biol, 2009. 7(8): p. e1000176.

137. Nomura, H., C.H. Tator, and M.S. Shoichet, Bioengineered strategies for spinal cord repair. Journal of neurotrauma, 2006. 23(3-4): p. 496-507.

138. Chevallay, B. and D. Herbage, Collagen-based biomaterials as 3D scaffold for cell cultures: applications for tissue engineering and gene therapy. Medical and Biological Engineering and Computing, 2000. 38(2): p. 211-218.

139. Wallace, D.G. and J. Rosenblatt, Collagen gel systems for sustained delivery and tissue engineering. Advanced drug delivery reviews, 2003. 55(12): p. 1631-1649.

140. Drury, J.L. and D.J. Mooney, Hydrogels for tissue engineering: scaffold design variables and applications. Biomaterials, 2003. 24(24): p. 4337-4351.

141. Thompson, J.M. and D.J. Pelto, Attachment, survival and neurite extension of chick embryo retinal neurons on various culture substrates. Developmental neuroscience, 1982. 5(5-6): p. 447-457.

142. Zhong, Y. and R.V. Bellamkonda, Biomaterials for the central nervous system. Journal of the Royal Society Interface, 2008. 5(26): p. 957-975.

143. Kaspar, M., L. Zardi, and D. Neri, Fibronectin as target for tumor therapy. International journal of cancer, 2006. 118(6): p. 1331-1339.

144. Singh, P., C. Carraher, and J.E. Schwarzbauer, Assembly of fibronectin extracellular matrix. Annual review of cell and developmental biology, 2010. 26: p. 397.

145. Venstrom, K.A. and L.F. Reichardt, Extracellular matrix. 2: Role of extracellular matrix molecules and their receptors in the nervous system. The FASEB journal, 1993. 7(11): p. 996-1003.

146. Shiga, T. and R.W. Oppenheim, Immunolocalization studies of putative guidance molecules used by axons and growth cones of intersegmental

interneurons in the chick embryo spinal cord. Journal of Comparative Neurology, 1991. 310(2): p. 234-252.

147. Myers, J.P., M. Santiago-Medina, and T.M. Gomez, Regulation of axonal outgrowth and pathfinding by integrin–ECM interactions. Developmental neurobiology, 2011. 71(11): p. 901-923.

148. Khoshnoodi, J., V. Pedchenko, and B.G. Hudson, Mammalian collagen IV. Microscopy research and technique, 2008. 71(5): p. 357-370.

149. Ali, S.A., I.S. Pappas, and J.G. Parnavelas, Collagen type IV promotes the differentiation of neuronal progenitors and inhibits astroglial differentiation in cortical cell cultures. Developmental brain research, 1998. 110(1): p. 31-38.

150. Hirose, H., T. Kitaguchi, and T. Tabira, Neurite promoting activity of collagens on embryonic neurons: decreased effect at the postnatal stage. The Tohoku journal of experimental medicine, 1993. 170(4): p. 207-218.

151. Barczyk, M., S. Carracedo, and D. Gullberg, Integrins. Cell and tissue research, 2010. 339(1): p. 269-280.

152. Letourneau, P.C., et al., Immunoreactivity for laminin in the developing ventral longitudinal pathway of the brain. Developmental biology, 1988. 125(1): p. 135-144.

153. Eagleson, K.L., R.T. Ferri, and P. Levitt, Complementary distribution of collagen type IV and the epidermal growth factor receptor in the rat embryonic telencephalon. Cerebral Cortex, 1996. 6(3): p. 540-549.

154. Kleinman, H.K. and G.R. Martin. Matrigel: basement membrane matrix with biological activity. Elsevier.

155. Hughes, C.S., L.M. Postovit, and G.A. Lajoie, Matrigel: a complex protein mixture required for optimal growth of cell culture. Proteomics, 2010. 10(9): p. 1886-1890.

156. Lutolf, M.P. and J.A. Hubbell, Synthetic biomaterials as instructive extracellular microenvironments for morphogenesis in tissue engineering. Nature biotechnology, 2005. 23(1): p. 47-55.

157. Ma, W., et al., Cell-extracellular matrix interactions regulate neural differentiation of human embryonic stem cells. BMC developmental biology, 2008. 8(1): p. 90.

158. Uemura, M., et al., Matrigel supports survival and neuronal differentiation of grafted embryonic stem cell-derived neural precursor cells. Journal of neuroscience research, 2010. 88(3): p. 542-551.

159. Weissman, I.L., D.J. Anderson, and F. Gage, Stem and progenitor cells: origins, phenotypes, lineage commitments, and transdifferentiations. Annual review of cell and developmental biology, 2001. 17(1): p. 387-403.

160. Daadi, M.M., A.-L. Maag, and G.K. Steinberg, Adherent self-renewable human embryonic stem cell-derived neural stem cell line: functional engraftment in experimental stroke model. PLoS One, 2008. 3(2): p. e1644.

161. Bjorklund, A. and J.H. Kordower, Cell therapy for Parkinson's disease: what next? Movement Disorders, 2013. 28(1): p. 110-115.

162. Solyanik, G.I., et al., Different growth patterns of a cancer cell population as a function of its starting growth characteristics: analysis by mathematical modelling. Cell proliferation, 1995. 28(5): p. 263-278.

163. Steel, G.G., Growth kinetics of tumours: cell population kinetics in relation to the growth and treatment of cancer. 1977: Oxford University Press, USA.

164. Williams, R.W., Mapping genes that modulate mouse brain development: a quantitative genetic approach, in Mouse brain development. 2000, Springer. p. 21-49.

165. Wu, H.-H., et al., Autoregulation of neurogenesis by GDF11. Neuron, 2003. 37(2): p. 197-207.

166. Caviness, V.S., T. Takahashi, and R.S. Nowakowski, Numbers, time and neocortical neuronogenesis: a general developmental and evolutionary model. Trends in neurosciences, 1995. 18(9): p. 379-383.

167. Johnston, M.D., et al., Mathematical modeling of cell population dynamics in the colonic crypt and in colorectal cancer. Proceedings of the National Academy of Sciences, 2007. 104(10): p. 4008-4013.

168. Aguirre, A., M.E. Rubio, and V. Gallo, Notch and EGFR pathway interaction regulates neural stem cell number and self-renewal. Nature, 2010. 467(7313): p. 323-327.

169. Liu, X., et al., Nonsynaptic GABA signaling in postnatal subventricular zone controls proliferation of GFAP-expressing progenitors. Nature neuroscience, 2005. 8(9): p. 1179-1187.

170. Alfonso, J., et al., Diazepam binding inhibitor promotes progenitor proliferation in the postnatal SVZ by reducing GABA signaling. Cell Stem Cell, 2012. 10(1): p. 76-87.

171. Krishan, A. and R.M. Hamelik, Click-iT Proliferation Assay with Improved DNA Histograms, in Current Protocols in Cytometry. 2001, John Wiley & Sons, Inc.

172. Sandberg, M.L., et al., c-Myb and p300 regulate hematopoietic stem cell proliferation and differentiation. Developmental cell, 2005. 8(2): p. 153-166.

173. Close, J.L., B. Gumuscu, and T.A. Reh, Retinal neurons regulate proliferation of postnatal progenitors and Müller glia in the rat retina via TGFβ signaling. Development, 2005. 132(13): p. 3015-3026.

174. Horsley, V., et al., NFATc1 balances quiescence and proliferation of skin stem cells. Cell, 2008. 132(2): p. 299-310.

175. Plikus, M.V., et al., Cyclic dermal BMP signalling regulates stem cell activation during hair regeneration. Nature, 2008. 451(7176): p. 340-344.

176. Cameron, H.A. and R.D.G. McKay, Adult neurogenesis produces a large pool of new granule cells in the dentate gyrus. The Journal of Comparative Neurology, 2001. 435(4): p. 406-417.

177. Hayes, N.L. and R.S. Nowakowski, Dynamics of cell proliferation in the adult dentate gyrus of two inbred strains of mice. Developmental Brain Research, 2002. 134(1–2): p. 77-85.

178. Salomoni, P. and F. Calegari, Cell cycle control of mammalian neural stem cells: putting a speed limit on G1. Trends in cell biology, 2010. 20(5): p. 233-243.

179. Kornack, D.R. and P. Rakic, Changes in cell-cycle kinetics during the development and evolution of primate neocortex. Proceedings of the National Academy of Sciences, 1998. 95(3): p. 1242-1246.

180. Lukaszewicz, A., et al., G1 Phase Regulation, Area-Specific Cell Cycle Control, and Cytoarchitectonics in the Primate Cortex. Neuron, 2005. 47(3): p. 353-364.

181. Storch, A., et al., Long-Term Proliferation and Dopaminergic Differentiation of Human Mesencephalic Neural Precursor Cells. Experimental Neurology, 2001. 170(2): p. 317-325.

182. Lindvall, O., Z. Kokaia, and A. Martinez-Serrano, Stem cell therapy for human neurodegenerative disorders–how to make it work. Nature Medicine 2004. 10: p. 42-50.

183. Kelly, S., et al., Transplanted human fetal neural stem cells survive, migrate, and differentiate in ischemic rat cerebral cortex. Proceedings of the National Academy of Sciences of the United States of America, 2004. 101(32): p. 11839-11844.

184. Daadi, M.M., et al., Molecular and magnetic resonance imaging of human embryonic stem cell–derived neural stem cell grafts in ischemic rat brain. Molecular Therapy, 2009. 17(7): p. 1282-1291.

185. Laflamme, M.A., et al., Cardiomyocytes derived from human embryonic stem cells in pro-survival factors enhance function of infarcted rat hearts. Nature biotechnology, 2007. 25(9): p. 1015-1024.

186. Contreras, J.L., et al., Cytoprotection of pancreatic islets before and early after transplantation using gene therapy. Kidney international, 2002. 61: p. S79-S84.

187. Skuk, D., et al., Resetting the Problem of Cell Death Following Muscle-Derived Cell Transplantation: Detection, Dynamics and Mechanisms. Journal of Neuropathology & Experimental Neurology, 2003. 62(9): p. 951-967.

188. Sakata, H., et al., Neural stem cells genetically modified to overexpress Cu/Zn-superoxide dismutase enhance amelioration of ischemic stroke in mice. Stroke, 2012. 43(9): p. 2423-2429.

189. Greenberger, J.S., Gene therapy approaches for stem cell protection. Gene therapy, 2008. 15(2): p. 100-108.

190. Trivedi, P., et al., Mesenchymal stem cell therapy for treatment of cardiovascular disease: helping people sooner or later. Stem cells and development, 2010. 19(7): p. 1109-1120.

191. Nowakowski, A., et al., Genetic engineering of stem cells for enhanced therapy. Acta Neurobiol Exp (Wars), 2013. 73(1): p. 1-18.

192. Sart, S., T. Ma, and Y. Li, Preconditioning stem cells for in vivo delivery. BioResearch open access, 2014. 3(4): p. 137-149.

193. Wei, L., et al., Transplantation of hypoxia preconditioned bone marrow mesenchymal stem cells enhances angiogenesis and neurogenesis after cerebral ischemia in rats. Neurobiology of disease, 2012. 46(3): p. 635-645.

194. Dings, J., et al., Clinical experience with 118 brain tissue oxygen partial pressure catheter probes. Neurosurgery, 1998. 43(5): p. 1082-1094.

195. Bouvier, M.M. and C. Mytilineou, Basic fibroblast growth factor increases division and delays differentiation of dopamine precursors in vitro. The Journal of neuroscience, 1995. 15(11): p. 7141-7149.

196. Shi, Y., et al., Human cerebral cortex development from pluripotent stem cells to functional excitatory synapses. Nature neuroscience, 2012. 15(3): p. 477-486.

197. Francis, F., et al., Doublecortin is a developmentally regulated, microtubule-associated protein expressed in migrating and differentiating neurons. Neuron, 1999. 23(2): p. 247-256.

198. Nacher, J., C. Crespo, and B.S. McEwen, Doublecortin expression in the adult rat telencephalon. European Journal of Neuroscience, 2001. 14(4): p. 629-644.

199. Francis, K.R. and L. Wei, Human embryonic stem cell neural differentiation and enhanced cell survival promoted by hypoxic preconditioning. Cell death & disease, 2010. 1(2): p. e22.

200. Cavallaro, M., et al., Impaired generation of mature neurons by neural stem cells from hypomorphic Sox2 mutants. Development, 2008. 135(3): p. 541-557.

201. Ilieva, M. and M. Dufva, SOX2 and OCT4 mRNA-expressing cells, detected by molecular beacons, localize to the center of neurospheres during differentiation. PloS one, 2013. 8(8): p. e73669.

202. Valorani, M.G., et al., Hypoxia increases Sca-1/CD44 co-expression in murine mesenchymal stem cells and enhances their adipogenic differentiation potential. Cell and tissue research, 2010. 341(1): p. 111-120.

203. Shin, J.M., et al., Enhancement of differentiation efficiency of hESCs into vascular lineage cells in hypoxia via a paracrine mechanism. Stem cell research, 2011. 7(3): p. 173-185.

204. Segers, V.F.M. and R.T. Lee, Stem-cell therapy for cardiac disease. Nature, 2008. 451(7181): p. 937-942.

205. Doetsch, F., A niche for adult neural stem cells. Current opinion in genetics & development, 2003. 13(5): p. 543-550.

206. Fuchs, E., T. Tumbar, and G. Guasch, Socializing with the neighbors: stem cells and their niche. Cell, 2004. 116(6): p. 769-778.

207. Morrison, S.J. and A.C. Spradling, Stem cells and niches: mechanisms that promote stem cell maintenance throughout life. Cell, 2008. 132(4): p. 598-611.

208. Peerani, R. and P.W. Zandstra, Enabling stem cell therapies through synthetic stem cell–niche engineering. The Journal of clinical investigation, 2010. 120(1): p. 60.

209. Jacques, T.S., et al., Neural precursor cell chain migration and division are regulated through different beta1 integrins. Development, 1998. 125(16): p. 3167-3177.

210. Kazanis, I., et al., Quiescence and activation of stem and precursor cell populations in the subependymal zone of the mammalian brain are associated with distinct cellular and extracellular matrix signals. The Journal of Neuroscience, 2010. 30(29): p. 9771-9781.

211. Lathia, J.D., et al., Patterns of laminins and integrins in the embryonic ventricular zone of the CNS. Journal of Comparative Neurology, 2007. 505(6): p. 630-643.

212. Hay, E.D., Extracellular matrix. The Journal of cell biology, 1981. 91(3): p. 205s-223s.

213. Mercier, F., J.T. Kitasako, and G.I. Hatton, Anatomy of the brain neurogenic zones revisited: fractones and the fibroblast/macrophage network. Journal of Comparative Neurology, 2002. 451(2): p. 170-188.

214. Pearlman, A.L. and A.M. Sheppard, Extracellular matrix in early cortical development. Progress in brain research, 1995. 108: p. 117-134.

215. Gavrieli, Y., Y. Sherman, and S.A. Ben-Sasson, Identification of programmed cell death in situ via specific labeling of nuclear DNA fragmentation. The Journal of cell biology, 1992. 119(3): p. 493-501.

216. Hall, P.E., J.D. Lathia, and M.A. Caldwell, Laminin enhances the growth of human neural stem cells in defined culture media. BMC neuroscience, 2008. 9(1): p. 71.

217. Hall, P.E., et al., Integrins are markers of human neural stem cells. Stem Cells, 2006. 24(9): p. 2078-2084.

218. Frisch, S.M. and H. Francis, Disruption of epithelial cell-matrix interactions induces apoptosis. The Journal of cell biology, 1994. 124(4): p. 619-626.

219. Frisch, S.M. and E. Ruoslahti, Integrins and anoikis. Current opinion in cell biology, 1997. 9(5): p. 701-706.

220. Kleinman, H.K., et al., Isolation and characterization of type IV procollagen, laminin, and heparan sulfate proteoglycan from the EHS sarcoma. Biochemistry, 1982. 21(24): p. 6188-6193.

221. Leone, D.P., et al., Regulation of neural progenitor proliferation and survival by β1 integrins. Journal of cell science, 2005. 118(12): p. 2589-2599.

222. Gospodarowicz, D. and J. Cheng, Heparin protects basic and acidic FGF from inactivation. Journal of cellular physiology, 1986. 128(3): p. 475-484.

223. Whalen, G.F., Y. Shing, and J. Folkman, The fate of intravenously administered bFGF and the effect of heparin. Growth Factors, 1989. 1(2): p. 157-164.

224. Nguyen, T.H., et al., A heparin-mimicking polymer conjugate stabilizes basic fibroblast growth factor. Nature chemistry, 2013. 5(3): p. 221-227.